

IERS TECHNICAL NOTE 21

IERS Conventions (1996)

Dennis D. McCarthy
U.S. Naval Observatory

July 1996

TABLE OF CONTENTS

INTRODUCTION	1
Differences Between This Document and IERS Technical Note 13	1
1. CONVENTIONAL CELESTIAL REFERENCE SYSTEM	4
Equator	4
Origin of Right Ascension	4
Precision and Accuracy	5
Availability of the Frame	5
2. CONVENTIONAL DYNAMICAL REFERENCE FRAME	8
3. CONVENTIONAL TERRESTRIAL REFERENCE SYSTEM	10
Definition	10
Realization	10
Transformation Parameters of World Coordinate Systems and Datums	11
Plate Motion Model	13
4. NUMERICAL STANDARDS	18
5. TRANSFORMATION BETWEEN THE CELESTIAL AND TERRESTRIAL SYSTEMS	20
Coordinate Transformation Referred to the Equinox	20
The IAU 1980 Theory of Nutation	22
The IERS 1996 Theory of Precession/Nutation	25
The Multipliers of the Fundamental Arguments of Nutation Theory	32
Conversion to Prograde and Retrograde Nutation Amplitudes	33
Coordinate Transformation Referred to the Nonrotating Origin	33
Geodesic Nutation	37
6. GEOPOTENTIAL	40
Effect of Solid Earth Tides	40
Solid Earth Pole Tide	46
Treatment of the Permanent Tide	47
Effect of the Ocean Tides	47
7. SITE DISPLACEMENT	52
Ocean Loading	52
Ocean Loading	52
Effects of the Solid Earth Tides	56
Displacement due to degree 2 tides	60
Displacement due to degree 3 tides	61
Contributions to the transverse	62
Out of phase contributions	62
Correction for frequency	63
Permanent deformation	65
Rotational Deformation Due to Polar Motion	66
Antenna Deformation	67
Atmospheric Loading	67
Postglacial Rebound	69
8. TIDAL VARIATIONS IN THE EARTH'S ROTATION	72
9. TROPOSPHERIC MODEL	78
Optical Techniques	78
Radio Techniques	78
10. RADIATION PRESSURE REFLECTANCE MODEL	81

Global Positioning System	81
11. GENERAL RELATIVISTIC MODELS FOR TIME, COORDINATES AND EQUATIONS OF MOTION	83
Equations of Motion for an Artificial Earth Satellite	83
Equations of Motion in the Barycentric Frame	83
Scale Effect and Choice of Time Coordinate	84
12. GENERAL RELATIVISTIC MODELS FOR PROPAGATION	87
VLBI Time Delay	87
Gravitational Delay	89
Geometric Delay	90
Observations Close to the Sun	91
Summary	91
Propagation Correction for Laser Ranging	92
GLOSSARY	95

INTRODUCTION

This document is intended to define the standard reference system to be used by the International Earth Rotation Service (IERS). It is based on the Project MERIT Standards (Melbourne *et al.*, 1983) and the IERS Standards (McCarthy, 1989; McCarthy, 1992) with revisions being made to reflect improvements in models or constants since the IERS Standards were published. If contributors to IERS do not fully comply with these guidelines, they will carefully identify the exceptions. In these cases, the institution is obliged to provide an assessment of the effects of the departures from the conventions so that its results can be referred to the IERS Reference System. Contributors may use models equivalent to those specified herein. Different observing methods have varying sensitivity to the adopted standards and reference systems. No attempt has been made in this document to assess the sensitivity of each technique to the adopted reference systems and standards.

The recommended system of astronomical constants corresponds closely to those of the previous IERS Standards with the exception of the changes listed below. The units of length, mass, and time are in the International System of Units (SI) (*Le Système International d'Unités (SI)*, 1991) as expressed by the meter (m), kilogram (kg) and second (s). The astronomical unit of time is the day containing 86400 SI seconds. The Julian century contains 36525 days.

Differences Between This Document and IERS Technical Note 13

Most chapters of IERS Technical Note 13 have been revised, and known typographical errors contained in that work have been corrected in this edition. There are some major differences between the current work and the past IERS Standards. The following is a brief list of the major modifications by chapter.

CHAPTER 2 IERS Dynamical Reference Frame

The JPL DE 403 ephemeris (Standish *et al.*, 1995) replaces the DE 200 model of IERS Technical Note 13.

CHAPTER 3 IERS Terrestrial Reference System

The NUVEL NNR-1A Model (DeMets *et al.*, 1994) for plate motion has replaced the Nuvel NNR-1 Model of IERS Technical Note 13.

CHAPTER 4 Numerical Standards

Numerical values are now given only for the most fundamental constants along with their uncertainties and references. Constants which have been changed include the astronomical unit in seconds and meters, precession, obliquity, equatorial radius, flattening factor and dynamical form factor of the Earth, constant of gravitation, geocentric and heliocentric gravitational constant.

CHAPTER 5 Transformation Between Celestial and Terrestrial Reference Systems

An empirical model to be used to predict the difference in the celestial pole coordinates between those published by the IERS and those given by the IAU model is added.

CHAPTER 6 Geopotential

The JGM3 model replaces the GEM-T3. Love Numbers are revised.

CHAPTER 7 Local Site Displacements

The printed table of the components of site displacement due to ocean loading is no longer included. References to machine-readable files are given. Love Numbers are revised. Atmospheric loading and postglacial rebound are included.

CHAPTER 8 Tidal Variations in UT1

The subdaily and daily tidal variations in Earth orientation due to the effect of ocean tides has been added.

CHAPTER 12 General Relativistic Models for Propagation

The formulation has been modified to be consistent with IAU/IUGG resolutions.

Contributors

Z. Altamimi	S. R. Dickman	R. Langley	J. R. Ray
B. Archinal	R. Eanes	B. Luzum	R. Ray
E. F. Arias	T. M. Eubanks	C. Ma	J. Ries
S. Bettadpur	M. Feissel	P. M. Mathews	M. Rothacher
K. Borkowski	H. Fliegel	D. N. Matsakis	H.-G. Scherneck
C. Boucher	T. Fukushima	V. Mendes	B. E. Schutz
P. Brosche	J. Gipson	A. E. Niell	P. Schwintzer
M. Burša	R. Gross	R. Noomen	P. K. Seidelmann
N. Capitaine	E. Groten	T. Otsubo	E. M. Standish
M. S. Carter	T. A. Herring	S. Pagiatakis	J. A. Steppe
P. Cook	G. H. Kaplan	E. C. Pavlis	T. vanDam
V. Dehant	J. Kovalevsky	W. R. Peltier	J. Verheijen

Errata from Technical Note 13

- p. 9: GPS Block II $dz = 0.9519m$ vice $1.0229m$.
- p. 18: Table 3.1, first line, last value should be -0.0070 vice 0.0070 .
- p. 83: Hobart Q1 EW tangential phase should be 160.4 vice -160.4 .
- p. 89: Malibu M2 EW tangential phase should be -142.4 vice 142.4 .
- p. 98: Pearblossom M2 radial phase should be -24.14 vice 24.1 .
- p. 137: paragraph 3, read ... of the International **Astronomical** Union.
- p. 137: the formula reads

$$ds^2 = -c^2 d\tau^2$$
$$= -\left(1 - \frac{2U}{c^2}\right)(dx^0)^2 + \left(1 + \frac{2U}{c^2}\right)[(dx^1)^2 + (dx^2)^2 + (dx^3)^2].$$

(the minus sign was omitted in the second line)

p. 140, note 2: the formulae giving TCB-TCG read

$$TCB - TCG = c^{-2} \left[\int_{t_0}^t (v_e^2/2 + U_{ext}(x_e)) dt + v_e \cdot (x - x_e) \right].$$

$$TCB - TCG = L_C \times (JD - 2443144.5) \times 86400 + c^{-2} v_e \cdot (x - x_e) + P.$$

(the “.” in the vector product $v_e \cdot (x - x_e)$ was omitted)

References

- DeMets, C., Gordon, R. G., Argus, D. F., and Stein, S., 1994, “Effect of Recent Revisions to the Geomagnetic Reversal Time Scale on Estimates of Current Plate Motions,” *Geophys. Res. Lett.*, **21**, pp. 2191–2194.
- Fricke, W., 1982, “Determination of the Equinox and Equator of the FK5,” *Astron. Astrophys.*, **107**, pp. L13–16.
- Le Système International d’Unités (SI)*, 1991, Bureau International des Poids et Mesures, Sèvres, France.
- Melbourne, W., Anderle, R., Feissel, M., King, R., McCarthy, D., Smith, D., Tapley, B., Vicente, R., 1983, Project MERIT Standards, U.S. Naval Observatory Circular No. 167.
- McCarthy, D. D., 1989, IERS Standards, IERS Technical Note 3, Observatoire de Paris, Paris.
- McCarthy, D. D., 1992, IERS Standards, IERS Technical Note 13, Observatoire de Paris, Paris.
- Standish, E. M., Newhall, X X, Williams, J. G., and Folkner, W. F., 1995, “JPL Planetary and Lunar Ephemerides, DE 403/LE 403,” JPL IOM 314.10-127, to be submitted to *Astron. Astrophys.*

CHAPTER 1 CONVENTIONAL CELESTIAL REFERENCE SYSTEM

In 1991 the International Astronomical Union (IAU) decided that the IAU celestial reference system would be realized by a celestial reference frame defined by the precise coordinates of extragalactic radio sources. The related IAU recommendations (see McCarthy, 1992) specify that the origin is to be at the barycenter of the solar system and the directions of the axes are to be fixed with respect to the quasars. In compliance with this recommendation, the IERS Celestial Reference System (ICRS) is realized by the IERS Celestial Reference Frame (ICRF) defined by the J2000.0 equatorial coordinates of extragalactic objects determined from Very Long Baseline Interferometry (VLBI) observations. It is a frame whose directions are consistent with those of the FK5 (Fricke *et al.*, 1988). The origin is located at the barycenter of the solar system through appropriate modeling of observations in the framework of General Relativity (see Chapters 2 and 12). The rotational stability of the frame is based on the assumption that the sources have no proper motions. Checks are performed regularly to ensure the validity of this constraint (Ma and Shaffer, 1991; Eubanks *et al.*, 1994). The HIPPARCOS reference frame is planned to be linked astrometrically to the ICRF to unify the radio and optical coordinate systems at the level of $\pm 0''.0005$ in direction and $\pm 0''.0005/\text{year}$ in rotation (Lindgren and Kovalevsky, 1995). The ICRS is recommended for the IAU conventional celestial system by the IAU Working Group on Reference Frames under the name “International Celestial Reference System.” See Arias *et al.* (1995).

Equator

The IAU recommendations call for the principal plane of the conventional reference frame to be close to the mean equator at J2000.0. The VLBI observations which are used to establish the extragalactic reference frame also provide the monitoring of the motion of the celestial pole in the sky (precession and nutation). In this way, the VLBI analyses provide corrections to the conventional IAU models for precession and nutation (Lieske *et al.*, 1977; Seidelmann, 1982) and the accurate estimation of the shift of the mean pole at J2000.0 relative to its conventional one, to which the pole of the ICRS is attached. Based on the VLBI observations available in early 1995 and the IERS correction model for precession and nutation (see Chapters 4 and 5), one can estimate the shift of the pole at J2000.0 relative to the IERS celestial pole to be 17.3 ± 0.2 mas in the direction 12^{h} and 5.1 ± 0.2 mas in the direction 18^{h} .

On the other hand, the IAU recommendations stipulate that the direction of the new conventional celestial pole be consistent with that of the FK5. The uncertainty in the direction of the FK5 pole can be estimated by considering (1) that the systematic part is dominated by a correction of $-0''.25/\text{cy}$ to the precession constant imbedded in the FK5 System, and (2) by adopting Fricke’s (1982) estimation of the accuracy of the FK5 equator ($\pm 0''.02$), and Schwan’s (1988) estimation of the limit of the residual rotation ($\pm 0''.07/\text{cy}$), taking the epochs of observations from Fricke *et al.* (1988). Assuming that the error in the precession rate is absorbed by the proper motions of stars, the uncertainty in the FK5 pole position relative to the mean pole at J2000.0 estimated in this way is ± 50 mas. The IERS celestial pole is therefore consistent with that of the FK5 within the uncertainty of the latter.

Origin of Right Ascension

The IAU recommends that the origin of right ascensions of the new celestial reference system be close to the dynamical equinox at J2000.0. The x axis of the IERS celestial system was implicitly defined in the initial realization (Arias *et al.*, 1988) by adopting the mean right ascension of 23 radio

sources in a group of catalogs that were compiled by fixing the right ascension of 3C 273B to the usual (Hazard *et al.*, 1971) conventional FK5 value ($12^{\text{h}}29^{\text{m}}6^{\text{s}}6997$ at J2000.0) (Kaplan *et al.*, 1982).

The uncertainty in the FK5 origin of right ascensions can be derived from the quadratic sum of the accuracies given by Fricke (1982) and Schwan (1988), considering a mean epoch of 1955 for the proper motions in right ascension. The uncertainty thus obtained is ± 80 mas. Folkner *et al.* (1994), comparing VLBI and LLR Earth orientation and terrestrial frames and the estimated frame tie of planetary ephemerides, show that the mean equinox of J2000.0 is shifted from the right ascension origin of the IERS system by 78 ± 10 mas (direct rotation around the polar axis). This shows that the ICRS origin of right ascension complies with the IAU recommendations.

Precision and Accuracy

The estimation of coordinates performed by the Central Bureau of the IERS is based on individual frames contributed by the IERS Analysis Centers. Several extragalactic frames are produced each year by independent VLBI groups. Selected realizations are used to form the ICRF. The algorithm used for the compilation is designed primarily to maintain the three directions of axes fixed for successive realizations while the precision of coordinates of individual sources is improved. Successive realizations produced up to now have maintained the initial definition of the axes within $\pm 0''0001$.

The inaccuracy of the conventional IAU 1976 Precession and IAU 1980 Theory of Nutation would give rise to systematic errors in the source positions and to misorientation of the axes of the frames, both at the level of a few milliarcseconds, in the analysis of VLBI observations. Therefore, the usual practice in catalog work is to estimate additional parameters which describe the motion of the celestial pole relative to its conventional position (see Sovers, 1991). Another type of possible systematic error is related to low elevation observations in cases where the observing network has a modest north-south extension. This effect can be modelled as a linear dependence of declination errors on declination which can reach 0.01 mas per degree and create a tilt of the frame equator of up to 0.6 mas (Feissel *et al.*, 1995). However, for recent global analyses these systematic differences are at the level of 0.001 mas per degree and 0.1 mas respectively (IERS, 1995). No other type of systematic differences can be found above this level in the present-day VLBI celestial reference frames (Feissel *et al.*, 1995, Eubanks *et al.*, 1994). After taking into account the small systematic errors mentioned above, the precision of the source coordinates is a white noise function of the number of observations, with a typical value of ± 0.2 mas for 100 observations (Arias *et al.*, 1995).

Availability of the Frame

The catalog of source coordinates published in the 1994 IERS Annual Report (July 1995) provides access to the ICRS. It includes a total of 608 objects, among which 236 with good observational histories attach the frame to the ICRS. In the future, based on new observations and new analyses, the stability of the source coordinates will be monitored, and the appropriate warnings and updates will appear in IERS publications.

The direct access to the quasars is most precise through VLBI observations, a technique which is not widely available to users. Therefore, while VLBI is used for the maintenance of the frame, the tie of the ICRF to the major practical reference frames may be obtained through use of the IERS Terrestrial Reference Frame (ITRF, see Chapter 3), the HIPPARCOS Galactic Reference Frame, and the JPL ephemerides of the solar system (see Chapter 2).

The principles on which the ITRF is established and maintained are described in Chapter 3. The IERS Earth orientation parameters provide the permanent tie of the ICRF to the ITRF. They describe the orientation of the Celestial Ephemeris Pole in the terrestrial system and in the celestial system (polar coordinates x, y ; nutation offsets $d\psi, d\epsilon$) and the orientation of the Earth around this axis (UT1-TAI), as a function of time. This tie is available daily with an accuracy of ± 0.5 mas in the IERS publications.

The other ties to major celestial frames are established by differential VLBI observations of solar system probes, galactic stars relative to quasars and other ground- or space-based astrometry projects. The tie of the solar system ephemerides of the Jet Propulsion Laboratory (JPL) is described by Standish *et al.* (1995). Its estimated precision is ± 3 mas, according to Folkner *et al.* (1994). The tie of the galactic frame to ICRS is a part of the HIPPARCOS project. It is described in some detail by Lindegren and Kovalevsky (1995). Its expected accuracy is ± 0.5 mas at the HIPPARCOS mean epoch of observation (1991.25) and ± 0.5 mas/year for the time evolution.

References

- Arias E. F., Charlot P., Feissel M., Lestrade J.-F., 1995, “The Extragalactic Reference System of the International Earth Rotation Service, ICRS,” *Astron. Astrophys.*, **303**, pp. 604–608.
- Arias, E. F., Feissel, M., and Lestrade, J.-F., 1988, “An Extragalactic Celestial Reference Frame Consistent with the BIH Terrestrial System (1987),” *BIH Annual Rep. for 1987*, pp. D-113–D-121.
- Eubanks, T. M., Matsakis, D. N., Josties, F. J., Archinal, B. A., Kingham, K. A., Martin, J. O., McCarthy, D. D., Klioner, S. A., Herring, T. A., 1994, “Secular motions of extragalactic radio sources and the stability of the radio reference frame,” *Proc. IAU Symposium 166*, J. Kovalevsky (ed.).
- Feissel, M., Ma, C., Sovers, O., and Jacobs, C., 1995, “Sub-milliarcsecond VLBI celestial frames: problem areas,” (unpublished contribution).
- Folkner, W. M., Charlot, P., Finger, M. H., Williams, J. G., Sovers, O. J., Newhall, X X, and Standish, E. M., 1994, “Determination of the extragalactic-planetary frame tie from joint analysis of radio interferometric and lunar laser ranging measurements,” *Astron. Astrophys.*, **287**, pp. 279–289.
- Fricke, W., 1982, “Determination of the Equinox and Equator of the FK5,” *Astron. Astrophys.*, **107**, p. L13–16.
- Fricke, W., Schwan, H., and Lederle, T., 1988, *Fifth Fundamental Catalogue, Part I. Veroff. Astron. Rechen Inst.*, Heidelberg.
- Hazard, C., Sutton, J., Argue, A. N., Kenworthy, C. N., Morrison, L. V., and Murray, C. A., 1971, “Accurate radio and optical positions of 3C273B,” *Nature Phys. Sci.*, **233**, p. 89.
- IERS, 1995, 1994 International Earth Rotation Service Annual Report, Observatoire de Paris, Paris.
- Kaplan, G. H., Josties, F. J., Angerhofer, P. E., Johnston, K. J., and Spencer, J. H., 1982, “Precise Radio Source Positions from Interferometric Observations,” *Astron. J.*, **87**, pp. 570–576.

- Lieske, J. H., Lederle, T., Fricke, W., and Morando, B., 1977, "Expression for the Precession Quantities Based upon the IAU (1976) System of Astronomical Constants," *Astron. Astrophys.*, **58**, pp. 1–16.
- Lindgren, L. and Kovalevsky, J., 1995, "Linking the Hipparcos catalogue to the extragalactic reference frame," *Astron. Astrophys.*, **304**, pp. 189–201.
- Ma, C. and Shaffer, D. B., 1991, "Stability of the extragalactic reference frame realized by VLBI," in *Reference Systems*, J. A. Hughes, C. A. Smith, and G. H. Kaplan (eds), U. S. Naval Observatory, Washington, pp. 135–144.
- McCarthy D.D. (ed.), 1992, "IERS Standards," *IERS Technical Note 13*, Observatoire de Paris, Paris.
- Schwan, H., 1988, "Precession and galactic rotation in the system of FK5," *Astron. Astrophys.*, **198**, pp. 116–124.
- Seidelmann, P. K., 1982, "1980 IAU Nutation: The Final Report of the IAU Working Group on Nutation," *Celest. Mech.*, **27**, pp. 79–106.
- Sovers, O. J., 1991, "Consistency of Nutation Modeling in Radio Source Position Comparisons," in *Reference Systems*, J. A. Hughes, C. A. Smith, and G. H. Kaplan (eds), U. S. Naval Observatory, Washington, pp. 130–134.
- Standish, E. M., Newhall, X X, Williams, J. G., and Folkner, W. F., 1995, "JPL Planetary and Lunar Ephemerides, DE403/LE403," JPL IOM 314.10-127, to be submitted to *Astron. Astrophys.*

CHAPTER 2 CONVENTIONAL DYNAMICAL REFERENCE FRAME

The planetary and lunar ephemerides recommended for the IERS standards are the JPL Development Ephemeris DE403 and the Lunar Ephemeris LE403 (Standish *et al.*, 1995). The reference frame of these new ephemerides is that of ICRF. The ephemerides have been adjusted to all relevant observational data, including recent observations taken with respect to the IERS frame. It is expected that DE403/LE403 will eventually replace DE200/LE200 (Standish, 1990) as the basis for the international almanacs.

Table 2.1 shows the IAU 1976 values of the planetary masses and the values used in the creation of both DE200/LE200 and of DE403/LE403. Also shown in the table are references for the DE403 set, the current best estimates.

Also associated with the ephemerides is the set of astronomical constants used in the ephemeris creation; these are listed in Table 2.2.

The constants which are provided directly with the ephemerides should be considered to be an integral part of them; they will sometimes differ from a more standard set, but the differences are necessary for the optimal fitting of the data.

Availability of DE403

Sections of DE403 are now available from the anonymous ftp site: “navigator.jpl.nasa.gov” [128.149.23.82]. For a “navio” version (in-house JPL format), the following “navio” and “nioftp” versions are available, covering 1980-2010:

“navigator:/ephem/navio/de403s” and “navigator:/ephem/navio/de403s.ftp”

For other time-spans, contact F A McCreary (faith@viviane.jpl) or E M Standish (ems@smyles.jpl). An outside user is advised to first get and read the file, “navigator:/ephem/export/READ.ME”; it should answer most questions about retrieving and using the JPL ephemerides.

Table 2.1. 1976 IAU, DE200 and DE403 planetary mass values, expressed in reciprocal solar masses.

Planet	1976 IAU	DE200	DE403	Reference for DE403 value
Mercury	6023600.	6023600.	6023600.	Anderson <i>et al.</i> , 1987
Venus	408523.5	408523.5	408523.71	Sjogren <i>et al.</i> , 1990
Earth & Moon	328900.5	328900.55	328900.560392...	Williams <i>et al.</i> , 1995
Mars	3098710.	3098710.	3098708.	Null, 1969
Jupiter	1047.355	1047.350	1047.3486	Campbell and Synott, 1985
Saturn	3498.5	3498.0	3497.898	Campbell and Anderson, 1989
Uranus	22869.	22960.	22902.98	Jacobson <i>et al.</i> , 1992
Neptune	19314.	19314.	19412.24	Jacobson <i>et al.</i> , 1991
Pluto	3000000.	130000000.	135200000.	Tholen and Buie, 1996

Table 2.2. Auxiliary constants from the JPL Planetary and Lunar Ephemerides DE403/LE403.

Scale (km/au)	149597870.691
Scale (secs/au)	499.0047838061...
Speed of light (km/sec)	299792.458
Obliquity of the ecliptic	23°26'21".412
Earth-Moon mass ratio	81.300585
GM_{Ceres}	$4.64 \times 10^{-10} GM_{Sun}$
GM_{Pallas}	$1.05 \times 10^{-10} GM_{Sun}$
GM_{Vesta}	$1.34 \times 10^{-10} GM_{Sun}$
density _{classC}	1.80
density _{classS}	2.40
density _{classM}	5.00

References

- Anderson, J. D., Colombo, G., Esposito, P. B., Lau, E. L., and Trager, G. B., 1987, “The Mass Gravity Field and Ephemeris of Mercury,” *Icarus*, **71**, pp. 337–349.
- Campbell, J. K. and Anderson, J. D., 1989, “Gravity Field of the Saturnian System from Pioneer and Voyager Tracking Data,” *Astron. J.*, **97**, pp. 1485–1495.
- Campbell, J. K. and Synott, S. P., 1985, “Gravity Field of the Jovian System from Pioneer and Voyager Tracking Data,” *Astron. J.*, **90**, pp. 364–372.
- Jacobson, R. A., Riedel, J. E. and Taylor, A. H., 1991, “The Orbits of Triton and Nereid from Spacecraft and Earth-based Observations”, *Astron. Astrophys.*, **247**, pp. 565–575.
- Jacobson, R. A., Campbell, J. K., Taylor, A. H. and Synnott, S. P., 1992, “The Masses of Uranus and its Major Satellites from Voyager Tracking Data and Earth-based Uranian Satellite Data”, *Astron J.*, **103**(6), pp. 2068–2078.
- Null, G. W., 1969, “A Solution for the Mass and Dynamical Oblateness of Mars Using Mariner-IV Doppler Data,” *Bull. American Astron. Soc.*, **1**, p. 356.
- Sjogren, W. L., Trager, G. B., and Roldan G. R., 1990, “Venus: A Total Mass Estimate,” *Geophys. Res. Let.*, **17**, pp. 1485–1488.
- Standish, E. M., 1990, “The Observational Basis for JPL’s DE200, the Planetary Ephemerides of the Astronomical Almanac,” *Astron. Astrophys.*, **233**, pp. 252–271.
- Standish, E. M., Newhall, X X, Williams, J. G. and Folkner, W. F., 1995, “JPL Planetary and Lunar Ephemerides, DE403/LE403,” JPL IOM 314.10-127, to be submitted to *Astron. Astrophys.*
- Tholen, D. J. and Buie, M. W., 1996, “The Orbit of Charon. I. New Hubble Space Telescope Observations”, submitted to *Icarus*.
- Williams, J. G., Newhall, X X, and Standish, E. M., 1995, (result from least squares adjustment of DE403/LE403).

CHAPTER 3 CONVENTIONAL TERRESTRIAL REFERENCE SYSTEM

Definition

The Terrestrial Reference System adopted for either the analysis of individual data sets by techniques (VLBI, SLR, LLR, GPS, DORIS, PRARE...) or the combination of individual solutions into a unified set of data (station coordinates, Earth orientation parameters, etc...) follows these criteria (Boucher, 1990):

- a) It is geocentric, the center of mass being defined for the whole Earth, including oceans and atmosphere.
- b) Its scale is that of a local Earth frame, in the meaning of a relativistic theory of gravitation.
- c) Its orientation was initially given by the BIH orientation at 1984.0.
- d) Its time evolution in orientation will create no residual global rotation with regards to the crust.

Realization

A Conventional Terrestrial Reference System (CTRS) can be realized through a reference frame *i.e.* a set of coordinates for a network of stations. Such a realization will be specified by cartesian equatorial coordinates X , Y , and Z , by preference. If geographical coordinates are needed, the GRS80 ellipsoid is recommended ($a=6378137.0$ m, $e^2=0.00669438003$). The CTRS which is monitored by IERS is called the International Terrestrial Reference System (ITRS) and is specified by the IUGG Resolution no. 2 adopted at the 20th IUGG General Assembly of Vienna in 1991.

Each analysis center should compare its reference frame to a realization of the ITRS. Within IERS, each Terrestrial Reference Frame (TRF) is either directly, or after transformation, expressed as a realization of the ITRS. The position of a point located on the surface of the solid Earth should be expressed by

$$\vec{X}(t) = \vec{X}_0 + \vec{V}_0(t - t_0) + \sum_i \Delta \vec{X}_i(t),$$

where $\Delta \vec{X}_i$ are corrections due to various time changing effects, and \vec{X}_0 and \vec{V}_0 are position and velocity at the epoch t_0 . The corrections to be considered are solid Earth tide displacement (full correction including permanent effect, see Chapter 7), ocean loading, post glacial rebound, and atmospheric loading. Further corrections could be added if they are at mm level or greater, and can be computed by a suitable model.

Realizations of the ITRS are produced by IERS under the name International Terrestrial Reference Frames (ITRF), which consist of lists of coordinates (and velocities) for a selection of IERS sites (tracking stations or related ground markers). Currently, ITRF-yy is published annually by the IERS in the *Technical Notes* (*cf.* Boucher *et al.*, 1996). The numbers (yy) following the designation "ITRF" specify the last year whose data were used in the formation of the frame. Hence ITRF94 designates the frame of coordinates and velocities constructed in 1995 using all of the IERS data available through 1994. More recently, since 1993, other special realizations have been produced, such as solutions for IGS core stations (ITRF-Py series) (IGS, 1995). It is also anticipated that monthly series may be determined.

Terrestrial reference frames may be defined within systems which account for the effect of the permanent tide differently. In the terminology of Ekman (1989), Rapp (1991) and Poutanen *et al.* (1996) the permanent or “zero–frequency” tide is retained in the “zero–tide” system. In this system the crust corresponds to the realistic time average of the crust which varies because of the action of the luni–solar tides. In a different system referred to as “tide–free,” all of the effects of the permanent tide are removed. This is not realistic since the crust in this case cannot be “observed,” nor are the Love Numbers required to describe the permanent tide known adequately. No error is associated with either convention as long as it is clear which system is employed in the analysis of the data. A third “mean–tide” system has been defined in which the crust is equivalent to that of the tide–free system and, in which, the effect of the permanent tide is also removed from the geoid.

Coordinates of the ITRF are given in a conventional frame where the effects of all tides are removed as recommended in IERS Technical Note 13 (McCarthy, 1992). There, it is recommended that equation 6 on p. 57 be used to account for the permanent tide. Note that this is in contradiction to Resolution 16 of the General Assembly of the IAG in 1983. The corresponding equation in this publication is equation 8 of Chapter 7. To place the coordinates in a zero-tide system it is necessary to apply equation 8 of IERS Technical Note 13 (McCarthy, 1992) or the corresponding version, equation 17 of Chapter 7 in this publication.

In data analysis, \vec{X}_0 and \vec{V}_0 should be considered as solve-for parameters. In particular, if a non-linear change occurs (earthquake, volcanic event ...), a new \vec{X}_0 should be adopted. When adjusting parameters, particularly velocities, the IERS orientation should be kept at all epochs, ensuring the alignment at a reference epoch and the time evolution through a no net rotation condition. The way followed by various analysis centers depends on their own view of modelling, and on the techniques themselves. For the origin, only data which can be modelled by dynamical techniques (currently SLR, LLR, GPS or DORIS for IERS) can determine the center of mass. The VLBI system can be referred to a geocentric system by adopting for a station its geocentric position at a reference epoch as provided from external information.

The scale is obtained by appropriate relativistic modelling. Specifically, according to IAU and IUGG resolutions, the scale is consistent with the TCG time coordinate for a geocentric local frame. A detailed treatment can be found in Chapter 11. The orientation is defined by adopting IERS (or BIH) Earth orientation parameters at a reference epoch. In the case of dynamical techniques, an additional constraint in longitude is necessary to remove ill-conditioning.

The unit of length is the meter (SI). The IERS Reference Pole (IRP) and Reference Meridian (IRM) are consistent with the corresponding directions in the BIH Terrestrial System (BTS) within $\pm 0''005$. The BIH reference pole was adjusted to the Conventional International Origin (CIO) in 1967; it was then kept stable independently until 1987. The uncertainty of the tie of the IRP with the CIO is $\pm 0''03$. The time evolution of the orientation will be ensured by using a no-net-rotation condition with regards to horizontal tectonic motions over the whole Earth.

Transformation Parameters to World Coordinate Systems and Various Datums

The seven-parameter similarity transformation between any two Cartesian systems, *e.g.*, from (x, y, z) to (xs, ys, zs) can be written as

$$\begin{pmatrix} xs \\ ys \\ zs \end{pmatrix} = \begin{pmatrix} x \\ y \\ z \end{pmatrix} + \begin{pmatrix} T1 \\ T2 \\ T3 \end{pmatrix} + \begin{pmatrix} D & -R3 & R2 \\ R3 & D & -R1 \\ -R2 & R1 & D \end{pmatrix} \begin{pmatrix} x \\ y \\ z \end{pmatrix}, \quad (1)$$

where $T1, T2, T3$ = coordinates of the origin of the frame (x_s, y_s, z_s) in the frame (x, y, z) ; $R1, R2, R3$ = differential rotations (expressed in radians) respectively, around the axes (x_s, y_s, z_s) to establish parallelism with the (x, y, z) frame; and D = differential scale change.

The use of the previous algorithm to transform coordinates from one datum to another must be done with care. At some level of accuracy, each reference system has multiple realizations. In many cases, two such realizations of the same system have nonzero transformation parameters. The usual reason is that such parameters are currently adjusted between two sets of coordinates. In this case, any global systematic error which can be mapped into a scale, shift or rotation will go into these seven parameters.

Therefore we give here (Table 3.1) only parameters from ITRF94 to previous ITRF series. These numbers are the responsibility of the IERS. For other transformations, either to global systems (such as WGS84) or regional (such as NAD83 or ETRS89), or even local systems, users should contact relevant agencies. For WGS84, the main result is that the most recent realizations of WGS84 based on GPS are consistent with the ITRF realization at the 0.1 meter level (Malys and Slater, 1994). Otherwise, one can refer to IAG bodies, such as Commission X on Global and Regional Geodetic Networks (Geodesist's Handbook, 1996).

Table 3.1. Transformation parameters from ITRF94 to past ITRFs. "ppb" refers to parts per billion (10^9). Rates must be applied for ITRF93. The units for rate are understood to be "per year."

Coordinate System (datum)	T1 (cm)	T2 (cm)	T3 (cm)	D (ppb)	R1 (mas)	R2 (mas)	R3 (mas)	Epoch
ITRF88	1.8	0.0	-9.2	7.4	0.1	0.0	0.0	1988.0
ITRF89	2.3	3.6	-6.8	4.3	0.0	0.0	0.0	1988.0
ITRF90	1.8	1.2	-3.0	0.9	0.0	0.0	0.0	1988.0
ITRF91	2.0	1.6	-1.4	0.6	0.0	0.0	0.0	1988.0
ITRF92	0.8	0.2	-0.8	-0.8	0.0	0.0	0.0	1988.0
ITRF93	0.6	-0.5	-1.5	0.4	-0.39	0.80	-0.96	1988.0
rates	-0.29	0.04	0.08	0.00	-0.11	-0.19	0.05	

Once the Cartesian coordinates (x, y, z) are known, they can be transformed to "datum" or curvilinear geodetic coordinates (λ, ϕ, h) referred to an ellipsoid of semi-major axis a and flattening f , using the following code (Borkowski, 1989). First compute $\lambda = \tan^{-1}(\frac{y}{x})$ properly determining the quadrant from x and y ($0 \leq \lambda < 2\pi$) and $r = \sqrt{x^2 + y^2}$.

```

subroutine GEOD(r,z,fi,h)
c Program to transform Cartesian to geodetic coordinates
c based on the exact solution (Borkowski,1989)
c Input : r, z = equatorial [m] and polar [m] components
c Output: fi, h = geodetic coord's (latitude [rad], height [m])
      implicit real*8(a-h,o-z)
c GRS80 ellipsoid: semimajor axis (a) and inverse flattening (fr)
      data a,fr /6378137.d0,298.257222101d0/
      b = dsign(a - a/fr,z)
      E = ((z + b)*b/a - a)/r
      F = ((z - b)*b/a + a)/r

```

```

c Find solution to: t**4 + 2*E*t**3 + 2*F*t - 1 = 0
  P = (E*F + 1.)*4.d0/3.d0
  Q = (E*E - F*F)*2.d0
  D = P*P*P + Q*Q
    if(D.ge.0d0) then
  s = dsqrt(D) + Q
  s = dsign(dexp(dlog(dabs(s))/3.d0),s)
  v = P/s - s
c Improve the accuracy of numeric values of v
  v = -(Q + Q + v*v*v)/(3.d0*P)
    else
  v = 2.d0*dsqrt(-P)*dcos(dacos(Q/P/dsqrt(-P))/3.d0)
    endif
  G = .5d0*(E + dsqrt(E*E + v))
  t = dsqrt(G*G + (F - v*G)/(G + G - E)) - G
  fi = datan((1.d0 - t*t)*a/(2.d0*b*t))
  h = (r - a*t)*dcos(fi) + (z - b)*dsin(fi)
  return
end

```

Plate Motion Model

One of the factors which affect Earth rotation results is the motion of the tectonic plates which make up the Earth's surface. As the plates move, fixed coordinates for the observing stations become inconsistent with each other. The rates of relative motions for some observing sites are 5 cm per year or larger. The observations of plate motions by modern methods appear to be roughly consistent with the average rates over the last few million years derived from the geological record and other geophysical information. Thus, the NNR-NUVEL1A model for plate motions given by DeMets *et al.* (1994) is recommended.

If a velocity has not yet been determined in the ITRF for a particular station, the velocity \vec{V}_0 should be expressed as

$$\vec{V}_0 = \vec{V}_{plate} + \vec{V}_r$$

where \vec{V}_{plate} is the horizontal velocity computed from the NNR-NUVEL1A model (DeMets *et al.*, 1994) and \vec{V}_r a residual velocity.

The Cartesian rotation vector for each of the major plates is given in Table 3.2. A subroutine called ABSMO_NUVEL is also included below. It computes the new site position from the old site position using the recommended plate motion model. Fig. 3.1 shows the plates on a map of the world.

Figure 3.1. Map of the tectonic plates.

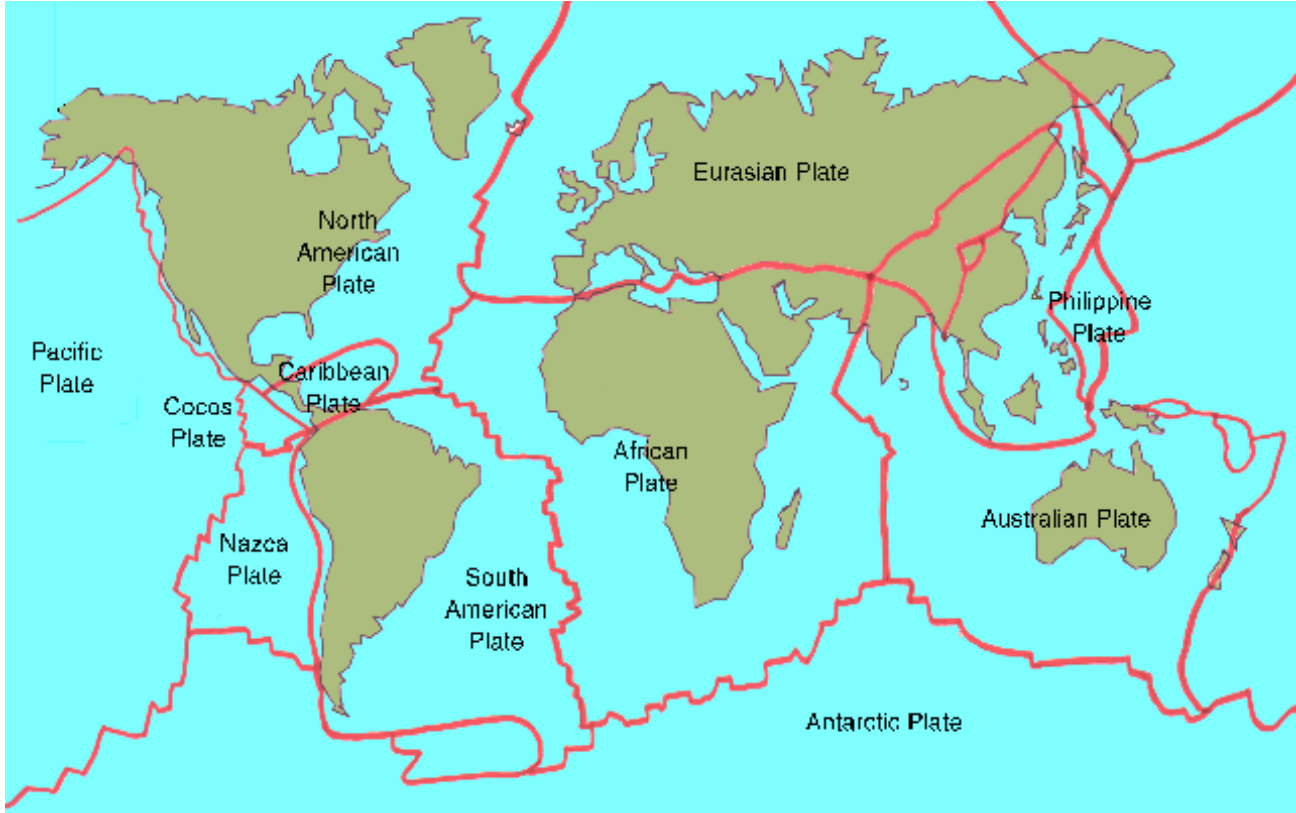


Table 3.2. Cartesian rotation vector for each plate using the NNR-NUVEL1A kinematic plate model (no net rotation).

Plate Name	Ω_x rad/My.	Ω_y rad/My.	Ω_z rad/My.
Pacific	-0.001510	0.004840	-0.009970
Cocos	-0.010425	-0.021605	0.010925
Nazca	-0.001532	-0.008577	0.009609
Caribbean	-0.000178	-0.003385	0.001581
South America	-0.001038	-0.001515	-0.000870
Antarctica	-0.000821	-0.001701	0.003706
India	0.006670	0.000040	0.006790
Australia	0.007839	0.005124	0.006282
Africa	0.000891	-0.003099	0.003922
Arabia	0.006685	-0.000521	0.006760
Eurasia	-0.000981	-0.002395	0.003153
North America	0.000258	-0.003599	-0.000153
Juan de Fuca	0.005200	0.008610	-0.005820
Philippine	0.010090	-0.007160	-0.009670
Rivera	-0.009390	-0.030960	0.012050
Scotia	-0.000410	-0.002660	-0.001270

The NNR-NUVEL1A model should be used as a default, for stations which appear to follow

reasonably its values. For some stations, particularly in the vicinity of plate boundaries, users may benefit by estimating velocities or using specific values not derived from NNR-NUVEL1A. This is also a way to take into account now some non-negligible vertical motions. Published station coordinates should include the epoch associated with the coordinates.

The original subroutine was a coding of the AM0-2 model from J. B. Minster. Changes have been made to represent NNR-NUVEL1A model (DeMets *et al.*, 1994).

```

      SUBROUTINE ABSMO_NUVEL(PSIT,T0,X0,Y0,Z0,T,X,Y,Z)
C
C  ABSMO_NUVEL takes a site specified by its initial coordinates
C  X0,Y0,Z0 at time T0, and computes its updated positions X,Y,Z
C  at time T, based on the geological "absolute".
C
C
C
C  Original author:  J.B. Minster, Science Horizons.
C  DFA: Revised by Don Argus, Northwestern University
C  DFA: uses absolute model NNR-NUVEL1
C
C  Transcribed from USNO Circular 167 "Project Merit Standards"
C  by Tony Mallama with slight modification to the documentation
C  and code.
C
C  Times are given in years, e.g. 1988.0 for Jan 1, 1988.
C
C  PSIT is the four character abbreviation for the plate name,
C  if PSIT is not recognized then the new positions are returned
C  as zero.
C
      IMPLICIT NONE
      CHARACTER*4 PSIT,PNM(16)
      REAL*8  OMX(16),OMY(16),OMZ(16)
      REAL*8  X0,Y0,Z0
      REAL*8  X,Y,Z,T,TO
      INTEGER*2 IPSIT,I
C
C  DFA: NNR-NUVEL1A
C
      DATA (PNM(I), OMX(I), OMY(I), OMZ(I),
& I = 1,16)
& /'PCFC', -0.001510, 0.004840, -0.009970,
& 'AFRC', 0.000891, -0.003099, 0.003922,
& 'ANTA', -0.000821, -0.001701, 0.003706,
& 'ARAB', 0.006685, -0.000521, 0.006760,
& 'AUST', 0.007839, 0.005124, 0.006282,
& 'CARB', -0.000178, -0.003385, 0.001581,
& 'COCO', -0.010425, -0.021605, 0.010925,
& 'EURA', -0.000981, -0.002395, 0.003153,

```

```

& 'INDI', 0.006670, 0.000040, 0.006790,
& 'NAZC', -0.001532, -0.008577, 0.009609,
& 'NOAM', 0.000258, -0.003599, -0.000153,
& 'SOAM', -0.001038, -0.001515, -0.000870,
& 'JUFU', 0.005200, 0.008610, -0.005820,
& 'PHIL', 0.010090, -0.007160, -0.009670,
& 'RIVR', -0.009390, -0.030960, -0.012050,
& 'SCOT', -0.000410, -0.002660, -0.001270/
C
C
C Initialize things properly
C
      IPSIT = -1
      X = 0.0D0
      Y = 0.0D0
      Z = 0.0D0
C
C Look up the plate in the list.
C
      DO 20 I = 1,16
      20 IF (PSIT .EQ. PNM(I)) IPSIT = I
C
C If plate name is not recognized return the new plate position
C as zero.
C
      IF (IPSIT .EQ. -1) RETURN
C
C Compute the new coordinates
C
      X = XO + (ORY*ZO - ORZ*YO) * (T-T0)/1.0D+6
      Y = YO + (ORZ*XO - ORX*ZO) * (T-T0)/1.0D+6
      Z = ZO + (ORX*YO - ORY*XO) * (T-T0)/1.0D+6
C
C Finish up
C
      RETURN
      END

```

References

- Borkowski, K. M., 1989, "Accurate Algorithms to Transform Geocentric to Geodetic Coordinates," *Bull. Geod.*, **63**, pp. 50–56.
- Boucher, C., 1990, "Definition and Realization of Terrestrial Reference Systems for Monitoring Earth Rotation," *Variations in Earth Rotation*, D. D. McCarthy and W. E. Carter (eds), pp. 197–201.
- Boucher, C., Altamimi, Z., Feissel, M., and Sillard, P., 1996, *Results and Analysis of the ITRF94*, IERS Technical Note 20, Observatoire de Paris, Paris.

- DeMets, C., Gordon, R. G., Argus, D. F., and Stein, S., 1994, "Effect of recent revisions to the geomagnetic reversal time scale on estimates of current plate motions," *Geophys. Res. Let.*, **21**, pp. 2191–2194.
- Ekman, M., 1989, "Impacts of Geodetic Phenomena on Systems for Height and Gravity," *Bull. Geod.*, **63**, pp. 281–296.
- Geodesist's Handbook*, 1996, International Association of Geodesy, in press.
- IGS, 1995, International GPS Service for Geodynamics 1994 Annual Report. IGS Central Bureau, JPL, Pasadena.
- Malys, S. and Slater, J. A., 1994, "Maintenance and enhancement of the World Geodetic System 1984," ION GPS 94, Salt Lake City, Utah.
- Poutanen, M., Vermeer, M., and Mekinen, J., 1996, "The Permanent Tide in GPS Positioning," *J. of Geod.*, **70**, pp. 499–504.
- Rapp, R. H., 1989, "The treatment of permanent tidal effects in the analysis of satellite altimeter data for sea surface topography," *Man. Geod.*, **14**, pp. 368–372.
- Soler, T. and Hothem, L. D., 1989, "Important Parameters Used in Geodetic Transformations," *J. Surv. Engrg.*, **115**, pp. 414–417.

CHAPTER 4 NUMERICAL STANDARDS

Table 4.1 listing numerical standards is organized into 5 columns: item, value, uncertainty, reference, comment. All values are given in terms of SI units (*Le Système International d'Unités (SI)*, 1991). The SI second, the basic unit of the TT time scale, is specifically assumed. If the TDB time scale is used, new units of time, t_{TDB} , and length, ℓ_{TDB} , are implicitly defined by the expressions (Seidelmann and Fukushima, 1992)

$$t_{TDB} = t/(1 - L_B), \text{ and}$$
$$\ell_{TDB} = \ell/(1 - L_B),$$

where t and ℓ are the SI units and L_B is a derived constant given in Table 4.1. Chapter 11 provides further details on the transformations between time scales.

The 1976 IAU System of Astronomical Constants (*Astronomical Almanac for the Year 1984*) is adopted for all astronomical constants which do not appear in Table 4.1.

References

Astronomical Almanac for the Year 1984, U.S. Government Printing Office, Washington, DC.

- [1] Burša, M., 1995, Report of the I.A.G. Special Commission SC3, Fundamental Constants, XXI, I.A.G. General Assembly.
- [2] Cohen, E. R. and Taylor, B. N., 1973, *J. Phys. Chem. Ref. Data*, **2**, p. 663.
- [3] Cohen, E. R. and Taylor, B. N., 1986, “The 1986 Adjustment of the Fundamental Physical Constants,” CODATA Bulletin, Bureau International des Poids et Mesures.
- [4] Fukushima, T., 1994, “Time Ephemeris,” *Astron. Astrophys.*, **294**, pp. 895–906.
- [5] Herring, T., 1996, “KSV-1 Precession/Nutation,” personal communication.

Le Système International d'Unités (SI), 1991, Bureau International des Poids et Mesures, Sèvres, France.

Seidelmann, P. K. and Fukushima, T., 1992, “Why New Time Scales?” *Astron. Astrophys.*, **265**, pp. 833–838.

- [6] Standish, E. M., 1994, Report of the IAU WGAS Sub-group on Numerical Standards.
- [7] Standish, E. M., Newhall, X X, Williams, J. G., and Folkner, W. F., 1995 “JPL Planetary and Lunar Ephemerides, DE403/LE403,” JPL IOM 314.10–127 to be submitted to *Astron. Astrophys.*

Table 4.1. IERS Numerical Standards.

ITEM	VALUE	UNCERTAINTY	REF.	COMMENTS
c	$299792458ms^{-1}$	Defining	[2]	Speed of light
L_B	$1.550519748 \times 10^{-8}$	4×10^{-17}	[4]	Average value of $d(\text{TCB})/d(\text{TT})-1$
L_C	$1.4808268457 \times 10^{-8}$	1×10^{-17}	[4]	Average value of $d(\text{TCB})/d(\text{TCG})-1$
L_G	$6.9692903 \times 10^{-10}$	1×10^{-17}	[4]	Average value of $d(\text{TCG})/d(\text{TT})-1$
W_0	$62636856.85m^2s^{-2}$	$1.0m^2s^{-2}$	[1]	Potential of the geoid
τ_A	$499.0047838061s$	$0.00000002s$	[7]	Astronomical unit in seconds
$c\tau_A$	$149597870691m$	$30m$	[7]	Astronomical unit in meters
P	$5029^{\circ}0965/century$	$0^{\circ}3/century$	[5]	General precession in longitude at J2000.0
ϵ_0	$84381^{\circ}412$	$0^{\circ}005$	[7]	Obliquity of the ecliptic at J2000.0
a_E	$6378136.49m$	$0.10m$	[1]	Equatorial radius of the Earth
$1/f$	298.25645	0.00001	[1]	Flattening factor of the Earth
$J_{2\oplus}$	1.0826359×10^{-3}	1.0×10^{-10}	[1]	Dynamical form-factor of the Earth
G	$6.67259 \times 10^{-11}m^3kg^{-1}s^{-2}$	$8.54 \times 10^{-15}m^3kg^{-1}s^{-2}$	[3]	Constant of gravitation
GM_{\oplus}	$3.986004418 \times 10^{14}m^3s^{-2}$	$8 \times 10^5m^3s^{-2}$	[1]	Geocentric gravitational constant
μ	0.0123000345	5×10^{-10}	[7]	Moon-Earth mass ratio
ω	$7.292115 \times 10^{-5}rads^{-1}$	variable	[1]	Nominal mean angular velocity of the Earth
GM_{\odot}	$1.327124 \times 10^{20}m^3s^{-2}$		[6]	Heliocentric gravitational constant
g_e	$9.780327ms^{-2}$	$1 \times 10^{-6}ms^{-2}$	[1]	Mean equatorial gravity
$R_0 = GM_{\oplus}/W_0$	$6363672.461m$	$0.1m$	[1]	Geopotential scale factor

Some geodetic parameters are affected by tidal variations (see Chapter 3). The values given in Table 4.1 are in the zero-tide system so that they correspond to a realistic time-averaged crust. This is done to be consistent with XVIII IAG General Assembly Resolution 16.

CHAPTER 5 TRANSFORMATION BETWEEN THE CELESTIAL AND TERRESTRIAL SYSTEMS

The coordinate transformation to be used from the TRS to the CRS at the date t of the observation can be written as:

$$[\text{CRS}] = PN(t)R(t)W(t) [\text{TRS}],$$

where $PN(t)$, $R(t)$ and $W(t)$ are the transformation matrices arising from the motion of the Celestial Ephemeris Pole (CEP) in the CRS, from the rotation of the Earth around the axis of the CEP, and from polar motion respectively.

Two equivalent options can be used. These two options have been shown to be consistent within ± 0.05 milliseconds of arc (mas) both theoretically (Capitaine, 1990) and numerically using existing astrometric data (Capitaine and Chollet, 1991) or simulated data over two centuries (Capitaine and Gontier, 1991).

Option 1, corresponding to the classical procedure, makes use of the equinox for realizing the intermediate reference frame of date t . It uses apparent Greenwich Sidereal Time in the transformation matrix $R(t)$ and the classical precession and nutation parameters in the transformation matrix $PN(t)$,

Option 2 makes use of the Conventional Ephemeris Origin (CEO) originally referred to as the nonrotating origin (Guinot, 1979) to realize the intermediate reference frame of date t : it uses the stellar angle (from the origin in the TRS to the CEO in the CRS) in the transformation matrix $R(t)$ and the two coordinates of the Celestial Ephemeris Pole in the CRS (Capitaine, 1990) in the transformation matrix $PN(t)$. This leads to very simple expressions of the partial derivatives of observables with respect to polar coordinates, UT1, and celestial pole offsets.

The following sections give the details of these two options as well as the standard expressions necessary to obtain the numerical values of the relevant parameters at the date of the observation. Subroutines for options 1 and 2 of the coordinate transformation from the TRS to the CRS are available from the Central Bureau on request together with the development of the parameters.

The expressions of the precession and nutation quantities have been developed originally as functions of barycentric dynamical time (TDB) defined by IAU recommendations of 1976 and 1979. In 1991 the IAU adopted definitions of other time scales. See Chapter 11 for the relationships among these time scales. The parameter t is defined by

$$t = (\text{TT} - 2000 \text{ January } 1\text{d } 12\text{h TT}) \text{ in days}/36525.$$

This definition is consistent with Resolution C7 passed at the 1994 Hague General Assembly of the IAU which recommends that J2000.0 be defined at the geocenter and at the date 2000.0 January 1.5 TT = Julian Date 2451545.0 TT. In the following, R_1 , R_2 and R_3 denote direct rotations about the axes 1, 2 and 3 of the coordinate frame.

Coordinate Transformation Referred to the Equinox

Option 1 uses the form of the coordinate transformation

$$[\text{CRS}] = PN'(t)R'(t)W'(t) [\text{TRS}], \tag{1}$$

in which the three fundamental components are (Mueller, 1969)

$$W'(t) = R_1(y_p) \cdot R_2(x_p),$$

x_p and y_p being the “polar coordinates” of the CEP in the TRS;

$$R'(t) = R_3(-\text{GST}),$$

GST being Greenwich True Sidereal Time at date t , including both the effect of Earth rotation and the accumulated precession and nutation in right ascension; and

$$PN'(t) = [P][N],$$

$$\text{with } [P] = R_3(\zeta_A) \cdot R_2(-\theta_A) \cdot R_3(z_A)$$

for the transformation matrix corresponding to the precession between the reference epoch and the date t ,

$$[N] = R_1(-\epsilon_A) \cdot R_3(\Delta\psi) \cdot R_1(\epsilon_A + \Delta\epsilon)$$

for the transformation matrix corresponding to the nutation at date t .

Standard values of the parameters to be used in form (1) of the transformation are explained below.

The standard polar coordinates to be used for the parameters x_p and y_p (if not estimated from the observations) are those published by the IERS. Apparent Greenwich Sidereal Time GST at the date t of the observation, must be derived from the following expressions:

(i) the relationship between Greenwich Mean Sidereal Time (GMST) and Universal Time as given by Aoki *et al.* (1982):

$$\text{GMST}_{0\text{h UT1}} = 6^{\text{h}} 41^{\text{m}} 50^{\text{s}} 54841 + 8640184^{\text{s}} 812866 T'_u + 0^{\text{s}} 093104 T'^2_u - 6^{\text{s}} 2 \times 10^{-6} T'^3_u,$$

with $T'_u = d'_u/36525$, d'_u being the number of days elapsed since 2000 January 1, 12h UT1, taking on values $\pm 0.5, \pm 1.5, \dots$,

(ii) the interval of GMST from 0h UT1 to the hour of the observation in UT1,

$$\text{GMST} = \text{GMST}_{0\text{h UT1}} + r[(\text{UT1} - \text{UTC}) + \text{UTC}],$$

where r is the ratio of universal to sidereal time as given by Aoki *et al.* (1982),

$$r = 1.002737909350795 + 5.9006 \times 10^{-11} T'_u - 5.9 \times 10^{-15} T'^2_u$$

and the UT1-UTC value to be used (if not estimated from the observations) is the IERS value.

(iii) accumulated precession and nutation in right ascension (Aoki and Kinoshita, 1983),

$$\text{GST} = \text{GMST} + \Delta\psi \cos \epsilon_A + 0'' 00264 \sin \Omega + 0'' 000063 \sin 2\Omega,$$

where Ω is the mean longitude of the ascending node of the lunar orbit. The last two terms have not been included in the IERS Standards previously. They should not be included in (iii) until 1 January

1997 when their use will begin. This date is chosen to minimize any discontinuity in UT1. The effect of these terms on the estimation of UT1 has been described by Capitaine and Gontier (1993).

The numerical expression for the precession quantities ζ_A , θ_A , z_A and ϵ_A have been given by Lieske *et al.* (1977) as functions of two time parameters t and T (the last parameter representing Julian centuries from J2000.0 to an arbitrary epoch). The simplified expressions when the arbitrary epoch is chosen to be J2000.0 (*i.e.* $T = 0$) are

$$\zeta_A = 2306''.2181t + 0''.30188t^2 + 0''.017998t^3,$$

$$\theta_A = 2004''.3109t - 0''.42665t^2 - 0''.041833t^3,$$

$$z_A = 2306''.2181t + 1''.09468t^2 + 0''.018203t^3,$$

$$\epsilon_A = 84381''.448 - 46''.8150t - 0''.00059t^2 + 0''.001813t^3.$$

The nutation quantities $\Delta\psi$ and $\Delta\epsilon$ to be used are the nutation angles in longitude and obliquity.

For observations requiring values of the nutation angles with an accuracy of ± 1 mas, it is necessary to add (if those quantities are not estimated from the observations) the IERS published values (observed or predicted) for the “celestial pole offsets” (*i.e.* corrections dpsi and deps).

The IAU 1980 Theory of Nutation

The IAU 1980 Theory of Nutation (Seidelmann, 1982; Wahr, 1981) is based on a modification of a rigid Earth theory published by Kinoshita (1977) and on the geophysical model 1066A of Gilbert and Dziewonski (1975). It therefore includes the effects of a solid inner core and a liquid outer core and a “distribution of elastic parameters inferred from a large set of seismological data.” The constants defining the theory are given in Table 5.1.

VLBI and LLR observations have shown that there are deficiencies in the IAU 1976 Precession and in the IAU 1980 Theory of Nutation. However, these models are kept as part of the IERS Standards and the observed differences ($\delta\Delta\psi$ and $\delta\Delta\epsilon$, equivalent to dpsi and deps in the IERS Bulletins) with respect to the conventional celestial pole position defined by the models are monitored and reported by the IERS as “celestial pole offsets.” Using these offsets the corrected nutation is given by

$$\Delta\psi = \Delta\psi(\text{IAU 1980}) + \delta\Delta\psi,$$

and

$$\Delta\epsilon = \Delta\epsilon(\text{IAU1980}) + \delta\Delta\epsilon.$$

This is practically equivalent to replacing N with the rotation described by Lieske (1991),

$$\tilde{N} = \mathcal{R}N_{\text{IAU}}.$$

where

$$\mathcal{R} = \begin{pmatrix} 1 & -\delta\Delta\psi \cos \epsilon_t & -\delta\Delta\psi \sin \epsilon_t \\ \delta\Delta\psi \cos \epsilon_t & 1 & \delta\Delta\epsilon \\ \delta\Delta\psi \sin \epsilon_t & \delta\Delta\epsilon & 1 \end{pmatrix},$$

$\epsilon_t = \epsilon_A + \Delta\epsilon$, and N_{IAU} represents the IAU 1980 Theory of Nutation according to which

$$\Delta\psi = \sum_{i=1}^{106} (A_i + A'_i t) \sin(\text{ARGUMENT}), \quad \Delta\epsilon = \sum_{i=1}^{106} (B_i + B'_i t) \cos(\text{ARGUMENT}).$$

Here

$$\text{ARGUMENT} = \sum N_i F_i,$$

the $N_i, (i = 1, \dots, 5)$ being integers multiplying the Fundamental Arguments F_i of nutation theory, namely,

$$\begin{aligned} F_1 \equiv l &= \text{Mean Anomaly of the Moon} \\ &= 134^\circ 96340251 + 1717915923'' 2178t + 31'' 8792t^2 + 0'' 051635t^3 - 0'' 00024470t^4, \end{aligned}$$

$$\begin{aligned} F_2 \equiv l' &= \text{Mean Anomaly of the Sun} \\ &= 357^\circ 52910918 + 129596581'' 0481t - 0'' 5532t^2 - 0'' 000136t^3 - 0'' 00001149t^4, \end{aligned}$$

$$\begin{aligned} F_3 \equiv F &= L - \Omega \\ &= 93^\circ 27209062 + 1739527262'' 8478t - 12'' 7512t^2 - 0'' 001037t^3 + 0'' 00000417t^4, \end{aligned}$$

$$\begin{aligned} F_4 \equiv D &= \text{Mean Elongation of the Moon from the Sun} \\ &= 297^\circ 85019547 + 1602961601'' 2090t - 6'' 3706t^2 + 0'' 006593t^3 - 0'' 00003169t^4, \end{aligned}$$

$$\begin{aligned} F_5 \equiv \Omega &= \text{Mean Longitude of the Ascending Node of the Moon} \\ &= 125^\circ 04455501 - 6962890'' 2665t + 7'' 4722t^2 + 0'' 007702t^3 - 0'' 00005939t^4, \end{aligned}$$

where t is measured in Julian Centuries of 36525 days of 86400 seconds of Dynamical Time since J2000.0 and where $1^\circ = 360^\circ = 1296000'' 0$ (Simon *et al.*, 1994). L is the Mean Longitude of the Moon.

The reader is cautioned that there may be an ambiguity in the assignment of the set of five multipliers N_j to any particular term of the nutation series. This ambiguity is illustrated, and a convention for unique assignment of multipliers for prograde and retrograde circular nutations is presented, in a note at the end of this chapter.

Table 5.1. IAU 1980 Theory of Nutation in longitude $\Delta\psi$ and obliquity $\Delta\epsilon$, referred to the mean equator and equinox of date, with t measured in Julian centuries from epoch J2000.0. The signs of the fundamental arguments, periods, and coefficients may differ from the original publication. These have been changed to be consistent with other portions of this chapter.

$$\Delta\psi = \sum_{i=1}^{106} (A_i + A'_i t) \sin(\text{ARGUMENT}), \quad \Delta\epsilon = \sum_{i=1}^{106} (B_i + B'_i t) \cos(\text{ARGUMENT}).$$

MULTIPLIERS OF					PERIOD	LONGITUDE		OBLIQUITY	
l	l'	F	D	Ω	(days)	A_i	A'_i	B_i	B'_i
0	0	0	0	1	-6798.4	-171996	-174.2	92025	8.9
0	0	2	-2	2	182.6	-13187	-1.6	5736	-3.1
0	0	2	0	2	13.7	-2274	-0.2	977	-0.5
0	0	0	0	2	-3399.2	2062	0.2	-895	0.5
0	-1	0	0	0	-365.3	-1426	3.4	54	-0.1
1	0	0	0	0	27.6	712	0.1	-7	0.0
0	1	2	-2	2	121.7	-517	1.2	224	-0.6
0	0	2	0	1	13.6	-386	-0.4	200	0.0
1	0	2	0	2	9.1	-301	0.0	129	-0.1
0	-1	2	-2	2	365.2	217	-0.5	-95	0.3
-1	0	0	2	0	31.8	158	0.0	-1	0.0
0	0	2	-2	1	177.8	129	0.1	-70	0.0
-1	0	2	0	2	27.1	123	0.0	-53	0.0
1	0	0	0	1	27.7	63	0.1	-33	0.0
0	0	0	2	0	14.8	63	0.0	-2	0.0
-1	0	2	2	2	9.6	-59	0.0	26	0.0
-1	0	0	0	1	-27.4	-58	-0.1	32	0.0
1	0	2	0	1	9.1	-51	0.0	27	0.0
-2	0	0	2	0	-205.9	-48	0.0	1	0.0
-2	0	2	0	1	1305.5	46	0.0	-24	0.0
0	0	2	2	2	7.1	-38	0.0	16	0.0
2	0	2	0	2	6.9	-31	0.0	13	0.0
2	0	0	0	0	13.8	29	0.0	-1	0.0
1	0	2	-2	2	23.9	29	0.0	-12	0.0
0	0	2	0	0	13.6	26	0.0	-1	0.0
0	0	2	-2	0	173.3	-22	0.0	0	0.0
-1	0	2	0	1	27.0	21	0.0	-10	0.0
0	2	0	0	0	182.6	17	-0.1	0	0.0
0	2	2	-2	2	91.3	-16	0.1	7	0.0
-1	0	0	2	1	32.0	16	0.0	-8	0.0
0	1	0	0	1	386.0	-15	0.0	9	0.0
1	0	0	-2	1	-31.7	-13	0.0	7	0.0
0	-1	0	0	1	-346.6	-12	0.0	6	0.0
2	0	-2	0	0	-1095.2	11	0.0	0	0.0
-1	0	2	2	1	9.5	-10	0.0	5	0.0
1	0	2	2	2	5.6	-8	0.0	3	0.0
0	-1	2	0	2	14.2	-7	0.0	3	0.0
0	0	2	2	1	7.1	-7	0.0	3	0.0
1	1	0	-2	0	-34.8	-7	0.0	0	0.0
0	1	2	0	2	13.2	7	0.0	-3	0.0
-2	0	0	2	1	-199.8	-6	0.0	3	0.0
0	0	0	2	1	14.8	-6	0.0	3	0.0
2	0	2	-2	2	12.8	6	0.0	-3	0.0
1	0	0	2	0	9.6	6	0.0	0	0.0
1	0	2	-2	1	23.9	6	0.0	-3	0.0
0	0	0	-2	1	-14.7	-5	0.0	3	0.0
0	-1	2	-2	1	346.6	-5	0.0	3	0.0
2	0	2	0	1	6.9	-5	0.0	3	0.0
1	-1	0	0	0	29.8	5	0.0	0	0.0
1	0	0	-1	0	411.8	-4	0.0	0	0.0
0	0	0	1	0	29.5	-4	0.0	0	0.0
0	1	0	-2	0	-15.4	-4	0.0	0	0.0
1	0	-2	0	0	-26.9	4	0.0	0	0.0
2	0	0	-2	1	212.3	4	0.0	-2	0.0
0	1	2	-2	1	119.6	4	0.0	-2	0.0
1	1	0	0	0	25.6	-3	0.0	0	0.0
1	-1	0	-1	0	-3232.9	-3	0.0	0	0.0
-1	-1	2	2	2	9.8	-3	0.0	1	0.0
0	-1	2	2	2	7.2	-3	0.0	1	0.0
1	-1	2	0	2	9.4	-3	0.0	1	0.0
3	0	2	0	2	5.5	-3	0.0	1	0.0
-2	0	2	0	2	1615.7	-3	0.0	1	0.0
1	0	2	0	0	9.1	3	0.0	0	0.0
-1	0	2	4	2	5.8	-2	0.0	1	0.0
1	0	0	0	2	27.8	-2	0.0	1	0.0
-1	0	2	-2	1	-32.6	-2	0.0	1	0.0

0	-2	2	-2	1	6786.3	-2	0.0	1	0.0
-2	0	0	0	1	-13.7	-2	0.0	1	0.0
2	0	0	0	1	13.8	2	0.0	-1	0.0
3	0	0	0	0	9.2	2	0.0	0	0.0
1	1	2	0	2	8.9	2	0.0	-1	0.0
0	0	2	1	2	9.3	2	0.0	-1	0.0
1	0	0	2	1	9.6	-1	0.0	0	0.0
1	0	2	2	1	5.6	-1	0.0	1	0.0
1	1	0	-2	1	-34.7	-1	0.0	0	0.0
0	1	0	2	0	14.2	-1	0.0	0	0.0
0	1	2	-2	0	117.5	-1	0.0	0	0.0
0	1	-2	2	0	-329.8	-1	0.0	0	0.0
1	0	-2	2	0	23.8	-1	0.0	0	0.0
1	0	-2	-2	0	-9.5	-1	0.0	0	0.0
1	0	2	-2	0	32.8	-1	0.0	0	0.0
1	0	0	-4	0	-10.1	-1	0.0	0	0.0
2	0	0	-4	0	-15.9	-1	0.0	0	0.0
0	0	2	4	2	4.8	-1	0.0	0	0.0
0	0	2	-1	2	25.4	-1	0.0	0	0.0
-2	0	2	4	2	7.3	-1	0.0	1	0.0
2	0	2	2	2	4.7	-1	0.0	0	0.0
0	-1	2	0	1	14.2	-1	0.0	0	0.0
0	0	-2	0	1	-13.6	-1	0.0	0	0.0
0	0	4	-2	2	12.7	1	0.0	0	0.0
0	1	0	0	2	409.2	1	0.0	0	0.0
1	1	2	-2	2	22.5	1	0.0	-1	0.0
3	0	2	-2	2	8.7	1	0.0	0	0.0
-2	0	2	2	2	14.6	1	0.0	-1	0.0
-1	0	0	0	2	-27.3	1	0.0	-1	0.0
0	0	-2	2	1	-169.0	1	0.0	0	0.0
0	1	2	0	1	13.1	1	0.0	0	0.0
-1	0	4	0	2	9.1	1	0.0	0	0.0
2	1	0	-2	0	131.7	1	0.0	0	0.0
2	0	0	2	0	7.1	1	0.0	0	0.0
2	0	2	-2	1	12.8	1	0.0	-1	0.0
2	0	-2	0	1	-943.2	1	0.0	0	0.0
1	-1	0	-2	0	-29.3	1	0.0	0	0.0
-1	0	0	1	1	-388.3	1	0.0	0	0.0
-1	-1	0	2	1	35.0	1	0.0	0	0.0
0	1	0	1	0	27.3	1	0.0	0	0.0

$$\epsilon_0 = 23^\circ 26' 21''.448$$

$$\sin \epsilon_0 = 0.39777716$$

The IERS 1996 Theory of Precession/Nutation

At the request of the IERS, T. Herring (1996) has analyzed the most recent VLBI and LLR data for geophysical parameters required to adjust the rigid Earth theory of nutation to the non-rigid theory. The non-rigid Earth theory coefficients resulting from this procedure are shown in Table 5.2. Table 5.3 contains the planetary nutation terms and the necessary planetary arguments. These coefficients are meant to be used for prediction purposes and by those requiring accurate *a priori* estimates of nutation. They are not meant to replace the IAU Theory. The IERS will continue to publish observed estimates of the corrections to the IAU 1976 Precession and the IAU 1980 Theory of Nutation in its publications.

The use of the IERS 1996 Theory of nutation must also be associated with the use of improved numerical values for the precession rate of the equator in longitude and obliquity:

$$\delta\psi_A = -0.299''/c \text{ and } \delta\omega_A = -0.024''/c$$

Table 5.2. IERS 1996 series for nutation in longitude $\Delta\psi$ and obliquity $\Delta\epsilon$, referred to the mean equator and equinox of date, with t measured in Julian centuries from epoch J2000.0. The signs of the fundamental arguments, periods, and coefficients may differ from the original publication. These have been changed to be consistent with other portions of this chapter.

$$\Delta\psi = \sum_{i=1}^{263} (A_i + A'_i t) \sin(\text{ARGUMENT}) + A''_i \cos(\text{ARGUMENT}),$$

$$\Delta\epsilon = \sum_{i=1}^{263} (B_i + B'_i t) \cos(\text{ARGUMENT}) + B''_i \sin(\text{ARGUMENT}).$$

MULTIPLIERS OF					PERIOD	LONGITUDE (0.001mas)		OBLIQUITY (0.001mas)		A''_i	B''_i
l	l'	F	D	Ω	(days)	A_i	A'_i	B_i	B'_i		
0	0	0	0	1	-6798.35	-17206277	-17419	9205356	886	3645	1553
0	0	2	-2	2	182.62	-1317014	-156	573058	-306	-1400	-464
0	0	2	0	2	13.66	-227720	-23	97864	-48	269	136
0	0	0	0	2	-3399.18	207429	21	-89747	47	-71	-29
0	-1	0	0	0	-365.26	-147538	364	7388	-19	1121	198
0	1	2	-2	2	121.75	-51687	123	22440	-68	-54	-18
1	0	0	0	0	27.55	71118	7	-687	0	-94	39
0	0	2	0	1	13.63	-38752	-37	20076	2	34	32
1	0	2	0	2	9.13	-30137	-4	12896	-6	77	35
0	-1	2	-2	2	365.22	21583	-49	-9591	30	6	12
0	0	2	-2	1	177.84	12820	14	-6897	-1	18	4
-1	0	2	0	2	27.09	12353	1	-5334	3	2	0
-1	0	0	2	0	31.81	15699	1	-127	0	-18	9
1	0	0	0	1	27.67	6314	6	-3323	0	3	-1
-1	0	0	0	1	-27.44	-5797	-6	3141	0	-19	-8
-1	0	2	2	2	9.56	-5965	-1	2554	-1	14	7
1	0	2	0	1	9.12	-5163	-4	2635	0	12	8
-2	0	2	0	1	1305.48	4590	5	-2424	-1	1	1
0	0	0	2	0	14.77	6336	1	-125	0	-15	3
0	0	2	2	2	7.10	-3854	0	1643	0	15	6
-2	0	0	2	0	-205.89	-4774	0	48	0	-2	-3
2	0	2	0	2	6.86	-3102	0	1323	-1	12	5
1	0	2	-2	2	23.94	2863	0	-1235	1	0	0
-1	0	2	0	1	26.98	2044	2	-1076	0	1	0
2	0	0	0	0	13.78	2923	0	-62	0	-8	1
0	0	2	0	0	13.61	2585	0	-56	0	-7	1
0	1	0	0	1	386.00	-1406	-3	857	0	8	-4
-1	0	0	2	1	31.96	1517	1	-801	0	1	0
0	2	2	-2	2	91.31	-1578	7	685	-4	-2	-1
0	0	-2	2	0	-173.31	2178	0	-15	0	1	1
1	0	0	-2	1	-31.66	-1286	-1	694	0	-4	-2
0	-1	0	0	1	-346.64	-1269	1	642	1	6	2
-1	0	2	2	1	9.54	-1022	-1	522	0	2	1
0	-2	0	0	0	-182.63	-1671	8	14	0	-1	-1
1	0	2	2	2	5.64	-768	0	325	0	4	2
-2	0	2	0	0	1095.18	-1102	0	10	0	-1	0
0	1	2	0	2	13.17	757	-2	-326	-2	-1	0
0	0	2	2	1	7.09	-664	-1	335	-1	2	1
0	-1	2	0	2	14.19	-714	2	307	2	1	0
0	0	0	2	1	14.80	-631	-1	327	0	0	0
1	0	2	-2	1	23.86	580	1	-307	0	0	0
2	0	2	-2	2	12.81	643	0	-277	0	-1	0
-2	0	0	2	1	-199.84	-579	-1	304	0	-1	0
2	0	2	0	1	6.85	-533	0	269	0	2	1
0	-1	2	-2	1	346.60	-477	-1	271	-1	0	0
0	0	0	-2	1	-14.73	-493	-1	272	0	-2	-1
-1	-1	0	2	0	34.85	735	0	-5	0	-1	0
2	0	0	-2	1	212.32	405	0	-220	0	1	0
1	0	0	2	0	9.61	657	0	-20	0	-2	0
0	1	2	-2	1	119.61	361	0	-194	0	1	0

1	-1	0	0	0	29.80	471	0	-4	0	-1	0
-2	0	2	0	2	1615.76	-311	0	131	0	0	0
3	0	2	0	2	5.49	-289	0	124	0	2	1
0	-1	0	2	0	15.39	435	0	-9	0	-1	0
1	-1	2	0	2	9.37	-287	0	123	0	1	0
-1	-1	2	2	2	9.81	-282	0	122	0	1	0
0	0	0	1	0	29.53	-422	0	3	0	1	0
-1	0	2	0	0	26.88	-404	0	4	0	1	0
0	-1	2	2	2	7.24	-264	0	114	0	1	0
-2	0	0	0	1	-13.75	-228	0	126	0	-1	0
1	1	2	0	2	8.91	246	0	-106	0	-1	0
2	0	0	0	1	13.81	218	0	-114	0	0	0
-1	1	0	1	0	3232.87	327	0	-1	0	0	0
1	1	0	0	0	25.62	-338	0	4	0	0	0
1	0	2	0	0	9.11	334	0	-11	0	-1	0
-1	0	2	-2	1	-32.61	-199	0	107	0	-1	0
1	0	0	0	2	27.78	-197	0	85	0	0	0
-1	0	0	1	0	-411.78	405	0	-55	0	-35	-14
0	0	2	1	2	9.34	165	0	-72	0	0	0
-1	0	2	4	2	5.80	-151	0	66	0	1	0
0	-2	2	-2	1	6786.31	-130	0	69	0	0	0
-1	1	0	1	1	6164.17	132	0	-68	0	0	0
1	0	2	2	1	5.64	-133	0	66	0	1	0
-2	0	2	2	2	14.63	139	0	-60	0	0	0
-1	0	0	0	2	-27.33	139	0	-60	0	0	0
1	1	2	-2	2	22.47	128	0	-55	0	0	0
-2	0	2	4	2	7.35	-121	0	52	0	0	0
-1	0	4	0	2	9.06	115	0	-49	0	0	0
2	0	2	-2	1	12.79	101	0	-54	0	0	0
2	0	2	2	2	4.68	-108	0	47	0	1	0
1	0	0	2	1	9.63	-95	0	49	0	0	0
3	0	0	0	0	9.18	157	0	-5	0	-1	0
3	0	2	-2	2	8.75	94	0	-40	0	0	0
0	0	4	-2	2	12.66	91	0	-39	0	0	0
0	0	-2	2	1	-169.00	87	0	-44	0	0	0
0	1	2	0	1	13.14	81	0	-42	0	0	0
0	0	2	-2	3	187.66	123	0	-20	0	0	0
-1	0	0	4	0	10.08	133	0	-4	0	0	0
2	0	-2	0	1	-943.23	71	0	-38	0	0	0
2	0	0	-4	0	-15.91	-128	0	1	0	0	0
-1	-1	0	2	1	35.03	75	0	-39	0	0	0
-2	-1	0	2	0	-131.67	-115	0	1	0	0	0
0	-1	2	0	1	14.16	-66	0	35	0	0	0
-1	0	0	1	1	-388.27	101	0	-49	0	-3	-1
0	0	-2	0	1	-13.58	-68	0	36	0	0	0
0	1	0	0	2	409.23	69	0	-33	0	-1	0
0	0	2	-1	2	25.42	-74	0	31	0	0	0
0	0	2	4	2	4.79	-69	0	29	0	0	0
1	1	0	-2	1	-34.67	-61	0	32	0	0	0
-1	1	0	2	0	29.26	-94	0	0	0	0	0
1	-1	2	2	2	5.73	-59	0	25	0	0	0
1	-1	0	0	1	29.93	51	0	-27	0	0	0
0	1	-2	2	0	-329.79	-90	0	3	0	0	0
3	0	2	0	1	5.49	-50	0	25	0	0	0
-1	1	2	2	2	9.31	56	0	-24	0	0	0
0	1	2	2	2	6.96	54	0	-22	0	0	0
-1	0	0	-2	1	-9.60	-50	0	27	0	0	0
-1	1	0	1	2	66079.30	-52	0	23	0	0	0
0	-1	2	2	1	7.23	-44	0	24	0	0	0
1	0	2	-4	1	-38.74	-47	0	24	0	0	0
-1	0	-2	2	0	-23.77	77	0	0	0	0	0
-1	-1	2	2	1	9.80	-46	0	24	0	0	0
0	-1	0	0	2	-329.82	59	0	-25	0	0	0
2	-1	2	0	2	6.99	-48	0	21	0	0	0
1	-1	2	0	1	9.35	-42	0	22	0	0	0
0	0	0	2	2	14.83	-46	0	20	0	0	0
0	1	0	2	0	14.19	-67	0	0	0	0	0
-1	1	2	0	2	25.22	47	0	-20	0	0	0
0	3	2	-2	2	73.05	-44	0	19	0	0	0
0	-1	-2	2	0	-117.54	66	0	0	0	0	0

0	0	0	1	1	29.66	-37	0	20	0	0	0
1	0	-2	-2	0	-9.53	-64	0	1	0	0	0
1	1	2	0	1	8.90	36	0	-18	0	0	0
2	1	2	0	2	6.73	40	0	-17	0	0	0
0	1	0	1	0	27.32	57	0	0	0	0	0
1	0	-2	2	0	32.76	-58	0	0	0	0	0
1	1	0	0	1	25.72	-34	0	19	0	0	0
-2	0	0	-2	0	-7.13	-59	0	1	0	0	0
-1	0	0	2	2	32.11	-38	0	17	0	0	0
0	0	0	-1	1	-29.40	33	0	-18	0	0	0
0	1	0	-2	1	-15.35	-33	0	18	0	0	0
-1	0	2	-2	2	-32.45	36	0	-16	0	0	0
-1	1	0	0	1	-29.67	-31	0	17	0	0	0
1	0	2	1	2	6.98	33	0	-14	0	0	0
0	0	0	-4	0	-7.38	-48	0	1	0	0	0
0	0	2	1	1	9.33	27	0	-14	0	0	0
1	0	0	-2	2	-31.52	32	0	-14	0	0	0
1	0	2	-1	2	13.22	-33	0	13	0	0	0
1	-1	0	2	0	9.87	48	0	0	0	0	0
-1	0	2	4	1	5.80	-26	0	13	0	0	0
0	0	-2	-2	0	-7.08	-41	0	1	0	0	0
1	0	-2	0	1	-26.77	27	0	-14	0	0	0
-1	0	2	-1	1	313.04	-23	0	14	0	0	0
1	1	2	-2	1	22.40	23	0	-12	0	0	0
4	0	2	0	2	4.58	-26	0	11	0	0	0
0	1	2	1	2	9.11	-24	0	10	0	0	0
-2	0	-2	0	0	-6.85	-36	0	1	0	0	0
2	1	2	-2	2	12.38	25	0	-10	0	0	0
2	-1	0	0	0	14.32	38	0	0	0	0	0
-1	-1	0	0	1	-25.53	21	0	-12	0	0	0
-2	0	2	2	1	14.60	22	0	-11	0	0	0
0	0	0	0	3	-2266.12	-22	0	10	0	0	0
1	0	4	-2	2	8.68	23	0	-9	0	0	0
2	0	2	2	1	4.68	-19	0	10	0	0	0
-2	0	2	4	1	7.34	-20	0	10	0	0	0
0	1	0	2	1	14.22	18	0	-9	0	0	0
1	0	0	1	0	14.25	-33	0	0	0	0	0
-1	0	0	4	1	10.10	-18	0	9	0	0	0
-1	0	4	0	1	9.05	19	0	-9	0	0	0
0	0	2	-3	2	-35.23	-20	0	8	0	0	0
0	0	4	0	2	6.82	19	0	-8	0	0	0
2	1	0	0	0	13.28	-28	0	0	0	0	0
0	0	2	-4	1	-16.10	-16	0	9	0	0	0
-1	-1	2	4	2	5.90	-17	0	7	0	0	0
-1	-2	0	2	0	38.52	27	0	0	0	0	0
0	0	0	4	1	7.39	-16	0	7	0	0	0
0	-1	0	2	1	15.42	-14	0	7	0	0	0
1	0	2	4	2	4.08	-16	0	7	0	0	0
-2	0	0	2	2	-194.13	18	0	-8	0	0	0
-2	2	0	2	0	1616.44	-22	0	0	0	0	0
-2	-1	2	0	1	-507.16	9	0	-5	0	0	0
-3	0	0	0	1	-9.17	-14	0	7	0	0	0
0	0	2	0	3	13.69	20	0	0	0	0	0
0	0	2	4	1	4.79	-12	0	6	0	0	0
0	0	4	-2	1	12.64	12	0	-7	0	0	0
0	-2	0	2	0	16.06	21	0	0	0	0	0
1	0	0	-1	1	438.33	17	0	-5	0	-3	1
1	1	2	2	2	5.56	15	0	-6	0	0	0
3	0	2	-2	1	8.73	12	0	-7	0	0	0
-1	-1	2	0	2	29.26	-16	0	6	0	0	0
-2	-1	0	2	1	-129.17	-13	0	7	0	0	0
0	0	0	-2	2	-14.70	13	0	-5	0	0	0
0	-2	2	2	2	7.38	-13	0	5	0	0	0
1	0	0	-4	1	-10.07	-12	0	6	0	0	0
-1	1	0	2	1	29.39	-10	0	6	0	0	0
-2	0	0	4	1	15.94	11	0	-6	0	0	0
0	0	2	-1	1	25.33	-10	0	5	0	0	0
0	2	0	0	1	187.67	-9	0	5	0	0	0
0	2	2	-2	1	90.10	8	0	-5	0	0	0
2	0	0	2	1	7.13	-9	0	5	0	0	0

2	0	0	-4	1	-15.87	-11	0	5	0	0	0
2	0	2	-4	1	95.42	10	0	-5	0	0	0
-1	0	-2	0	1	-9.10	-10	0	5	0	0	0
-1	1	2	0	1	25.13	9	0	-5	0	0	0
-1	1	2	-2	1	-35.80	-11	0	5	0	0	0
-1	-1	0	4	0	10.37	15	0	0	0	0	0
-3	0	0	4	0	37.63	16	0	0	0	0	0
3	0	2	2	2	4.00	-14	0	0	0	0	0
2	-1	0	-2	0	471.89	-9	0	1	0	-1	0
0	2	-2	2	0	-3396.16	-9	0	0	0	0	0
0	-1	2	4	2	4.86	-9	0	0	0	0	0
0	-1	2	-1	2	27.32	9	0	0	0	0	0
1	1	0	2	0	9.37	-10	0	0	0	0	0
2	0	0	-2	2	219.17	-11	0	0	0	0	0
2	-1	2	2	2	4.74	-9	0	0	0	0	0
4	0	0	0	0	6.89	9	0	0	0	0	0
4	0	2	-2	2	6.64	12	0	0	0	0	0
-1	0	0	3	0	15.31	-10	0	0	0	0	0
-1	0	4	-2	2	23.43	-9	0	0	0	0	0
-1	-2	2	2	2	10.08	-9	0	0	0	0	0
-2	-1	0	4	0	16.63	12	0	0	0	0	0
-2	-1	2	4	2	7.50	-12	0	0	0	0	0
0	1	2	2	1	6.95	7	0	0	0	0	0
0	2	2	0	2	12.71	7	0	0	0	0	0
0	-2	2	0	2	14.77	-8	0	0	0	0	0
1	0	0	4	0	5.82	8	0	0	0	0	0
1	0	2	2	0	5.63	8	0	0	0	0	0
1	0	2	-4	2	-38.52	7	0	0	0	0	0
1	-1	2	2	1	5.73	-8	0	0	0	0	0
1	-1	2	-2	2	25.62	-7	0	0	0	0	0
1	-2	0	0	0	32.45	8	0	0	0	0	0
2	0	0	0	2	13.83	-8	0	0	0	0	0
2	1	0	-2	1	134.27	8	0	0	0	0	0
3	0	0	0	1	9.20	7	0	0	0	0	0
-1	0	2	1	2	14.13	8	0	0	0	0	0
-1	0	2	3	2	7.22	8	0	0	0	0	0
-1	0	-2	4	0	38.96	-7	0	0	0	0	0
-1	1	2	2	1	9.30	7	0	0	0	0	0
-1	2	0	2	0	27.09	-8	0	0	0	0	0
-1	-1	2	-1	1	2189.73	7	0	0	0	0	0
-2	0	2	-2	1	-14.93	-8	0	0	0	0	0
-2	0	4	0	2	13.49	-7	0	0	0	0	0
-2	0	-2	2	0	-12.76	8	0	0	0	0	0
-2	1	2	0	1	285.41	9	0	0	0	0	0
-3	0	2	0	1	-28.15	-8	0	0	0	0	0
0	1	0	1	1	27.43	5	0	0	0	0	0
0	-1	0	4	0	7.53	6	0	0	0	0	0
0	-1	0	-2	1	-14.16	5	0	0	0	0	0
0	-2	0	0	1	-177.85	-6	0	0	0	0	0
1	0	2	1	1	6.97	5	0	0	0	0	0
1	0	2	-3	2	126.51	-6	0	0	0	0	0
1	0	-2	1	0	-299.26	-7	0	0	0	0	0
1	1	0	1	0	13.72	5	0	0	0	0	0
1	-1	0	-2	1	-29.14	6	0	0	0	0	0
2	0	2	-1	2	8.93	-6	0	0	0	0	0
2	1	2	0	1	6.73	5	0	0	0	0	0
2	-1	2	0	1	6.98	-6	0	0	0	0	0
2	-1	2	-2	2	13.28	5	0	0	0	0	0
3	0	0	2	0	5.66	5	0	0	0	0	0
3	-1	2	0	2	5.58	-5	0	0	0	0	0
-1	-1	2	0	1	29.14	-6	0	0	0	0	0
-2	0	0	0	2	-13.72	6	0	0	0	0	0
-2	0	0	3	0	34.48	-5	0	0	0	0	0
-2	0	0	-2	1	-7.12	-5	0	0	0	0	0
-2	0	2	2	0	14.57	-6	0	0	0	0	0
-2	-1	2	0	0	-548.04	-5	0	0	0	0	0
-2	-1	2	2	2	15.24	6	0	0	0	0	0
0	0	1	0	0	27.21	0	0	0	0	8	0
0	0	1	0	1	27.32	0	0	0	0	-16	-14
-1	0	1	0	0	2190.35	0	0	0	0	33	0

-1	0	1	0	1	3231.51	0	0	0	0	-105	-89
-1	0	1	0	2	6159.22	0	0	0	0	36	18
-1	0	1	0	3	65514.10	0	0	0	0	-6	0

Table 5.3. IERS 1996 Series for planetary nutation in longitude $\Delta\psi$ and obliquity $\Delta\epsilon$, referred to the mean equator and equinox of date, with t measured in Julian centuries from epoch J2000.0. The signs of the fundamental arguments, periods, and coefficients may differ from the original publication. These have been changed to be consistent with other portions of this chapter.

$$\Delta\psi = \sum_{i=1}^{118} (A_i + A'_i t) \sin(\text{ARGUMENT}), \quad \Delta\epsilon = \sum_{i=1}^{118} (B_i + B'_i t) \cos(\text{ARGUMENT}).$$

MULTIPLIERS OF										PERIOD	LONGITUDE		OBLIQUITY	
l_{Ve}	l_E	l_{Ma}	l_J	l_{Sa}	p_a	D	F	l	Ω	(days)	A_i	A'_i	B_i	B'_i
0	2	0	-2	0	0	2	0	-2	1	100171.17	28	0	0	-15
18	-16	0	0	0	0	0	0	-1	0	99728.92	23	10	0	0
8	-12	0	0	0	0	1	-1	0	-1	88074.16	-120	-60	32	-64
0	0	2	0	0	0	1	-1	0	0	38036.19	27	-8	0	0
0	1	-2	0	0	0	0	0	0	-1	-37884.54	46	43	-23	25
3	-4	0	0	0	0	1	0	-1	0	-34988.76	0	13	0	0
5	-6	0	0	0	0	2	-2	0	0	18185.76	0	23	0	0
6	-8	0	0	0	0	2	0	-2	0	-17494.38	8	-2	0	0
0	8	-15	0	0	0	0	0	0	0	14765.98	5	-2	0	0
0	-2	0	3	0	0	-2	0	2	1	-13630.86	9	-2	0	-5
0	2	0	-3	0	0	2	0	-2	0	-13562.72	-35	-6	0	0
0	1	0	-1	0	0	1	0	-1	0	12732.58	-5	0	0	0
0	1	0	1	0	0	1	-1	0	0	11960.41	-2	-8	0	0
0	0	0	1	0	0	0	0	0	1	11945.37	2	-7	0	0
0	1	0	0	1	0	1	-1	0	-1	10771.42	-17	-8	4	-9
0	0	0	0	1	0	0	0	0	0	10759.23	1	6	0	0
0	0	0	0	1	1	0	0	0	0	10746.94	5	0	0	0
0	-1	0	0	1	0	-1	1	0	1	10747.06	-7	-1	0	0
8	-13	0	0	0	0	0	0	0	1	-7372.72	5	7	0	0
18	-16	0	0	0	0	0	0	-1	1	-7295.69	-7	-3	0	0
0	0	0	-2	5	0	0	0	0	1	-6944.70	8	2	0	0
0	4	-8	3	0	0	0	0	0	-1	6870.05	-8	-30	16	-4
0	4	-8	3	0	0	0	0	0	1	-6728.13	-8	29	16	4
0	0	0	2	-5	0	0	0	0	1	-6658.05	-7	2	0	0
0	2	0	-2	0	0	2	0	-2	0	6366.29	-44	0	0	0
-18	16	0	0	0	0	0	0	1	1	-6364.50	6	-3	0	0
-8	13	0	0	0	0	0	0	0	1	-6307.01	-4	6	0	0
0	0	2	0	0	0	1	-1	0	-1	5767.51	-27	-8	4	-15
0	1	-2	0	0	0	0	0	0	0	-5764.01	-46	44	0	0
0	-2	2	0	0	0	-1	1	0	1	5760.51	0	-5	0	0
0	0	0	0	-2	-1	0	0	0	0	-5376.54	-5	-10	6	-3
0	-1	0	0	2	0	-1	1	0	1	5376.57	-5	-11	-6	3
0	0	0	0	2	2	0	0	0	0	5373.47	-12	0	0	5
5	-6	0	0	0	0	2	-2	0	-1	4948.47	2	44	-23	0
0	2	0	-3	0	0	2	0	-2	1	-4528.45	-5	0	0	0
0	-1	0	-1	0	0	-1	1	0	1	-4334.57	-5	19	10	3
0	0	0	1	0	-1	0	0	0	0	4334.58	2	6	0	0
0	0	0	1	0	0	0	0	0	0	4332.59	-8	25	0	0
0	0	0	1	0	1	0	0	0	0	4330.60	0	5	0	0
0	-1	0	1	0	0	-1	1	0	1	4330.61	0	-5	0	0
3	-3	0	0	0	0	2	0	-2	0	3561.67	-14	0	0	0
0	-2	0	2	0	0	-2	0	2	1	-3287.62	5	0	0	0
3	-5	0	0	0	0	0	0	0	0	-2959.21	-22	7	0	0
3	-5	0	0	0	-1	0	0	0	0	-2958.28	-1	-7	3	-1
3	-5	0	0	0	-2	0	0	0	0	-2957.35	211	0	0	96
0	2	-4	0	0	0	0	0	0	0	-2882.00	-8	14	0	0
0	2	-4	0	0	-2	0	0	0	0	-2880.24	5	0	0	0
5	-8	0	0	0	-2	0	0	0	0	2863.89	0	-26	13	0
5	-7	0	0	0	0	1	-1	0	-1	2863.01	-14	-3	1	-7

0	0	0	-2	0	-1	0	0	0	0	-2165.80	-4	-27	12	-2
0	1	0	-2	0	0	1	-1	0	-1	-2165.80	3	14	-8	1
0	0	0	2	0	2	0	0	0	0	2165.30	-116	0	0	51
-3	3	0	0	0	0	-2	2	0	1	2060.87	12	0	0	-6
0	-2	0	2	0	0	-2	2	0	1	1642.24	5	0	0	0
2	-3	0	0	0	0	0	0	0	0	1454.94	0	63	0	0
0	0	0	3	0	2	0	0	0	0	1443.75	-12	0	0	5
1	-2	0	0	0	0	0	0	0	0	-975.38	0	-9	0	0
0	2	-3	0	0	0	0	0	0	0	901.99	-8	5	0	0
0	1	-1	0	0	0	0	0	0	0	779.94	-6	0	0	0
4	-7	0	0	0	-2	0	0	0	0	-733.47	0	6	0	0
4	-6	0	0	0	-2	0	0	0	0	727.58	-52	0	0	-23
4	-6	0	0	0	-1	0	0	0	0	727.52	0	9	-5	1
1	-1	0	0	0	0	0	0	0	0	583.92	153	0	0	0
1	-1	0	0	0	1	0	0	0	0	583.89	0	-6	-5	-1
0	1	0	-3	0	-2	0	0	0	0	488.96	-11	0	0	-5
2	-4	0	0	0	-1	0	0	0	0	-487.66	0	-8	0	0
2	-4	0	0	0	-2	0	0	0	0	-487.64	47	0	0	20
0	1	0	-2	0	0	0	0	0	0	439.33	-18	27	0	0
0	3	-4	0	0	0	0	0	0	0	418.27	-8	5	0	0
3	-4	0	0	0	0	0	0	0	0	416.69	0	29	0	0
0	1	0	-1	0	0	0	0	0	0	398.88	-123	-3	0	0
0	2	-2	0	0	0	0	0	0	0	389.97	-38	0	0	0
0	1	0	0	-1	0	0	0	0	0	378.09	-8	0	0	0
0	0	2	0	0	2	0	0	0	0	343.46	-7	0	0	0
0	1	0	1	0	2	0	0	0	0	336.83	-25	0	0	11
3	-6	0	0	0	-2	0	0	0	0	-325.10	0	-5	0	0
5	-7	0	0	0	-2	0	0	0	0	323.94	-21	0	0	-9
0	1	0	2	0	2	0	0	0	0	312.54	-3	-5	0	0
2	-2	0	0	0	-1	0	0	0	0	291.97	0	5	0	0
2	-2	0	0	0	0	0	0	0	0	291.96	-60	0	0	0
1	-3	0	0	0	-2	0	0	0	0	-265.73	-11	0	0	-5
1	-3	0	0	0	-1	0	0	0	0	-265.73	0	-5	0	0
0	2	0	-3	0	0	0	0	0	0	209.07	8	2	0	0
2	-5	0	0	0	-2	0	0	0	0	-208.83	0	-13	6	0
6	-8	0	0	0	-2	0	0	0	0	208.35	-12	0	0	-5
0	2	0	-2	0	0	0	0	0	0	199.44	39	0	0	0
3	-3	0	0	0	0	0	0	0	0	194.64	10	0	0	0
3	-3	0	0	0	2	0	0	0	0	194.63	5	-2	0	0
0	-2	0	1	0	-2	0	0	0	0	-190.66	15	3	-1	7
0	3	-2	0	0	2	0	0	0	0	188.60	8	-7	0	0
8	-15	0	0	0	-2	0	0	0	0	-183.00	-6	-10	4	-3
0	6	-8	3	0	2	0	0	0	0	182.67	12	-42	-18	-5
0	2	0	0	0	2	0	0	0	0	182.62	-9	0	0	0
0	-2	8	-3	0	2	0	0	0	0	182.57	-12	42	18	5
-8	11	0	0	0	-2	0	0	0	0	-182.24	6	10	-4	13
0	1	2	0	0	2	0	0	0	0	177.01	-8	-7	0	0
0	2	0	1	0	2	0	0	0	0	175.23	17	-1	0	-7
3	-7	0	0	0	-2	0	0	0	0	-172.01	7	-2	0	0
2	-1	0	0	0	2	0	0	0	0	162.26	0	-17	-8	0
7	-9	0	0	0	-2	0	0	0	0	153.56	-7	0	0	0
4	-4	0	0	0	0	0	0	0	0	145.98	11	0	0	0
1	1	0	0	0	2	0	0	0	0	139.11	-30	0	0	13
0	3	0	-2	0	2	0	0	0	0	129.00	7	-9	-4	-3
3	-2	0	0	0	2	0	0	0	0	126.97	0	-11	-5	0
0	3	0	-1	0	2	0	0	0	0	125.27	52	2	0	-22
0	4	-2	0	0	2	0	0	0	0	124.38	14	0	0	-6
8	-10	0	0	0	-2	0	0	0	0	121.59	-5	0	0	0
5	-5	0	0	0	0	0	0	0	0	116.78	7	0	0	0
2	0	0	0	0	2	0	0	0	0	112.35	39	0	0	-17
0	4	0	-2	0	2	0	0	0	0	95.33	-18	0	0	8
-18	16	0	0	0	0	0	-2	1	-2	-13.66	13	6	-3	5
-18	16	0	0	0	0	0	2	1	2	13.66	13	-6	-3	-5

$$l_{V_e} = 181^{\circ}979800853 + 58517^{\circ}8156748 \times t$$

$$l_E = 100^{\circ}466448494 + 35999^{\circ}3728521 \times t$$

$$\begin{aligned}
l_{Ma} &= 355^\circ.433274605 + 19140^\circ.299314 \times t \\
l_{Ju} &= 34^\circ.351483900 + 3034^\circ.90567464 \times t \\
l_{Sa} &= 50^\circ.0774713998 + 1222^\circ.11379404 \times t \\
p_a &= 1^\circ.39697137214 \times t + 0^\circ.0003086 \times t^2
\end{aligned}$$

The multipliers of the fundamental arguments of nutation theory

Each of the lunisolar terms in the nutation series is characterized by a set of five integers N_j which determines the ARGUMENT for the term as a linear combination of the five Fundamental Arguments F_j , namely the Delaunay variables $(\ell, \ell', F, D, \Omega)$: ARGUMENT = $\sum_{j=1}^5 N_j F_j \equiv \vec{N} \cdot \vec{F}$, where \vec{N} is the five-vector composed of the values (N_1, \dots, N_5) which characterize the term, and \vec{F} is the five-vector (F_1, \dots, F_5) . The F_j are functions of time, and the angular frequency of the nutation described by the term is given by

$$\omega \equiv \frac{d(\text{ARGUMENT})}{dt}.$$

The frequency thus defined is positive for most terms, and negative for some. Planetary nutation terms differ from the above only in that ARGUMENT = $\sum_{j=1}^{10} N'_j F'_j$ as noted in Table 5.3.

Over time scales involved in nutation studies, the frequency ω is effectively time-independent, and one may write, for the s th term in the nutation series,

$$\text{ARGUMENT} = \omega_s t + \alpha_s.$$

Different tables of nutations in longitude and obliquity do not necessarily assign the same set of multipliers N_j to a particular term in the nutation series. Compare, for instance, the 31.8 day term in Table 5.1 wherein $\vec{N} = (-1, 0, 0, 2, 0)$ with the same term in Seidelmann (1982) where the assignment is $\vec{N} = (1, 0, 0, -2, 0)$. The differences in the assignments arises from the fact that the replacement $\vec{N}_j \rightarrow -\vec{N}_j$ accompanied by reversal of the sign of the coefficient of $\sin(\text{ARGUMENT}_j)$ in the series for $\Delta\psi$ and $\Delta\epsilon$ leaves these series unchanged. This freedom has led to some confusion in the assignment of multipliers of the Delaunay arguments for amplitudes of retrograde and prograde circular nutations.

The nutations in longitude and obliquity at a given frequency ω_s may be viewed as the superposition of a pair of prograde and retrograde circular nutations whose frequencies have the same absolute value, $|\omega_s|$, but with opposite signs. These circular nutation terms may be written as

$$A_s^{pro} e^{-iq_s(\omega_s t + \alpha_s)} \quad \text{and} \quad A_s^{ret} e^{iq_s(\omega_s t + \alpha_s)},$$

where q_s is the sign of ω_s :

$$q_s \omega_s = |\omega_s|.$$

With the convention that the exponential factor involving the frequency ν is to be written as $e^{-i\nu t}$, one sees from the above expressions that the frequency of the prograde nutation, $\omega_s^{pro} = (q_s \omega_s) \equiv |\omega_s|$, is positive, and that of the retrograde nutation is negative ($\omega_s^{ret} = -|\omega_s|$).

Now, given the vector \vec{N} of multipliers of the fundamental arguments for the nutations in longitude and obliquity of frequency ω_s , one can choose multipliers $\vec{N}^{(pro)}$ and $\vec{N}^{(ret)}$ for the corresponding prograde and retrograde nutations in such a manner as to ensure that

$$\omega_s^{pro} \equiv \vec{N}^{pro} \cdot \frac{d\vec{F}}{dt} = |\omega_s|, \quad \omega_s^{ret} \equiv \vec{N}^{ret} \cdot \frac{d\vec{F}}{dt} = -|\omega_s|.$$

This is accomplished by making the assignments

$$\vec{N}^{pro} = q_s \vec{N}; \quad \vec{N}^{ret} = -q_s \vec{N},$$

a practice that will be adhered to in this work. Note that $\vec{N}^{(pro)}$ and $\vec{N}^{(ret)}$ are unaffected by whether \vec{N} or $-\vec{N}$ is used to label the nutations in longitude and obliquity, because on switching from one to the other, the sign of ω_s also is switched simultaneously.

Conversion to Prograde and Retrograde Nutation Amplitudes

With the convention for the time dependence of the circular nutation amplitudes as stated above, the amplitudes of prograde and retrograde circular nutations are written as

$$A_s^{pro} = A_s^{pro\ ip} - iA_s^{pro\ op},$$

$$A_s^{ret} = A_s^{ret\ ip} - iA_s^{ret\ op},$$

where $A_s^{pro\ ip}$ and $A_s^{pro\ op}$ are the in-phase and out-of-phase parts of the prograde nutation with angular frequency $|\omega_s|$ as defined in the foregoing section, and $A_s^{ret\ ip}$ and $A_s^{ret\ op}$ are the in-phase and out-of-phase parts of the retrograde nutation with angular frequency $(-|\omega_s|)$. These amplitudes are related to the coefficients in longitude and obliquity through the following equations (see Defraigne *et al.*, 1995):

$$A_s^{pro\ ip} = -\frac{1}{2} (\Delta\epsilon_s^{ip} - q_s \Delta\psi_s^{ip} \sin \epsilon_0),$$

$$A_s^{ret\ ip} = -\frac{1}{2} (\Delta\epsilon_s^{ip} + q_s \Delta\psi_s^{ip} \sin \epsilon_0),$$

$$A_s^{pro\ op} = \frac{1}{2} (q_s \Delta\epsilon_s^{op} + \Delta\psi_s^{op} \sin \epsilon_0),$$

$$A_s^{ret\ op} = -\frac{1}{2} (q_s \Delta\epsilon_s^{op} - \Delta\psi_s^{op} \sin \epsilon_0).$$

$\Delta\epsilon_s^{ip}$ and $\Delta\epsilon_s$ are the in-phase (cosine) and out-of-phase (sine) parts of the nutation in obliquity for a nutation of frequency ω_s ; $\Delta\psi_s^{ip}$ and $\Delta\psi_s^{op}$ are the in-phase (sine) and out-of-phase (cosine) parts of the nutation in longitude for the same nutation.

The relations stated above are valid when the convention regarding the time dependence as stated in the previous section is followed, *i.e.*, when the time dependence of the prograde amplitude is $e^{-i|\omega_s|t}$ and that of the retrograde amplitude is $e^{i|\omega_s|t}$. However the opposite convention is often used in the literature. The amplitudes to be employed in such a case are the complex conjugates of those given above, *i.e.*, $(A_s^{pro\ ip} + iA_s^{pro\ op})$ goes together with $e^{i|\omega_s|t}$ for the prograde nutation and $(A_s^{ret\ ip} + iA_s^{ret\ op})$ with $e^{-i|\omega_s|t}$ for the retrograde nutation. Since the real parts are to be eventually taken, switching between mutually complex conjugates versions does not affect the results.

Coordinate Transformation Referred to the Nonrotating Origin

Option 2 uses form (2) of the coordinate transformation from the TRS to the CRS

$$[\text{CRS}] = PN''(t)R''(t)W''(t)[\text{TRS}], \quad (2)$$

where the three fundamental components of (2) are given below (Capitaine, 1990)

$$W''(t) = R_3(-s') \cdot R_1(y_p) \cdot R_2(x_p),$$

x_p and y_p being the “polar coordinates” of the CEP in the TRS and s' the accumulated displacement of the terrestrial origin on the true equator due to polar motion. The use of the quantity s' (which is neglected in the classical form (1)) provides an exact realization of the “instantaneous prime meridian.”

$$R''(t) = R_3(-\theta),$$

θ being the stellar angle at date t due to the Earth’s angle of rotation,

$$PN''(t) = R_3(-E) \cdot R_2(-d) \cdot R_3(E) \cdot R_3(S),$$

E and d being such that the coordinates of the CEP in the CRS are $X = \sin d \cos E$, $Y = \sin d \sin E$, $Z = \cos d$ and S being the accumulated rotation (between the epoch and the date t) of the celestial CEO on the true equator due to the celestial motion of the CEP. $PN''(t)$ can be given in an equivalent form involving directly X and Y (to which all the observations of a celestial object from the Earth are actually sensitive) as:

$$PN''(t) = Q_1 = \begin{pmatrix} 1 - aX^2 & -aXY & X \\ -aXY & 1 - aY^2 & Y \\ -X & -Y & 1 - a(X^2 + Y^2) \end{pmatrix} \cdot R_3(s),$$

with $a = 1/(1 + \cos d)$, which can also be written, with sufficient accuracy as $a = 1/2 + 1/8(X^2 + Y^2)$.

The standard values of the parameters to be used in the form (2) of the transformation are detailed below.

The standard pole coordinates to be used for the parameters x_p and y_p (if not estimated from the observations) are those published by the IERS. The quantity s' (of the order of 0.1 mas/cy) is:

$$s' = 0.0015(a_c^2/1.2 + a_a^2)t,$$

a_c and a_a being the average amplitudes (in arc seconds) of the Chandlerian and annual wobbles, respectively in the period considered (Capitaine *et al.*, 1986).

The stellar angle is obtained by the use of the conventional relationship between the stellar angle θ , the hour angle of the CEO and UT1 as given by Capitaine *et al.*, (1986),

$$\theta(T_u) = 2\pi(0.779057273264 + 1.00273781191135448T_u \times 36525),$$

where $T_u = (\text{Julian UT1 date} - 2451545.0)/36525$, and

UT1 = UTC + (UT1-UTC), or equivalently

$$\theta(T_u) = 2\pi(\text{UT1 Julian day number elapsed since } 2451545.0 + 0.779057273264 \\ + 0.00273781191135448T_u \times 36525),$$

the quantity UT1-UTC to be used (if not estimated from the observations) being the IERS value.

The celestial coordinates X and Y of the CEP to be used for consistency with the IAU 1980 theory of nutation are the standard values as derived from the series given in Table 5.4. These developments of the celestial polar coordinates have been derived (Capitaine, 1990) from the previous standard expressions for precession and nutation with a consistency of 5×10^{-5} sec. of arc after a century; such consistency has been numerically checked over two centuries (Gontier, 1990). For observations requiring values of the nutation angles with a milliarcsecond accuracy, it is necessary to add (if those quantities are not estimated from the observations) the IERS published values (observed or predicted) for the “celestial pole offsets” (*i.e.* corrections $dX = \Delta\psi \sin \epsilon_0$ and $dY = \Delta\epsilon$).

For consistency with the IERS 1995 series for nutation as given by Tables 5.2 and 5.3, it is necessary to use the following expressions for X and Y (Capitaine, 1990):

$$X = \sin \omega \sin \psi,$$

$$Y = -\sin \epsilon_0 \cos \omega + \cos \epsilon_0 \sin \omega \cos \psi,$$

where ϵ_0 is the obliquity of the ecliptic at J2000, ω is the inclination of the true equator of date on the fixed ecliptic of epoch and ψ is the longitude, on the ecliptic of epoch of the node of the true equator of date on the fixed ecliptic of epoch; these quantities are such that:

$$\omega = \omega_A + \Delta\epsilon_1, \psi = \psi_A + \Delta\psi_1,$$

where ψ_A and ω_A are the precession quantities in longitude and obliquity (Lieske *et al.* 1977) referred to the ecliptic of epoch and $\Delta\psi_1$, $\Delta\epsilon_1$ are the nutation angles in longitude and obliquity referred to the ecliptic of epoch. $\Delta\psi_1$, $\Delta\epsilon_1$ can be obtained with an accuracy better than one microarcsecond after one century from the nutation angles $\Delta\psi$, $\Delta\epsilon$ in longitude and obliquity referred to the ecliptic of date, following Aoki and Kinoshita (1983) by:

$$\Delta\psi_1 = \frac{(\Delta\psi \sin \epsilon_A \cos \chi_A - \Delta\epsilon \sin \chi_A)}{\sin \omega_A},$$

$$\Delta\epsilon_1 = \Delta\psi \sin \epsilon_A \sin \chi_A + \Delta\epsilon \cos \chi_A,$$

ω_A and ϵ_A being the precession quantities in obliquity referred to ecliptic of epoch and ecliptic of date respectively and χ_A the precession quantity for planetary precession along the equator (Lieske *et al.* 1977).

The standard value of s compatible with the IAU 1980 Theory of Nutation and the Lieske *et al.* (1977) precession can be derived with an accuracy of $5 \times 10^{-5}''$ after a century (Capitaine, 1990) from the following numerical development and the numerical values of X and Y (Table 5.3),

$$s = -XY/2 + 0''.00385t - 0''.07259t^3 - 0''.00264 \sin \Omega - 0''.00006 \sin 2\Omega \\ + 0''.00074t^2 \sin \Omega + 0''.00006t^2 \sin 2(F - D + \Omega)$$

Table 5.4 Series for the celestial coordinates X and Y of the CEP referred to the mean equator and equinox of epoch J2000.0, with t measured in Julian centuries from epoch J2000.0. The terms following the dotted line are identical in Tables 5.1 and 5.4. The signs of the fundamental arguments, periods, and coefficients may differ from the original publication. These have been changed to be consistent with other portions of this chapter.

$$X = 2004''.3109t - 0''.42665t^2 - 0''.198656t^3 + 0''.0000140t^4 \\ + 0''.00006t^2 \cos \Omega + \sin \epsilon_0 \left\{ \sum_{i=1,106} [(A_i + A'_i t) \sin(\text{ARGUMENT}) + A''_i t \cos(\text{ARGUMENT})] \right\} \\ + 0''.00204t^2 \sin \Omega + 0''.00016t^2 \sin 2(F - D + \Omega),$$

$$Y = -0''.00013 - 22''.40992t^2 + 0''.001836t^3 + 0''.0011130t^4 \\ + \sum_{i=1,106} [(B_i + B'_i t) \cos(\text{ARGUMENT}) + B''_i t \sin(\text{ARGUMENT})] \\ - 0''.00231t^2 \cos \Omega - 0''.00014t^2 \cos 2(F - D + \Omega)$$

MULTIPLIERS OF					PERIOD	LONGITUDE (0''.0001)			OBLIQUITY (0''.0001)		
l	l'	F	D	Ω	(days)	A_i	A'_i	A''_i	B_i	B'_i	B''_i
0	0	0	0	1	-6798.4	-171996	-84.2	5173.2	92025	8.9	1529.9
0	0	2	-2	2	182.6	-13187	5.3	322.2	5736	-3.1	117.3
0	0	2	0	2	13.7	-2274	1.0	54.8	977	-0.5	20.2
0	0	0	0	2	-3399.2	2053.2	-1.0	-50.5	-893.7	0.5	-18.3
0	-1	0	0	0	-365.3	-1426	4.3	3.0	54	-0.1	-12.7
1	0	0	0	0	27.6	712	0.1	0.0	-7	0.0	-6.3
0	1	2	-2	2	121.7	-517	1.5	12.6	224	-0.6	4.6
0	0	2	0	1	13.6	-386	-0.4	11.3	200	0.0	3.4
1	0	2	0	2	9.1	-301	0.0	7.3	129	-0.1	2.7
0	-1	2	-2	2	365.2	217	-0.5	-5.3	-95	0.3	-1.9
-1	0	0	2	0	31.8	158	0.0	0.0	-1	0.0	1.4
0	0	2	-2	1	177.8	129	0.1	-4.0	-70	0.0	-1.2
-1	0	2	0	2	27.1	123	0.0	-3.0	-53	0.0	-1.1
1	0	0	0	1	27.7	63	0.1	-1.8	-33	0.0	-0.6
0	0	0	2	0	14.8	63	0.0	0.0	-2	0.0	-0.6
-1	0	2	2	2	9.6	-59	0.0	1.5	26	0.0	0.5
-1	0	0	0	1	-27.4	-58	-0.1	1.8	32	0.0	0.5
1	0	2	0	1	9.1	-51	0.0	1.5	27	0.0	0.5
-2	0	0	2	0	-205.9	-48	0.0	0.0	1	0.0	0.0
-2	0	2	0	1	1305.5	46	0.0	-1.3	-24	0.0	0.0
.....											
0	0	2	2	2	7.1	-38	0.0		16	0.0	
2	0	2	0	2	6.9	-31	0.0		13	0.0	
2	0	0	0	0	13.8	29	0.0		-1	0.0	
1	0	2	-2	2	23.9	29	0.0		-12	0.0	
0	0	2	0	0	13.6	26	0.0		-1	0.0	
0	0	2	-2	0	173.3	-22	0.0		0	0.0	
-1	0	2	0	1	27.0	21	0.0		-10	0.0	
0	2	0	0	0	182.6	17	-0.1		0	0.0	
0	2	2	-2	2	91.3	-16	0.1		7	0.0	
1	0	0	2	1	32.0	16	0.0		-8	0.0	
0	1	0	0	1	386.0	-15	0.0		9	0.0	
1	0	0	-2	1	-31.7	-13	0.0		7	0.0	
0	-1	0	0	1	-346.6	-12	0.0		6	0.0	
2	0	-2	0	0	-1095.2	11	0.0		0	0.0	
-1	0	2	2	1	9.5	-10	0.0		5	0.0	
1	0	2	2	2	5.6	-8	0.0		3	0.0	
0	-1	2	0	2	14.2	-7	0.0		3	0.0	
0	0	2	2	1	7.1	-7	0.0		3	0.0	
1	1	0	-2	0	-34.8	-7	0.0		0	0.0	
0	1	2	0	2	13.2	7	0.0		-3	0.0	
-2	0	0	2	1	-199.8	-6	0.0		3	0.0	
0	0	0	2	1	14.8	-6	0.0		3	0.0	
2	0	2	-2	2	12.8	6	0.0		-3	0.0	
1	0	0	2	0	9.6	6	0.0		0	0.0	
1	0	2	-2	1	23.9	6	0.0		-3	0.0	
0	0	0	-2	1	-14.7	-5	0.0		3	0.0	
0	-1	2	-2	1	346.6	-5	0.0		3	0.0	

2	0	2	0	1	6.9	-5	0.0	3	0.0
1	-1	0	0	0	29.8	5	0.0	0	0.0
1	0	0	-1	0	411.8	-4	0.0	0	0.0
0	0	0	1	0	29.5	-4	0.0	0	0.0
0	1	0	-2	0	-15.4	-4	0.0	0	0.0
1	0	-2	0	0	-26.9	4	0.0	0	0.0
2	0	0	-2	1	212.3	4	0.0	-2	0.0
0	1	2	-2	1	119.6	4	0.0	-2	0.0
1	1	0	0	0	25.6	-3	0.0	0	0.0
1	-1	0	-1	0	-3232.9	-3	0.0	0	0.0
-1	-1	2	2	2	9.8	-3	0.0	1	0.0
0	-1	2	2	2	7.2	-3	0.0	1	0.0
1	-1	2	0	2	9.4	-3	0.0	1	0.0
3	0	2	0	2	5.5	-3	0.0	1	0.0
-2	0	2	0	2	1615.7	-3	0.0	1	0.0
1	0	2	0	0	9.1	3	0.0	0	0.0
-1	0	2	4	2	5.8	-2	0.0	1	0.0
1	0	0	0	2	27.8	-2	0.0	1	0.0
-1	0	2	-2	1	-32.6	-2	0.0	1	0.0
0	-2	2	-2	1	6786.3	-2	0.0	1	0.0
-2	0	0	0	1	-13.7	-2	0.0	1	0.0
2	0	0	0	1	13.8	2	0.0	-1	0.0
3	0	0	0	0	9.2	2	0.0	0	0.0
1	1	2	0	2	8.9	2	0.0	-1	0.0
0	0	2	1	2	9.3	2	0.0	-1	0.0
1	0	0	2	1	9.6	-1	0.0	0	0.0
1	0	2	2	1	5.6	-1	0.0	1	0.0
1	1	0	-2	1	-34.7	-1	0.0	0	0.0
0	1	0	2	0	14.2	-1	0.0	0	0.0
0	1	2	-2	0	117.5	-1	0.0	0	0.0
0	1	-2	2	0	-329.8	-1	0.0	0	0.0
1	0	-2	2	0	32.8	-1	0.0	0	0.0
1	0	-2	-2	0	-9.5	-1	0.0	0	0.0
1	0	2	-2	0	32.8	-1	0.0	0	0.0
1	0	0	-4	0	-10.1	-1	0.0	0	0.0
2	0	0	-4	0	-15.9	-1	0.0	0	0.0
0	0	2	4	2	4.8	-1	0.0	0	0.0
0	0	2	-1	2	25.4	-1	0.0	0	0.0
-2	0	2	4	2	7.3	-1	0.0	1	0.0
2	0	2	2	2	4.7	-1	0.0	0	0.0
0	-1	2	0	1	14.2	-1	0.0	0	0.0
0	0	-2	0	1	-13.6	-1	0.0	0	0.0
0	0	4	-2	2	12.7	1	0.0	0	0.0
0	1	0	0	2	409.2	1	0.0	0	0.0
1	1	2	-2	2	22.5	1	0.0	-1	0.0
3	0	2	-2	2	8.7	1	0.0	0	0.0
-2	0	2	2	2	14.6	1	0.0	-1	0.0
-1	0	0	0	2	-27.3	1	0.0	-1	0.0
0	0	-2	2	1	-169.0	1	0.0	0	0.0
0	1	2	0	1	13.1	1	0.0	0	0.0
-1	0	4	0	2	9.1	1	0.0	0	0.0
2	1	0	-2	0	131.7	1	0.0	0	0.0
2	0	0	2	0	7.1	1	0.0	0	0.0
2	0	2	-2	1	12.8	1	0.0	-1	0.0
2	0	-2	0	1	-943.2	1	0.0	0	0.0
1	-1	0	-2	0	-29.3	1	0.0	0	0.0
-1	0	0	1	1	-388.3	1	0.0	0	0.0
-1	-1	0	2	1	35.0	1	0.0	0	0.0
0	1	0	1	0	27.3	1	0.0	0	0.0
0	0	2	-2	3	177.8	-1.2	0.0	0	0.0

Geodesic Nutation

Fukushima (1991) has pointed out that, if extreme precision is required, the effect of geodesic nutation must be taken into account. For Option (1) this would require a correction in longitude of

$$\Delta\psi_g = -0''000153 \sin l' - 0''000002 \sin 2l',$$

where l' is the mean anomaly of the Sun. For Option (2) it would require a correction to X of

$$\Delta X_g = (-0''.0000609 \sin l' - 0''.0000008 \sin 2l') \sin \epsilon_0.$$

In both cases, the correction would be added to the uncorrected determination of ψ or X .

References

- Aoki, S., Guinot, B., Kaplan, G. H., Kinoshita, H., McCarthy, D. D., and Seidelmann, P. K., 1982, "The New Definition of Universal Time," *Astron. Astrophys.*, **105**, pp. 359–361.
- Aoki, S. and Kinoshita, H., 1983, "Note on the relation between the equinox and Guinot's non-rotating origin," *Celest. Mech.*, **29**, pp. 335–360.
- Capitaine, N., 1990, "The Celestial Pole Coordinates," *Celest. Mech. Dyn. Astr.*, **48**, pp. 127–143.
- Capitaine, N., Guinot, B., and Souchay, J., 1986, "A Non-rotating Origin on the Instantaneous Equator: Definition, Properties and Use," *Celest. Mech.*, **39**, pp. 283–307.
- Capitaine, N. and Chollet, F., 1991, "The use of the nonrotating origin in the computation of apparent places of stars for estimating Earth Rotation Parameters," in *Reference Systems*, J. A. Hughes, C. A. Smith, and G. H. Kaplan (eds), pp. 224–227.
- Capitaine, N. and Gontier A. -M., 1991, "Procedure for VLBI estimates of Earth Rotation Parameter referred to the nonrotating origin," in *Reference Systems*, J. A. Hughes, C. A. Smith, and G. H. Kaplan (eds), pp. 77–84.
- Capitaine, N. and Gontier A. -M., 1993, "Accurate procedure for deriving UT1 at a submilliarcsecond accuracy from Greenwich Sidereal Time or from stellar angle," *Astron. Astrophys.*, **275**, pp. 645–650.
- Defraigne, P., Dehant, V., and Pâquet, P., 1995, "Link between the retrograde-prograde nutations and nutations in obliquity and longitude," *Celest. Mech. Dyn. Astr.*, **62**, pp. 363–376.
- Fukushima, T., 1991, "Geodesic Nutation," *Astron. Astrophys.*, **244**, pp. L11–L12.
- Gilbert, F. and Dziewonski, A. M., 1975, "An Application of Normal Mode Theory to the Retrieval Structure Parameters and Source Mechanisms from Seismic Spectra," *Phil. Trans. Roy. Soc. Lond.*, **A278**, pp. 187–269.
- Gontier, A. -M., 1990, "Tests pour l'application de l'origine nontournante en radioastronomie," in *Journées 1990 Systèmes de Référence spatio-temporels*, pp. 281–286.
- Guinot, B., 1979, "Basic Problems in the Kinematics of the Rotation of the Earth," in *Time and the Earth's Rotation*, D. D. McCarthy and J. D. Pilkington (eds), D. Reidel Publishing Company, pp. 7–18.
- Herring, T., 1996, Private Communication.
- Kinoshita, H., 1977, "Theory of the Rotation of the Rigid Earth," *Celest. Mech.*, **15**, pp. 277–326.

- Lieske, J. H., Lederle, T., Fricke, W., and Morando, B., 1977, “Expression for the Precession Quantities Based upon the IAU (1976) System of Astronomical Constants,” *Astron. Astrophys.*, **58**, pp. 1–16.
- Lieske, J., 1991, Private Communication.
- Mueller, I. I., 1969, *Spherical and Practical Astronomy as applied to Geodesy*, F. Ungar Publishing Co., Inc.
- Seidelmann, P. K., 1982, “1980 IAU Nutation: The Final Report of the IAU Working Group on Nutation,” *Celest. Mech.*, **27**, pp. 79–106.
- Simon, J. L., Bretagnon, P., Chapront, J., Chapront-Touzé, M., Francou, G., Laskar, J., 1994, “Numerical Expressions for Precession Formulae and Mean Elements for the Moon and Planets,” *Astron. Astrophys.*, **282**, pp. 663–683.
- Wahr, J. M., 1981, “The Forced Nutations of an Elliptical, Rotating, Elastic, and Oceanless Earth,” *Geophys. J. Roy. Astron. Soc.*, **64**, pp. 705–727.

CHAPTER 6 GEOPOTENTIAL

The recommended geopotential field is the JGM-3 model (Tapley *et al.*, 1995). The GM_{\oplus} and a_e values reported with JGM-3 ($398600.4415 \text{ km}^3/\text{s}^2$ and 6378136.3 m) should be used as scale parameters with the geopotential coefficients. The recommended $GM_{\oplus} = 398600.4418$ should be used with the two-body term when working with SI units (398600.4415 or 398600.4356 should be used by those still working with TDT or TDB units, respectively). Although the JGM-3 model is given with terms through degree and order 70, only terms through degree and order twenty are required for Lageos.

Values for the C_{21} and S_{21} coefficients are included in the JGM-3 model. The C_{21} and S_{21} coefficients describe the position of the Earth's figure axis. When averaged over many years, the figure axis should closely coincide with the observed position of the rotation pole averaged over the same time period. Any differences between the mean figure and mean rotation pole averaged would be due to long-period fluid motions in the atmosphere, oceans, or Earth's fluid core (Wahr, 1987, 1990). At present, there is no independent evidence that such motions are important. The JGM-3 values for C_{21} and S_{21} give a mean figure axis that corresponds to the mean pole position recommended in Chapter 3 Terrestrial Reference Frame.

This choice for C_{21} and S_{21} is realized as follows. First, to use the geopotential coefficients to solve for a satellite orbit, it is necessary to rotate from the Earth-fixed frame, where the coefficients are pertinent, to an inertial frame, where the satellite motion is computed. This transformation between frames should include polar motion. We assume the polar motion parameters used are relative to the IERS Reference Pole. If \bar{x} and \bar{y} are the angular displacements of the Terrestrial Reference Frame described in Chapter 3 relative to the IERS Reference Pole, then the values

$$\bar{C}_{21} = \sqrt{3}\bar{x}\bar{C}_{20},$$

$$\bar{S}_{21} = -\sqrt{3}\bar{y}\bar{C}_{20},$$

where $\bar{x} = 0.223 \times 10^{-6}$ radians (equivalent to 0.046 arcsec) and $\bar{y} = 1.425 \times 10^{-6}$ radians (equivalent to 0.294 arcsec) (Nerem *et al.*, 1994) are those used in the geopotential model, so that the mean figure axis coincides with the pole described in Chapter 3. This gives normalized coefficients of

$$\bar{C}_{21}(\text{IERS}) = -0.187 \times 10^{-9},$$

$$\bar{S}_{21}(\text{IERS}) = 1.195 \times 10^{-9}.$$

JGM-3 is available via ftp at <ftp.csr.utexas.edu> on the directory `pub/grav` in file `JGM3.GEO.Z`. It can also be accessed by World Wide Web at <http://www.csr.utexas.edu> by clicking the "library of data files" selection.

Effect of Solid Earth Tides

The changes induced by the solid Earth tides in the free space potential are most conveniently modeled as variations in the standard geopotential coefficients C_{nm} and S_{nm} (Eanes *et al.*, 1983). The contributions ΔC_{nm} and ΔS_{nm} from the tides are expressible in terms of the k Love number. The effects of ellipticity and rotation of the Earth on tidal deformations necessitates the use, in general, of three k parameters, $k_{nm}^{(0)}$ and $k_{nm}^{(\pm)}$, to characterize the changes produced in the free space potential by

tides of spherical harmonic degree and order (nm) (Wahr, 1981). Within the diurnal tidal band, for $(mn) = (21)$, these parameters have a strong frequency dependence due to the Nearly Diurnal Free Wobble resonance. Anelasticity of the mantle causes $k_{nm}^{(0)}$ and $k_{nm}^{(\pm)}$ to acquire small imaginary parts (reflecting a phase lag in the deformational response of the Earth to tidal forces), and also gives rise to a further variation with frequency which is particularly pronounced within the long period band. Though modeling of anelasticity at the periods relevant to tidal phenomena (8 hours to 18.6 years) is not yet definitive, it is clear that the magnitudes of the contributions from anelasticity cannot be ignored (see below) Consequently the anelastic Earth model is recommended for use in precise data analysis.

The degree 2 tides produce time dependent changes in C_{2m} and S_{2m} , through $k_{2m}^{(0)}$, which can exceed 10^{-8} in magnitude. They also produce changes exceeding a cutoff of 3×10^{-12} in C_{4m} and S_{4m} through $k_{2m}^{(+)}$. (The direct contributions of the degree 4 tidal potential to these coefficients are negligible.) The only other changes exceeding this cutoff are in C_{3m} and S_{3m} , produced by the degree 3 part of the tide generating potential.

The computation of the tidal contributions to the geopotential coefficients is most efficiently done by a two-step procedure. In Step 1, the $(2m)$ part of the tidal potential is evaluated in the time domain for each m using lunar and solar ephemerides, and the corresponding changes ΔC_{2m} and ΔS_{2m} are computed using frequency independent nominal values k_{2m} for the respective $k_{2m}^{(0)}$. The contributions of the degree 3 tides to C_{3m} and S_{3m} through $k_{3m}^{(0)}$ and also those of the degree 2 tides to C_{4m} and S_{4m} through $k_{2m}^{(+)}$ may be computed by a similar procedure; they are at the level of 10^{-11} .

Step 2 corrects for the deviations of the $k_{21}^{(0)}$ of several of the constituent tides of the diurnal band from the constant nominal value k_{21} assumed for this band in the first step. Similar corrections need to be applied to a few of the constituents of the other two bands also.

With frequency-independent values k_{nm} (**Step 1**), changes induced by the (nm) part of the tide generating potential in the normalized geopotential coefficients having the same (nm) are given in the time domain by

$$\Delta \bar{C}_{nm} - i \Delta \bar{S}_{nm} = \frac{k_{nm}}{2n+1} \sum_{j=2}^3 \frac{GM_j}{GM_{\oplus}} \left(\frac{R_e}{r_j} \right)^{n+1} \bar{P}_{nm}(\sin \Phi_j) e^{-im\lambda_j} \quad (1)$$

(with $S_{n0} = 0$), where

k_{nm} = nominal degree Love number for degree n and order m ,

R_e = equatorial radius of the Earth,

GM_{\oplus} = gravitational parameter for the Earth,

GM_j = gravitational parameter for the Moon ($j = 2$) and Sun ($j = 3$),

r_j = distance from geocenter to Moon or Sun,

Φ_j = body fixed geocentric latitude of Moon or Sun,

λ_j = body fixed east longitude (from Greenwich) of Moon or Sun,

and \bar{P}_{nm} is the normalized associated Legendre function related to the classical (unnormalized) one by

$$\bar{P}_{nm} = N_{nm} P_{nm}, \quad (2a)$$

where

$$N_{nm} = \sqrt{\frac{(n-m)!(2n+1)(2-\delta_{om})}{(n+m)!}}. \quad (2b)$$

Correspondingly, the normalized geopotential coefficients ($\bar{C}_{nm}, \bar{S}_{nm}$) are related to the unnormalized coefficients (C_{nm}, S_{nm}) by

$$C_{nm} = N_{nm} \bar{C}_{nm}, \quad S_{nm} = N_{nm} \bar{S}_{nm}. \quad (3)$$

Equation (1) yields $\Delta\bar{C}_{nm}$ and $\Delta\bar{S}_{nm}$ for both $n = 2$ and $n = 3$ for all m , apart from the corrections for frequency dependence to be evaluated in Step 2. (The particular case $(nm) = (20)$ needs special consideration, however, because it includes a time-independent part which will be discussed below in the section on the permanent tide.)

One further computation to be done in Step 1 is that of the changes in the degree 4 coefficients produced by the degree 2 tides. They are given by

$$\Delta\bar{C}_{4m} - i\Delta\bar{S}_{4m} = \frac{k_{2m}^{(+)}}{5} \sum_{j=2}^3 \frac{GM_j}{GM_{\oplus}} \left(\frac{R_e}{r_j}\right)^3 \bar{P}_{2m}(\sin \Phi_j) e^{-im\lambda_j}, \quad (m = 0, 1, 2), \quad (4)$$

which has the same form as Equation (1) for $n = 2$ except for the replacement of k_{2m} by $k_{2m}^{(+)}$.

The parameter values for the computations of Step 1 are given in Table 6.1. The choice of these nominal values (which are complex for $m = 1$ and $m = 2$ in the anelastic case) has been made so as to minimize the number of terms for which corrections will have to be applied in Step 2. The nominal value for $m = 0$ has to be chosen real because the contribution to \bar{C}_{20} from the imaginary part of $k_{20}^{(0)}$. The frequency dependent values for use in Step 2 are taken from the results of computations by Mathews and Buffett (private communication) using the PREM elastic Earth model with the ocean layer replaced by solid, and for the evaluation of anelasticity effects, the Widmer *et al.* (1991) model of mantle Q . As in Wahr and Bergen (1986), a power law was assumed for the frequency dependence of Q with 200 s as the reference period; the value $\alpha = 0.15$ was used for the power law index. The anelasticity contribution (out of phase and in phase) to the tidal changes in the geopotential coefficients is at the level of one to two percent in-phase, and half to one percent out-of-phase, *i.e.*, of the order of 10^{-10} .

Table 6.1. Nominal values of solid Earth tide external potential Love numbers.

n	m	Elastic Earth		Anelastic Earth		
		k_{nm}	k_{nm}^+	Re k_{nm}	Im k_{nm}	k_{nm}^+
2	0	0.29525	-0.00087	0.30190	-0.00000	-0.00089
2	1	0.29470	-0.00079	0.29830	-0.00144	-0.00080
2	2	0.29801	-0.00057	0.30102	-0.00130	-0.00057
3	0	0.093	...			
3	1	0.093	...			
3	2	0.093	...			
3	3	0.094	...			

The frequency dependence corrections to the $\Delta\bar{C}_{nm}$ and $\Delta\bar{S}_{nm}$ values obtained from Step 1 are computed in **Step 2** as the sum of contributions from a number of tidal constituents belonging to the respective bands. The contribution to $\Delta\bar{C}_{20}$ from the long period tidal constituents of various frequencies f is

$$\text{Re} \sum_{f(2,0)} (A_0 \delta k_f H_f e^{i\theta_f}) = \sum_{f(2,0)} (A_0 H_f (\delta k_f^R \cos \theta_f - \delta k_f^I \sin \theta_f)), \quad (5a)$$

while the contribution to $(\Delta\bar{C}_{21} - i\Delta\bar{S}_{21})$ from the diurnal tidal constituents and to $\Delta\bar{C}_{22} - i\Delta\bar{S}_{22}$ from the semidiurnals are given by

$$\Delta\bar{C}_{2m} - i\Delta\bar{S}_{2m} = \eta_m \sum_{f(2,m)} (A_m \delta k_f H_f) e^{i\theta_f}, \quad (m = 1, 2), \quad (5b)$$

where

$$A_0 = \frac{1}{R_e \sqrt{4\pi}} = 4.4228 \times 10^{-8} \text{ m}^{-1}, \quad (5c)$$

$$A_m = \frac{(-1)^m}{R_e \sqrt{8\pi}} = (-1)^m (3.1274 \times 10^{-8}) \text{ m}^{-1}, \quad (m \neq 0), \quad (5d)$$

$$\eta_1 = -i, \eta_2 = 1, \quad (5e)$$

δk_f = difference between $k_f \equiv k_{2m}^{(0)}$ at frequency f and the nominal value k_{2m} , in the sense $k_f - k_{2m}$,

δk_f^R = real part, and δk_f^I = imaginary part, of δk_f ,

H_f = amplitude (m) of the term at frequency f from the harmonic expansion of the tide generating potential, defined according to the convention of Cartwright and Taylor (1971), and

$$\theta_f = \bar{n} \cdot \bar{\beta} = \sum_{i=1}^6 n_i \beta_i, \quad \text{or} \quad \theta_f = m(\theta_g + \pi) - \bar{N} \cdot \bar{F} = m(\theta_g + \pi) - \sum_{j=1}^5 N_j F_j,$$

where

$\bar{\beta}$ = six-vector of Doodson's fundamental arguments β_i , (τ, s, h, p, N', p_s) ,

\bar{n} = six-vector of multipliers n_i (for the term at frequency f) of the fundamental arguments,

\bar{F} = five-vector of fundamental arguments F_j (the Delaunay variables l, l', F, D, Ω) of nutation theory,

\bar{N} = five-vector of multipliers N_i of the Delaunay variables for the nutation of frequency $-f + d\theta_g/dt$,

and θ_g is the Greenwich Mean Sidereal Time expressed in angle units (*i.e.* $24^h = 360^\circ$; see Chapter 5).

(π in $(\theta_g + \pi)$ is now to be replaced by 180.)

For the fundamental arguments (l, l', F, D, Ω) of nutation theory and the convention followed here in choosing their multipliers N_j , see Chapter 5. For conversion of tidal amplitudes defined according to different conventions to the amplitude H_f corresponding to the Cartwright-Tayler convention, use Table 6.4 given at the end of this Chapter.

The correction due to the K_1 constituent, for example, is obtained as follows, given that $A_m = A_1 = -3.1274 \times 10^{-8}$, $H_f = 0.36871$, and $\theta_f = (\theta_g + \pi)$ for this tide. If anelasticity is ignored, $(k_{21}^{(0)})_{K_1} = 0.25377$, and the nominal value chosen is 0.29470. Hence δk_f is $0.25377 - 0.29470 = -0.04093$, and $A_m(\delta k)_f H_f$ reduces to 472.0×10^{-12} . The corrections to the (21) coefficients then become

$$\begin{aligned} (\Delta \bar{C}_{21})_{K_1} &= 472.0 \times 10^{-12} \sin(\theta_g + \pi), \\ (\Delta \bar{S}_{21})_{K_1} &= 472.0 \times 10^{-12} \cos(\theta_g + \pi). \end{aligned}$$

With anelasticity included, $(k_{21}^{(0)})_{K_1} = 0.25745 - i0.00148$, and on choosing the nominal value as $(0.29830 - i0.00144)$ one obtains the corrections to the coefficients by replacing δk_f in the above calculation by $(-0.04085 - i0.00004)$.

In general, if $\delta k_f = \delta k_f^R + i\delta k_f^I$,

$$\begin{aligned} (\Delta \bar{C}_{2m})_{K_1} &= A_m H_f (\delta k_f^R \sin \theta_f + \delta k_f^I \cos \theta_f), \\ (\Delta \bar{S}_{2m})_{K_1} &= A_m H_f (\delta k_f^R \cos \theta_f - \delta k_f^I \sin \theta_f). \end{aligned}$$

Table 6.2a lists the results for all tidal terms which contribute 10^{-13} or more, after round-off, to the $(nm) = (21)$ geopotential coefficient. A cutoff at this level is used for the individual terms in order that accuracy at the level of 3×10^{-12} be not affected by the accumulated contributions from the numerous smaller terms that are disregarded. The imaginary parts of the contributions are below cutoff and are not listed. Results relating to the (20) and (22) coefficients are presented in Tables (6.2b) and (6.2c), respectively.

Table 6.2a. Amplitudes $(A_1 \delta k_f H_f)$ of the corrections for frequency dependence of $k_{21}^{(0)}$, taking the nominal value k_{21} for the diurnal tides as 0.29470 for the elastic case, and $(0.29830 - i0.00144)$ for the anelastic case. Units: 10^{-12} . Multipliers of the Doodson arguments identifying the tidal terms are given, as also those of the Delaunay variables.

Name	deg/hr	Doodson No.	τ	s	h	p	N'	p_s	ℓ	ℓ'	F	D	Ω	δk_f^{el}	Amp. elas.	δk_f^{anel}	Amp. anel.
	13.39645	135,645	1	-2	0	1	-1	0	1	0	2	0	1	-0.00044	-0.1	-0.00045	-0.1
Q ₁	13.39866	135,655	1	-2	0	1	0	0	1	0	2	0	2	-0.00044	-0.7	-0.00046	-0.7
ρ_1	13.47151	137,455	1	-2	2	-1	0	0	-1	0	2	2	2	-0.00047	-0.1	-0.00049	-0.1
	13.94083	145,545	1	-1	0	0	-1	0	0	0	2	0	1	-0.00081	-1.2	-0.00082	-1.3
O ₁	13.94303	145,555	1	-1	0	0	0	0	0	0	2	0	2	-0.00081	-6.6	-0.00082	-6.7
N τ_1	14.41456	153,655	1	0	-2	1	0	0	1	0	2	-2	2	-0.00167	0.1	-0.00168	0.1
LK ₁	14.48741	155,455	1	0	0	-1	0	0	-1	0	2	0	2	-0.00193	0.4	-0.00193	0.4
NO ₁	14.49669	155,655	1	0	0	1	0	0	1	0	0	0	0	-0.00196	1.3	-0.00197	1.3
	14.49890	155,665	1	0	0	1	1	0	1	0	0	0	1	-0.00197	0.2	-0.00198	0.3
χ_1	14.56955	157,455	1	0	2	-1	0	0	-1	0	0	2	0	-0.00231	0.3	-0.00231	0.3
π_1	14.91787	162,556	1	1	-3	0	0	1	0	1	2	-2	2	-0.00834	-1.9	-0.00832	-1.9
	14.95673	163,545	1	1	-2	0	-1	0	0	0	2	-2	1	-0.01114	0.5	-0.01111	0.5
P ₁	14.95893	163,555	1	1	-2	0	0	0	0	0	2	-2	2	-0.01135	-43.3	-0.01132	-43.2
S ₁	15.00000	164,556	1	1	-1	0	0	1	0	1	0	0	0	-0.01650	2.0	-0.01642	2.0
	15.03886	165,545	1	1	0	0	-1	0	0	0	0	0	-1	-0.03854	-8.8	-0.03846	-8.8
K ₁	15.04107	165,555	1	1	0	0	0	0	0	0	0	0	0	-0.04093	472.0	-0.04085	471.0
	15.04328	165,565	1	1	0	0	1	0	0	0	0	0	1	-0.04365	68.3	-0.04357	68.2
	15.04548	165,575	1	1	0	0	2	0	0	0	0	0	2	-0.04678	-1.6	-0.04670	-1.6
ψ_1	15.08214	166,554	1	1	1	0	0	-1	0	-1	0	0	0	0.23083	-20.8	0.22609	-20.4
ϕ_1	15.12321	167,555	1	1	2	0	0	0	0	0	-2	2	-2	0.03051	-5.0	0.03027	-5.0
θ_1	15.51259	173,655	1	2	-2	1	0	0	1	0	0	-2	0	0.00374	-0.5	0.00371	-0.5
J ₁	15.58545	175,455	1	2	0	-1	0	0	-1	0	0	0	0	0.00329	-2.1	0.00325	-2.1
	15.58765	175,465	1	2	0	-1	1	0	-1	0	0	0	1	0.00327	-0.4	0.00324	-0.4
SO ₁	16.05697	183,555	1	3	-2	0	0	0	0	0	0	-2	0	0.00198	-0.2	0.00195	-0.2
OO ₁	16.13911	185,555	1	3	0	0	0	0	0	0	-2	0	-2	0.00187	-0.7	0.00184	-0.6
	16.14131	185,565	1	3	0	0	1	0	0	0	-2	0	-1	0.00187	-0.4	0.00184	-0.4

Table 6.2b. Corrections for frequency dependence of $k_{20}^{(0)}$ of the zonal tides due to anelasticity. Units: 10^{-12} . The nominal value k_{20} for the zonal tides is taken as 0.30190. The real and imaginary parts δk_f^R and δk_f^I of δk_f are listed, along with the corresponding in phase (ip) amplitude ($A_0 H_f \delta k_f^R$) and out of phase (op) amplitude ($-A_0 H_f \delta k_f^I$) to be used in equation (5a). In the elastic case, $k_{20}^{(0)} = 0.29525$ for all the zonal tides, and no second step corrections are needed.

Name	Doodson No.	deg/hr	τ	s	h	p	N'	p_s	ℓ	ℓ'	F	D	Ω	δk_f^R	Amp. (ip)	δk_f^I	Amp. (op)
		55,565	0.00221	0	0	0	0	1	0	0	0	0	1	0.01347	16.6	-0.00541	-6.7
		55,575	0.00441	0	0	0	2	0	0	0	0	0	2	0.01124	-0.1	-0.00488	0.1
S_a		56,554	0.04107	0	0	1	0	0	-1	0	-1	0	0	0.00547	-1.2	-0.00349	0.8
S_{sa}		57,555	0.08214	0	0	2	0	0	0	0	0	-2	2	0.00403	-5.5	-0.00315	4.3
		57,565	0.08434	0	0	2	0	1	0	0	0	-2	2	0.00398	0.1	-0.00313	-0.1
		58,554	0.12320	0	0	3	0	0	-1	0	-1	-2	2	0.00326	-0.3	-0.00296	0.2
M_{sm}		63,655	0.47152	0	1	-2	1	0	0	1	0	0	-2	0.00101	-0.3	-0.00242	0.7
		65,445	0.54217	0	1	0	-1	0	-1	0	0	0	-1	0.00080	0.1	-0.00237	-0.2

M_m	65,455	0.54438	0 1 0 -1	0 0	-1 0 0 0 0	0.00080	-1.2	-0.00237	3.7
	65,465	0.54658	0 1 0 -1	1 0	-1 0 0 0 1	0.00079	0.1	-0.00237	-0.2
	65,655	0.55366	0 1 0 1	0 0	1 0 -2 0 -2	0.00077	0.1	-0.00236	-0.2
M_{sf}	73,555	1.01590	0 2 -2 0	0 0	0 0 0 -2 0	-0.00009	0.0	-0.00216	0.6
	75,355	1.08875	0 2 0 -2	0 0	-2 0 0 0 0	-0.00018	0.0	-0.00213	0.3
M_f	75,555	1.09804	0 2 0 0	0 0	0 0 -2 0 -2	-0.00019	0.6	-0.00213	6.3
	75,565	1.10024	0 2 0 0	1 0	0 0 -2 0 -1	-0.00019	0.2	-0.00213	2.6
	75,575	1.10245	0 2 0 0	2 0	0 0 -2 0 0	-0.00019	0.0	-0.00213	0.2
M_{stm}	83,655	1.56956	0 3 -2 1	0 0	1 0 -2 -2 -2	-0.00065	0.1	-0.00202	0.2
M_{tm}	85,455	1.64241	0 3 0 -1	0 0	-1 0 -2 0 -2	-0.00071	0.4	-0.00201	1.1
	85,465	1.64462	0 3 0 -1	1 0	-1 0 -2 0 -1	-0.00071	0.2	-0.00201	0.5
M_{sqm}	93,555	2.11394	0 4 -2 0	0 0	0 0 -2 -2 -2	-0.00102	0.1	-0.00193	0.2
M_{qm}	95,355	2.18679	0 4 0 -2	0 0	-2 0 -2 0 -2	-0.00106	0.1	-0.00192	0.1

Table 6.2c. Amplitudes ($A_2 \delta k_f H_f$) of the corrections for frequency dependence of $k_{22}^{(0)}$, taking the nominal value k_{22} for the sectorial tides as 0.29801 for the elastic case, and $(0.30102 - i 0.00130)$ for the anelastic case. Units: 10^{-12} . The corrections are only to the real part, and are the same in both the elastic and the anelastic cases.

Name	Doodson No.	deg/hr	τ	s	h	p	N'	p_s	ℓ	ℓ'	F	D	Ω	δk_f^R	Amp.
N_2	245,655	28.43973	2	-1	0	1	0	0	1	0	2	0	2	0.00006	-0.3
M_2	255,555	28.98410	2	0	0	0	0	0	0	0	2	0	2	0.00004	-1.2

The total variation in geopotential coefficient \bar{C}_{20} is obtained by adding to the result of Step 1 the sum of the contributions from the tidal constituents listed in Table 6.2b computed using equation (5a). The tidal variations in \bar{C}_{2m} and \bar{S}_{2m} for the other m are computed similarly, except that equation (5b) is to be used together with Table 6.2a for $m = 1$ and Table 6.2c for $m = 2$.

Solid Earth Pole Tide

The pole tide is generated by the centrifugal effect of polar motion, characterized by the potential

$$\Delta V = -(\Omega^2 R_e^2 / 2) \sin 2\theta (x_p \cos \lambda - y_p \sin \lambda).$$

(See the section on Deformation due to Polar Motion in Chapter 7 for further details). The deformation which constitutes this tide produces a perturbation $k_2 \Delta V$ in the external potential which is equivalent to changes in the geopotential coefficients C_{21} and S_{21} . Using for k_2 the elastic Earth value 0.2977 appropriate to the polar tide yields

$$\Delta \bar{C}_{21} = -1.290 \times 10^{-9} (x_p),$$

$$\Delta \bar{S}_{21} = 1.290 \times 10^{-9} (y_p),$$

where x_p and y_p are in seconds of arc as defined in Chapter 7. For the anelastic Earth, k_2 has real and imaginary parts $k_2^R = 0.3111$ and $k_2^I = -0.0035$, leading to

$$\begin{aligned}\Delta\bar{C}_{21} &= -1.348 \times 10^{-9}(x_p + 0.0112y_p), \\ \Delta\bar{S}_{21} &= 1.348 \times 10^{-9}(y_p - 0.0112x_p).\end{aligned}$$

Treatment of the Permanent Tide

The degree 2 zonal tide generating potential has a mean (time average) value which is nonzero. This permanent (time independent) potential produces a permanent deformation which is reflected in the static figure of the Earth, and a corresponding time independent contribution to the geopotential which can be considered as part of the adopted value of \bar{C}_{20} , as in the JGM-3 model. Therefore, for $(nm) = (20)$, the zero frequency part should be excluded from the expression (1). Hereafter the symbol $\Delta\bar{C}_{20}$ is reserved for the temporally varying part of the tidal contribution to \bar{C}_{20} ; the expression (1) for $(mn) = (20)$ will be redesignated as \bar{C}_{20}^* .

$$\Delta\bar{C}_{20}^* = \frac{k_{20}}{5} \sum_{j=2}^3 \frac{GM_j}{GM_\oplus} \left(\frac{R_e}{r_j}\right)^3 \bar{P}_{20}(\sin \Phi_j).$$

Its zero frequency part is

$$\langle \Delta\bar{C}_{20} \rangle = A_0 H_0 k_{20} = (4.4228 \times 10^{-8})(-0.31460)k_{20}. \quad (6)$$

To represent the tide induced changes in the (20) geopotential, one should then use only the time variable part

$$\Delta\bar{C}_{20} = \Delta\bar{C}_{20}^* - \langle \Delta\bar{C}_{20} \rangle. \quad (7)$$

In evaluating it, the same value should be used for k_{20} in both $\Delta\bar{C}_{20}^*$ and $\langle \Delta\bar{C}_{20} \rangle$. If the elastic Earth value $k_{20} = 0.29525$ is used, $\langle \Delta\bar{C}_{20} \rangle = -4.108 \times 10^{-9}$, while with the value $k_{20} = 0.30190$ of the anelastic case, $\langle \Delta\bar{C}_{20} \rangle = -4.201 \times 10^{-9}$.

The restitution of the indirect effect of the permanent tide is done to be consistent with the XVIII IAG General Assembly Resolution 16; but to obtain the effect of the permanent tide on the geopotential, one can use the same formula as equation (6) using the fluid limit Love number which is $k = 0.94$.

Effect of the Ocean Tides

The dynamical effects of ocean tides are most easily incorporated by periodic variations in the normalized Stokes' coefficients. These variations can be written as

$$\Delta\bar{C}_{nm} - i\Delta\bar{S}_{nm} = F_{nm} \sum_{s(n,m)} \sum_{+}^{\bar{-}} (C_{snm}^{\pm} \mp iS_{snm}^{\pm}) e^{\pm i\theta_j}, \quad (8)$$

where

$$F_{nm} = \frac{4\pi G \rho_w}{g} \sqrt{\frac{(n+m)!}{(n-m)!(2n+1)(2-\delta_{om})}} \left(\frac{1+k'_n}{2n+1}\right),$$

g and G are given in Chapter 4, $\rho_w = \text{density of seawater} = 1025 \text{ kg m}^{-3}$,

$k'_n = \text{load deformation coefficients}$ ($k'_2 = -0.3075, k'_3 = -0.195, k'_4 = -0.132, k'_5 = -0.1032, k'_6 = -0.0892$),

$C_{snm}^\pm, S_{snm}^\pm = \text{ocean tide coefficients (m) for the tide constituent } s$

$\theta_s = \text{argument of the tide constituent } s \text{ as defined in the solid tide model (Chapter 7)}$.

The summation over + and - denotes the respective addition of the retrograde waves using the top sign and the prograde waves using the bottom sign. The C_{snm}^\pm and S_{snm}^\pm are the coefficients of a spherical harmonic decomposition of the ocean tide height for the ocean tide due to the constituent s of the tide generating potential.

For each constituent s in the diurnal and semi-diurnal tidal bands, these coefficients were obtained from the CSR 3.0 ocean tide height model (Eanes *et al.*, 1996), which was estimated from the TOPEX/Poseidon satellite altimeter data. For each constituent s in the long period band, the self-consistent equilibrium tide model of Ray and Cartwright (1994) was used. The list of constituents for which the coefficients were determined was obtained from the Cartwright and Tayler (1971) expansion of the tide raising potential.

These ocean tide height harmonics are related to the Schwiderski convention (Schwiderski, 1983) according to

$$C_{snm}^\pm - iS_{snm}^\pm = -i\hat{C}_{snm}^\pm e^{i(\epsilon_{snm}^\pm + \chi_s)}, \quad (9)$$

where

$\hat{C}_{snm}^\pm = \text{ocean tide amplitude for constituent } s \text{ using the Schwiderski notation}$,

$\epsilon_{snm}^\pm = \text{ocean tide phase for constituent } s$,

and χ_s is obtained from Table 6.3, with H_s being the Cartwright and Tayler (1971) amplitude at frequency s .

Table 6.3. Values of χ_s for long-period, diurnal and semidiurnal tides.

<u>Tidal Band</u>	<u>$H_s > 0$</u>	<u>$H_s < 0$</u>
Long Period	π	0
Diurnal	$\frac{\pi}{2}$	$-\frac{\pi}{2}$
Semidiurnal	0	π

For clarity, the terms in equation 1 are repeated in both conventions:

$$\Delta\bar{C}_{nm} = F_{nm} \sum_{s(n,m)} [(C_{snm}^+ + C_{snm}^-) \cos \theta_s + (S_{snm}^+ + S_{snm}^-) \sin \theta_s] \quad (10a)$$

or

$$\Delta\bar{C}_{nm} = F_{nm} \sum_{s(n,m)} [\hat{C}_{snm}^+ \sin(\theta_s + \epsilon_{snm}^+ + \chi_s) + \hat{C}_{snm}^- \sin(\theta_s + \epsilon_{snm}^- + \chi_s)], \quad (10b)$$

$$\Delta \bar{S}_{nm} = F_{nm} \sum_{s(n,m)} [(S_{snm}^+ + S_{snm}^-) \cos \theta_s - (C_{snm}^+ - C_{snm}^-) \sin \theta_s] \quad (10c)$$

or

$$\Delta \bar{S}_{nm} = F_{nm} \sum_{s(n,m)} [\hat{C}_{snm}^+ \cos(\theta_s + \epsilon_{snm}^+ + \chi_s) - \hat{C}_{snm}^- \cos(\theta_s + \epsilon_{snm}^- + \chi_s)]. \quad (10d)$$

The orbit element perturbations due to ocean tides can be loosely grouped into two classes. The resonant perturbations arise from coefficients for which the order (m) is equal to the first Doodson's argument multiplier n_1 of the tidal constituent s (See Note), and have periodicities from a few days to a few years. The non-resonant perturbations arise when the order m is not equal to index n_1 . The most important of these are due to ocean tide coefficients for which $m = n_1 + 1$ and have periods of about 1 day.

Certain selected constituents (*e.g.* S_a and S_2) are strongly affected by atmospheric mass distribution (Chapman and Lindzen, 1970). The resonant harmonics (for $m = n_1$) for some of these constituents were determined by their combined effects on the orbits of several satellites. These multi-satellite values then replaced the corresponding values from the CSR3.0 altimetric ocean tide height model.

Based on the predictions of the linear perturbation theory outlined in Casotto (1989), the relevant tidal constituents and spherical harmonics were selected for several geodetic and altimetric satellites. For geodetic satellites, both resonant and non-resonant perturbations were analyzed, whereas for altimetric satellites, only the non-resonant perturbations were analyzed. For the latter, the adjustment of empirical parameters during orbit determination removes the errors in modeling resonant accelerations. The resulting selection of ocean tidal harmonics was then merged into a single recommended ocean tide force model. With this selection the error of omission on TOPEX is approximately 5 mm along-track, and for Lageos it is 2 mm along-track. The recommended ocean tide harmonic selection is available via anonymous ftp from ftp.csr.utexas.edu.

For high altitude geodetic satellites like Lageos, in order to reduce the required computing time, it is recommended that out of the complete selection, only the constituents whose Cartwright and Tayler amplitudes H_s is greater than 0.5 mm be used, with their spherical harmonic expansion terminated at maximum degree and order 8. The omission errors from this reduced selection on Lageos is estimated at approximately 1 cm in the transverse direction for short arcs.

NOTE: The Doodson variable multipliers (\bar{n}) are coded into the argument number (A) after Doodson (1921) as:

$$A = n_1(n_2 + 5)(n_3 + 5)(n_4 + 5)(n_5 + 5)(n_6 + 5).$$

Conversion of tidal amplitudes defined according to different conventions

The definition used for the amplitudes of tidal terms in the recent high-accuracy tables differ from each other and from Cartwright and Tayler (1971). Hartmann and Wenzel (1995) tabulate amplitudes in units of the potential ($m^2 s^{-2}$), while the amplitudes of Roosbeek (1996), which follow the Doodson (1921) convention, are dimensionless. To convert them to the equivalent tide heights H_f of the Cartwright-Tayler convention, multiply by the appropriate factors from Table 6.4. The following values are used for the constants appearing in the conversion factors: Doodson constant $D_1 = 2.63358352855 m^2 s^{-2}$; $g_e \equiv g$ at the equatorial radius = 9.79828685 (from $GM = 3.986004415 \times 10^{14} m^3 s^{-2}$, $R_e = 6378136.55 m$).

Table 6.4 Factors for conversion to Cartwright-Taylor amplitudes from those defined according to Doodson's and Hartmann and Wenzel's conventions

From Doodson	From Hartmann & Wenzel
$f_{20} = -\frac{\sqrt{4\pi} D_1}{\sqrt{5} g_e} = -0.426105$	$f'_{20} = \frac{2\sqrt{\pi}}{g_e} = 0.361788$
$f_{21} = -\frac{2\sqrt{24\pi} D_1}{3\sqrt{5} g_e} = -0.695827$	$f'_{21} = -\frac{\sqrt{8\pi}}{g_e} = -0.511646$
$f_{22} = \frac{\sqrt{96\pi} D_1}{3\sqrt{5} g_e} = 0.695827$	$f'_{22} = \frac{\sqrt{8\pi}}{g_e} = 0.511646$
$f_{30} = -\frac{\sqrt{20\pi} D_1}{\sqrt{7} g_e} = -0.805263$	$f'_{30} = \frac{2\sqrt{\pi}}{g_e} = 0.361788$
$f_{31} = -\frac{\sqrt{720\pi} D_1}{8\sqrt{7} g_e} = -0.603947$	$f'_{31} = -\frac{\sqrt{8\pi}}{g_e} = -0.511646$
$f_{32} = \frac{\sqrt{1440\pi} D_1}{10\sqrt{7} g_e} = 0.683288$	$f'_{32} = \frac{\sqrt{8\pi}}{g_e} = 0.511646$
$f_{33} = -\frac{\sqrt{2880\pi} D_1}{15\sqrt{7} g_e} = -0.644210$	$f'_{33} = -\frac{\sqrt{8\pi}}{g_e} = -0.511646$

References

- Cartwright, D. E. and Taylor, R. J., 1971, "New Computations of the Tide-Generating Potential," *Geophys. J. Roy. Astron. Soc.*, **23**, pp. 45–74.
- Casotto, S., 1989, "Ocean Tide Models for TOPEX Precise Orbit Determination," Ph.D. Dissertation, The Univ. of Texas at Austin.
- Chapman, S. and Lindzen, R., 1970, *Atmospheric Tides*, D. Reidel, Dordrecht.
- Doodson, A. T., 1921, "The Harmonic Development of the Tide-Generating Potential," *Proc. R. Soc. A.*, **100**, pp. 305–329.
- Eanes, R. J., Schutz, B., and Tapley, B., 1983, "Earth and Ocean Tide Effects on Lageos and Starlette," in *Proceedings of the Ninth International Symposium on Earth Tides*, J. T. Kuo (ed), E. Sckweizerbart'sche Verlagabuchhandlung, Stuttgart.
- Eanes, R. J. and Bettadpur, S. V., 1996, "The CSR 3.0 global ocean tide model," in preparation.
- Hartmann, T. and Wenzel, H.-G., 1995, "The HW95 Tidal Potential Catalogue," *Geophys. Res. Lett.*, **22**, pp. 3553–3556.
- Mathews, P. M., Buffett, B. A., and Shapiro, I. I., 1995, "Love numbers for a rotating spheroidal Earth: New definitions and numerical values," *Geophys. Res. Lett.*, **22**, pp. 579–582.
- Nerem, R. S., Lerch, F. J., Marshall, J. A., Pavlis, E. C., Putney, B. H., Tapley, B. D., Eanes, R. J., Ries, J. C., Schutz, B. E., Shum, C. K., Watkins, M. M., Klosko, S. M., Chan, J. C., Luthcke, S. B., Patel, G. B., Pavlis, N. K., Williamson, R. G., Rapp, R. H., Biancale, R., Nouel, F., 1994, "Gravity Model Development for TOPEX/POSEIDON: Joint Gravity Models 1 and 2," *J. Geophys. Res.*, **99**, pp. 24421–24447.
- Ray, R. D. and Cartwright, D. E., 1994, "Satellite altimeter observations of the M_f and M_m ocean tides, with simultaneous orbit corrections," *Gravimetry and Space Techniques Applied to Geodynamics and Ocean Dynamics*, Geophysical Monograph 82, IUGG Volume 17, pp. 69–78.

- Roosbeek, F., 1996, "RATGP95: a harmonic development of the tide-generating potential using an analytical method," *Geophys. J. Int.*, **126**, pp. 197–204.
- Schwiderski, E., 1983, "Atlas of Ocean Tidal Charts and Maps, Part I: The Semidiurnal Principal Lunar Tide M2," *Marine Geodesy*, **6**, pp. 219–256.
- Tapley, B. D., M. M. Watkins, J. C. Ries, G. W. Davis, R. J. Eanes, S. R. Poole, H. J. Rim, B. E. Schutz, C. K. Shum, R. S. Nerem, F. J. Lerch, J. A. Marshall, S. M. Klosko, N. K. Pavlis, and R. G. Williamson, 1995, "The JGM-3 Gravity Model," to be submitted to *J. Geophys. Res.*
- Wahr, J. M., 1981, "The Forced Nutations of an Elliptical, Rotating, Elastic, and Oceanless Earth," *Geophys. J. Roy. Astron. Soc.*, **64**, pp. 705–727.
- Wahr, J., 1987, "The Earth's C_{21} and S_{21} gravity coefficients and the rotation of the core," *Geophys. J. Roy. Astr. Soc.*, **88**, pp. 265–276.
- Wahr, J., 1990, "Corrections and Update to 'The Earth's C_{21} and S_{21} gravity coefficients and the rotation of the core'," *Geophys. J. Int.*, **101**, pp. 709–711.
- Wahr, J. and Z. Bergen, 1986, "The effects of mantle elasticity on nutations, Earth tides, and tidal variations in the rotation rate" *Geophys. J. R. Astr. Soc.*, 633–668.
- Widmer, R., G. Masters, and F. Gilbert, 1991, "Spherically symmetric attenuation within the Earth from normal mode data", *Geophys. J. Int.*, **104**, pp. 541–553.

CHAPTER 7 SITE DISPLACEMENT

Local Site Displacement due to Ocean Loading

Local site displacement is understood as an effect of (visco-) elastic deformation of the Earth in response to time-varying surface loads. The reference point of zero deformation is the joint mass center of the solid Earth and the load, while the sites are attached to the solid Earth. This convention implies that the rigid body translation of the solid Earth that counterbalances the motion of the load's mass center is not contained in the local displacement model. This convention follows strictly Farrell (1972).

Ocean Loading

Three dimensional site displacements due to ocean tide loading are computed using the following scheme. Let Δc denote a displacement component (radial, west, south) at a particular site and time t . Let W denote the tide generating potential (*e.g.* Tamura, 1987; Cartwright and Tayler, 1971; Cartwright and Edden, 1973),

$$W = g \sum_j K_j P_2^{m_j}(\cos \psi) \cos(\omega_j t + \chi_j + m_j \lambda), \quad (1)$$

where only degree two harmonics are retained. The symbols designate colatitude ψ , longitude λ , tidal angular velocity ω_j , amplitude K_j and the astronomical argument χ_j at $t = 0^h$. Spherical harmonic order m_j distinguishes the fundamental bands, *i. e.* long-period ($m = 0$), diurnal ($m = 1$) and semi-diurnal ($m = 2$). The parameters K_j and ω_j are used to obtain the most completely interpolated form

$$\Delta c = \sum_j a_{cj} \cos(\omega_j t + \chi_j - \phi_{cj}), \quad (2)$$

with

$$a_{cj} \cos \phi_{cj} = K_j \left[\frac{A_{ck} \cos \Phi_{ck}}{\bar{K}_k} (1-p) + \frac{A_{c,k+1} \cos \Phi_{c,k+1}}{\bar{K}_{k+1}} p \right],$$

$$a_{cj} \sin \phi_{cj} = K_j \left[\frac{A_{ck} \sin \Phi_{ck}}{\bar{K}_k} (1-p) + \frac{A_{c,k+1} \sin \Phi_{c,k+1}}{\bar{K}_{k+1}} p \right].$$

For each site, the amplitudes A_{ck} and phases Φ_{ck} , $1 \leq k \leq 11$, are taken from Table 7.1. For clarity symbols written with bars overhead designate tidal potential quantities associated with the small set of partial tides represented in the table. These are the semi-diurnal waves M_2, S_2, N_2, K_2 , the diurnal waves K_1, O_1, P_1, Q_1 , and the long-period waves M_f, M_m , and S_{sa} .

Interpolation is possible only within a fundamental band, *i.e.* we demand

$$\bar{m}_k = m_j = \bar{m}_{k+1}. \quad (3)$$

Then

$$p = \frac{\omega_j - \bar{\omega}_k}{\bar{\omega}_{k+1} - \bar{\omega}_k}, \quad \bar{\omega}_k \leq \omega_j \leq \bar{\omega}_{k+1}.$$

If no $\bar{\omega}_k$ or $\bar{\omega}_{k+1}$ can be found meeting (3), p is set to zero or one, respectively.

A shorter form of (2) is obtained if the summation considers only the tidal species of Table 7.1 and corrections for the modulating effect of the lunar node. Then,

$$\Delta c = \sum_j f_j A_{ej} \cos(\omega_j t + \chi_j + u_j - \Phi_{ej}), \quad (4)$$

where f_j and u_j depend on the longitude of the lunar node according to Table 26 of Doodson (1928). The astronomical arguments needed in (4) can be computed with subroutine ARG below.

```

C  SUBROUTINE ARG(IYEAR, DAY, ANGLE)
C
C  COMPUTES THE ANGULAR ARGUMENT WHICH DEPENDS ON TIME FOR 11
C  TIDAL ARGUMENT CALCULATIONS
C
C
C  ORDER OF THE 11 ANGULAR QUANTITIES IN VECTOR ANGLE
C
C  01-M2  02-S2
C  03-N2  04-K2
C  05-K1  06-01
C  07-P1  08-Q1
C  09-Mf  10-Mm
C  11-Ssa
C
C  TAKEN FROM 'TABLE 1 CONSTANTS OF MAJOR TIDAL MODES'
C  WHICH DR. SCHWIDERSKI SENDS ALONG WITH HIS TAPE OF TIDAL
C  AMPLITUDES AND PHASES
C
C
C  INPUT--
C
C  IYEAR - EX. 79 FOR 1979
C  DAY - DAY OF YEAR GREENWICH TIME
C  EXAMPLE 32.5 FOR FEB 1 12 NOON
C  1.25 FOR JAN 1 6 AM
C
C  OUTPUT--
C
C  ANGLE - ANGULAR ARGUMENT FOR SCHWIDERSKI COMPUTATION
C
C*****
C
C
C  C A U T I O N
C
C  OCEAN LOADING PHASES COMPUTED FROM SCHWIDERSKI'S MODELS
C  REFER TO THE PHASE OF THE ASSOCIATED SOLID EARTH TIDE
C  GENERATING POTENTIAL AT THE ZERO MERIDIAN ACCORDING TO
C

```



```

C OL_DR = OL_AMP X COS (SE_PHASE" - OL_PHASE)
C
C WHERE OL = OCEAN LOADING TIDE,
C SE = SOLID EARTH TIDE GENERATING POTENTIAL.
C
C IF THE HARMONIC TIDE DEVELOPMENT OF CARTWRIGHT, ET AL.
C (= CTE) (1971, 1973) IS USED, MAKE SURE THAT SE_PHASE"
C TAKES INTO ACCOUNT
C
C (1) THE SIGN OF SE_AMP IN THE TABLES OF CARTWRIGHT ET AL.
C
C (2) THAT CTE'S SE_PHASE REFERS TO A SINE RATHER THAN A
C COSINE FUNCTION IF (N+M) = (DEGREE + ORDER) OF THE
C TIDE SPHERICAL HARMONIC IS ODD.
C
C I.E. SE_PHASE" = TAU(T) N1 + S(T) N2 + H(T) N3
C + P(T) N4 + N'(T) N5 + PS(T) N6
C + PI IF CTE'S AMPLITUDE COEFFICIENT < 0
C + PI/2 IF (DEGREE + N1) IS ODD
C
C WHERE TAU ... PS = ASTRONOMICAL ARGUMENTS,
C N1 ... N6 = CTE'S ARGUMENT NUMBERS.
C
C MOST TIDE GENERATING SOFTWARE COMPUTE SE_PHASE" (FOR
C USE WITH COSINES).
C
C THIS SUBROUTINE IS VALID ONLY AFTER 1973.
C
C*****
SUBROUTINE ARG(IYEAR,DAY,ANGLE)
IMPLICIT DOUBLE PRECISION (A-H,O-Z)
REAL ANGFAC(4,11)
DIMENSION ANGLE(11),SPEED(11)
C
C SPEED OF ALL TERMS IN RADIANS PER SEC
C
EQUIVALENCE (SPEED(1),SIGM2),(SPEED(2),SIGS2),(SPEED(3),SIGN2)
EQUIVALENCE (SPEED(4),SIGK2),(SPEED(5),SIGK1),(SPEED(6),SIGO1)
EQUIVALENCE (SPEED(7),SIGP1),(SPEED(8),SIGQ1),(SPEED(9),SIGMF)
EQUIVALENCE (SPEED(10),SIGMM),(SPEED(11),SIGSSA)
DATA SIGM2/1.40519D-4/
DATA SIGS2/1.45444D-4/
DATA SIGN2/1.37880D-4/
DATA SIGK2/1.45842D-4/
DATA SIGK1/.72921D-4/
DATA SIGO1/.67598D-4/
DATA SIGP1/.72523D-4/
DATA SIGQ1/.64959D-4/
DATA SIGMF/.053234D-4/

```

```

DATA SIGMM/.026392D-4/
DATA SIGSSA/.003982D-4/
DATA ANGFAC/2.E0,-2.E0,0.E0,0.E0,4*0.E0,
. 2.E0,-3.E0,1.E0,0.E0,2.E0,3*0.E0,
. 1.E0,2*0.E0,.25E0,1.E0,-2.E0,0.E0,-.25E0,
. -1.E0,2*0.E0,-.25E0,1.E0,-3.E0,1.E0,-.25E0,
. 0.E0,2.E0,2*0.E0,0.E0,1.E0,-1.E0,0.E0,
. 2.E0,3*0.E0/
DATA TWOPI/6.28318530718D0/
DATA DTR/.174532925199D-1/

C
C DAY OF YEAR
C
C ID=DAY
C
C FRACTIONAL PART OF DAY IN SECONDS
C
C FDAY=(DAY-ID)*86400.DO
C ICAPD=ID+365*(IYEAR-75)+((IYEAR-73)/4)
C CAPT=(27392.500528D0+1.000000035D0*ICAPD)/36525.DO
C
C MEAN LONGITUDE OF SUN AT BEGINNING OF DAY
C
C HO=(279.69668D0+(36000.768930485D0+3.03D-4*CAPT)*CAPT)*DTR
C
C MEAN LONGITUDE OF MOON AT BEGINNING OF DAY
C
C SO=(((1.9D-6*CAPT-.001133D0)*CAPT+481267.88314137D0)*CAPT
. +270.434358D0)*DTR
C
C MEAN LONGITUDE OF LUNAR PERIGEE AT BEGINNING OF DAY
C
C PO=((-1.2D-5*CAPT-.010325D0)*CAPT+4069.0340329577D0)*CAPT
. +334.329653D0)*DTR
C DO 500 K=1,11
C ANGLE(K)=SPEED(K)*FDAY+ANGFAC(1,K)*HO+ANGFAC(2,K)*SO
. +ANGFAC(3,K)*PO+ANGFAC(4,K)*TWOPI
C ANGLE(K)=DMOD(ANGLE(K),TWOPI)
C IF(ANGLE(K).LT.0.DO)ANGLE(K)=ANGLE(K)+TWOPI
500 CONTINUE
RETURN
END

```

Table 7.1 is available electronically by anonymous ftp to [maia.usno.navy.mil](ftp://maia.usno.navy.mil) or <ftp://gere.oso.chalmers.se/~pub/hgs/oload/README>. For sites not contained in the list the following is recommended: If the distance to the nearest site contained in the table is less than ten km, its data can be substituted. In other cases, coefficients and/or software can be requested from hgs@oso.chalmers.se (Hans-Georg Scherneck). The Tamura tide potential is available from the International Centre for Earth Tides, Observatoire Royal de Belgique, Bruxelles.

The coefficients of Table 7.1 have been computed according to Scherneck (1983, 1991). Tangential displacements are to be taken positive in west and south directions. The ocean tide maps adopted are due to LeProvost *et al.* (1994), Schwiderski (1983), Schwiderski and Szeto (1981), and Flather (1981). Refined coastlines have been derived from the topographic data sets ETOPO5 and Terrain Base (Row *et al.*, 1995) of the National Geophysical Data Center, Boulder, CO. Ocean tide mass budgets have been constrained using a uniform co-oscillating oceanic layer. Load convolution employed a disk-integrating Green's function method (Farrell, 1972; Zschau, 1983; Scherneck, 1990). An assessment of the accuracy of the loading model is given in Scherneck (1993). Adoption of more recent ocean tide results drawing from TOPEX/POSEIDON results is currently under consideration.

Table 7.1 Sample of ocean loading table file. Each site record shows a header with the site name, the CDP monument number, geographic coordinates and comments. First three rows of numbers designate amplitudes (meter), radial, west, south, followed by three lines with the corresponding phase values (degrees).

Columns designate partial tides $M_2, S_2, N_2, K_2, K_1, O_1, P_1, Q_1, M_f, M_m,$ and S_{sa} .

\$\$

ONSALA60 7213

\$\$

\$\$\$ Computed by H.G. Scherneck, Uppsala University, 1989

\$\$\$ ONSALA 7213 lon/lat: 11.9263 57.3947

.00384	.00091	.00084	.00019	.00224	.00120	.00071	.00003	.00084	.00063	.00057
.00124	.00034	.00031	.00009	.00042	.00041	.00015	.00006	.00018	.00010	.00010
.00058	.00027	.00021	.00008	.00032	.00017	.00009	.00004	.00007	.00001	.00020
-56.0	-46.1	-90.7	-34.4	-44.5	-123.2	-49.6	178.4	14.9	37.3	24.6
75.4	97.6	40.8	94.8	119.0	25.4	98.7	-14.1	-177.0	-126.7	-175.8
84.2	131.3	77.7	103.9	17.2	-55.0	25.2	-165.0	173.3	121.8	91.3

Effects of the Solid Earth Tides

Site displacements caused by tides of spherical harmonic degree and order (nm) are characterized by the Love number h_{nm} and the Shida number l_{nm} . The effective values of these numbers depend on station latitude and tidal frequency (Wahr, 1981). This dependence is a consequence of the ellipticity and rotation of the Earth, and includes a strong frequency dependence within the diurnal band due to the Nearly Diurnal Free Wobble resonance. A further frequency dependence, which is most pronounced in the long period tidal band, arises from mantle anelasticity which leads to corrections to the elastic Earth Love numbers; these corrections have a small imaginary part and cause the tidal displacements to lag slightly behind the tide generating potential. All these effects need to be taken into account when an accuracy of 1 *mm* is desired in determining station positions.

In order to account for the latitude dependence of the effective Love and Shida numbers, the representation in terms of multiple h and l parameters employed by Mathews *et al.* (1995) is used. In this representation, parameters $h^{(0)}$ and $l^{(0)}$ play the roles of h_{2m} and l_{2m} , while the latitude dependence is expressed in terms of additional parameters $h^{(2)}, h',$ and $l^{(1)}, l^{(2)}, l'$. These parameters are defined through their contributions to the site displacement as given by equations (5) below. Their numerical values as listed in Mathews *et al.* (1995) have since been revised, and the new values, presented in Table 7.2 are used here. These values pertain to the elastic Earth and anelasticity models referred to in Chapter 6.

The vector displacement due to a tidal term of frequency f is given in terms of the several parameters by the following expressions that result from evaluation of the defining equation (6) of Mathews *et al.* (1995):

For a long-period tide of frequency f :

$$\begin{aligned} \Delta \vec{r}_f = \sqrt{\frac{5}{4\pi}} H_f \left\{ \left[h(\phi) \left(\frac{3}{2} \sin^2 \phi - \frac{1}{2} \right) + \sqrt{\frac{4\pi}{5}} h' \right] \cos \theta_f \hat{r} + 3l(\phi) \sin \phi \cos \phi \cos \theta_f \hat{n} \right. \\ \left. + \cos \phi \left[3l^{(1)} \sin^2 \phi - \sqrt{\frac{4\pi}{5}} l' \right] \sin \theta_f \hat{e} \right\}. \end{aligned} \quad (5a)$$

For a diurnal tide of frequency f :

$$\begin{aligned} \Delta \vec{r}_f = -\sqrt{\frac{5}{24\pi}} H_f \left\{ h(\phi) 3 \sin \phi \cos \phi \sin(\theta_f + \lambda) \hat{r} \right. \\ \left. + \left[3l(\phi) \cos 2\phi - 3l^{(1)} \sin^2 \phi + \sqrt{\frac{24\pi}{5}} l' \right] \sin(\theta_f + \lambda) \hat{n} \right. \\ \left. + \left[\left(3l(\phi) - \sqrt{\frac{24\pi}{5}} l' \right) \sin \phi - 3l^{(1)} \sin \phi \cos 2\phi \right] \cos(\theta_f + \lambda) \hat{e} \right\}. \end{aligned} \quad (5b)$$

For a semidiurnal tide of frequency f :

$$\begin{aligned} \Delta \vec{r}_f = \sqrt{\frac{5}{96\pi}} H_f \{ [h(\phi) 3 \cos^2 \phi \cos(\theta_f + 2\lambda) \hat{r} - 6 \sin \phi \cos \phi [l(\phi) + l^{(1)}] \cos(\theta_f + 2\lambda) \hat{n} \\ - 6 \cos \phi [l(\phi) + l^{(1)} \sin^2 \phi] \sin(\theta_f + 2\lambda) \hat{e} \}. \end{aligned} \quad (5c)$$

In the above expressions,

$$h(\phi) = h^{(0)} + h^{(2)}[(3/2) \sin^2 \phi - 1/2], \quad l(\phi) = l^{(0)} + l^{(2)}[(3/2) \sin^2 \phi - 1/2], \quad (6)$$

H_f = amplitude (m) of the tidal term of frequency f ,

ϕ = geocentric latitude of station,

λ = east longitude of station,

θ_f = tide argument for tidal constituent with frequency f ,

\hat{e} = unit vector in the east direction,

\hat{n} = unit vector at right angles to \hat{r} in the northward direction.

The convention used in defining the tidal amplitude H_f is as in Cartwright and Taylor (1971). To convert amplitudes defined according to other conventions that have been employed in recent more accurate tables, use the conversion factors given in Chapter 6, Table 6.4.

Equations (5) assume that the Love and Shida number parameters are all real. Generalization to the case of complex parameters (anelastic earth) is done simply by making the following replacements for the combinations $L \cos(\theta_f + m\lambda)$ and $L \sin(\theta_f + m\lambda)$, wherever they occur in those equations:

$$L \cos(\theta_f + m\lambda) \rightarrow L^R \cos(\theta_f + m\lambda) - L^I \sin(\theta_f + m\lambda), \quad (7a)$$

$$L \sin(\theta_f + m\lambda) \rightarrow L^R \sin(\theta_f + m\lambda) + L^I \cos(\theta_f + m\lambda), \quad (7b)$$

where L is a generic symbol for $h(\phi)$, h' , $l(\phi)$, $l^{(1)}$, and l' , and L^R and L^I stand for their respective real and imaginary parts. Table 7.2 lists the values of the Love and Shida number parameters. The Earth model on which they are based is the 1 sec PREM, modified by replacement of the ocean layer by solid (Dehant, 1987, Wang, 1994) and by adjustment of the fluid core ellipticity to make the FCN period = 430 sidereal days as inferred from the resonance in nutations. The tidal frequencies shown in the table are in cycles per sidereal day (*cpsd*). Periods, in solar days, of the nutations associated with the diurnal tides are also shown.

Table 7.2. Displacement Love number parameters for degree 2 tides. Quantities with subscripts *elas* (*anelas*) are computed ignoring (including) anelasticity effects. Superscripts *R* and *I* identify the real and imaginary parts, respectively.

Name	Period	Frequency	$h_{elas}^{(0)}$	$h_{anelas}^{(0)R}$	$h_{anelas}^{(0)I}$	$h^{(2)}$	h'
Semidiurnal		-2 <i>cpsd</i>	.6026	.6078	-.0022	-.0006	
Diurnal							
Q ₁	9.13	-0.89080	.5971	.6033	-.0025	-.0006	
145,545	13.63	-0.92685	.5964	.6026	-.0025	-.0006	
O ₁	13.66	-0.92700	.5964	.6026	-.0025	-.0006	
NO ₁	27.55	-0.96381	.5941	.6003	-.0025	-.0006	
π ₁	121.75	-0.99181	.5813	.5876	-.0025	-.0007	
P ₁	182.62	-0.99454	.5753	.5816	-.0025	-.0007	
165,545	6798.38	-0.99985	.5214	.5280	-.0027	-.0007	
K ₁	infinity	-1.00000	.5166	.5232	-.0027	-.0008	
165,565	-6798.38	-1.00015	.5112	.5178	-.0027	-.0008	
ψ ₁	-365.26	-1.00273	1.0582	1.0534	.0020	-.0001	
φ ₁	-182.62	-1.00546	.6589	.6644	-.0022	-.0006	

Long period							
55,565	6798.38	.000015	.5998	.6344	-.0093	-.0006	.0001
S_{sa}	182.62	.000546	.5998	.6182	-.0054	-.0006	.0001
M_m	27.55	.003619	.5998	.6126	-.0041	-.0006	.0001
M_f	13.66	.007300	.5998	.6109	-.0037	-.0006	.0001
75,565	13.63	.007315	.5998	.6109	-.0037	-.0006	.0001

Name	Period	Frequency	$l_{elas}^{(0)}$	$l_{anelas}^{(0)R}$	$l_{anelas}^{(0)I}$	$l^{(1)}$	$l^{(2)}$	l'
Semidiurnal								
		-2 <i>cpsd</i>	.0831	.0847	-.0007	.0024	.0002	
Diurnal								
Q_1	9.13	-0.89080	.0829	.0848	-.0007	.0012	.0002	-.0002
145,545	13.63	-0.92685	.0829	.0848	-.0007	.0012	.0002	-.0002
O_1	13.66	-0.92700	.0829	.0848	-.0007	.0012	.0002	-.0002
M_1	27.55	-0.96381	.0830	.0849	-.0007	.0012	.0002	-.0002
π_1	121.75	-0.99181	.0834	.0853	-.0007	.0012	.0002	-.0002
P_1	182.62	-0.99454	.0836	.0855	-.0007	.0012	.0002	-.0002
165,545	6798.38	-0.99985	.0853	.0871	-.0007	.0011	.0002	-.0003
K_1	infinity	-1.00000	.0854	.0872	-.0007	.0011	.0002	-.0003
165,565	-6798.38	-1.00015	.0856	.0874	-.0007	.0011	.0002	-.0003
ψ_1	-365.26	-1.00273	.0684	.0710	-.0010	.0019	.0002	.0001
ϕ_1	-182.62	-1.00546	.0810	.0829	-.0008	.0013	.0002	-.0002
Long period								
55,565	6798.38	.000015	.0831	.0936	-.0028	.0000	.0002	
S_{sa}	182.62	.000546	.0831	.0886	-.0016	.0000	.0002	
M_m	27.55	.003619	.0831	.0870	-.0012	.0000	.0002	
M_f	13.66	.007300	.0831	.0864	-.0011	.0000	.0002	
75,565	13.63	.007315	.0831	.0864	-.0011	.0000	.0002	

Computation of the variations of station coordinates due to solid Earth tides, like that of geopotential variations, is done most efficiently by the use of a two-step procedure. The evaluations in the first step use the expression in the time domain for the full degree 2 tidal potential or for the parts that pertain to particular bands ($m = 0, 1$, or 2). Nominal values used for the Love and Shida numbers h_{2m} and l_{2m} are common to all the tidal constituents involved in the potential and to all stations. They are chosen with reference to the values in Table 7.2 so as to minimize the computational effort needed in Step 2. Along with expressions for the dominant contributions from $h^{(0)}$ and $l^{(0)}$ to the tidal displacements, relatively small contributions from some of the other parameters are included in Step 1 for reasons of computational efficiency. The displacements caused by the degree 3 tides are also computed in the first step, using constant values for h_3 and l_3 .

Corrections to the results of the first step are needed to take account of the frequency dependent deviations of the Love and Shida numbers from their respective nominal values, and also to compute

the out of phase contributions from the zonal tides. The scheme of computation is outlined in the chart below.

CORRECTIONS FOR THE STATION TIDAL DISPLACEMENTS

Step 1 : Corrections to be computed in the time domain

in phase	for degree 2 and 3 . for degree 2 → eq (8)	Nominal values $h_2 \rightarrow h(\phi) = h^{(0)} + h^{(2)}[(3 \sin^2 \phi - 1)/2]$ $l_2 \rightarrow l(\phi) = l^{(0)} + l^{(2)}[(3 \sin^2 \phi - 1)/2]$
	elastic	$h^{(0)} = 0.6026, h^{(2)} = -0.0006; l^{(0)} = 0.0831, l^{(2)} = 0.0002$
	anelastic	$h^{(0)} = 0.6078, h^{(2)} = -0.0006; l^{(0)} = 0.0847, l^{(2)} = 0.0002$
	. for degree 3 → eq (9)	$h_3 = 0.292$ and $l_3 = 0.015$
out-of-phase	for degree 2 only . diurnal tides → eq (13) . semi-diurnal tides → eq (14)	Nominal values $h^I = -0.0025$ and $l^I = -0.0007$ $h^I = -0.0022$ and $l^I = -0.0007$
contribution from latitude dependence	. diurnal tides → eq (11) . semi-diurnal tides → eq (12)	Nominal values $l^{(1)} = 0.0012$ $l^{(1)} = 0.0024$

Step 2 : Corrections to be computed in the frequency domain and to be added to results of Step 1

in phase for degree 2	. diurnal tides → eqs (15) → Sum over all the components of Table 7.3a . semi-diurnal tides negligible
in phase and out of phase for degree 2	. long-period tides → eqs (16) → Sum over all the components of Table 7.3b

Displacement due to degree 2 tides, with nominal values for $h_{2m}^{(0)}$ and $l_{2m}^{(0)}$

The first stage of the **Step 1** calculations employs real nominal values h_2 and l_2 common to all the degree 2 tides for the Love and Shida numbers. It is found to be computationally most economical to choose these to be the values for the semidiurnal tides (which have very little intraband variation). For the same reason, the nominal values used when anelasticity is included are different from the elastic case. (Anelasticity contributions are at the one percent level, which is about 4 mm in the radial displacement due to the full degree 2 tide.) The out of phase contributions due to anelasticity are dealt with separately below.

On using the nominal values, the vector displacement of the station due to the degree 2 tides is given by

$$\Delta \vec{r} = \sum_{j=2}^3 \frac{GM_j R_e^4}{GM_{\oplus} R_j^3} \left\{ h_2 \hat{r} \left(\frac{3}{2} (\hat{R}_j \cdot \hat{r})^2 - \frac{1}{2} \right) + 3l_2 (\hat{R}_j \cdot \hat{r}) [\hat{R}_j - (\hat{R}_j \cdot \hat{r}) \hat{r}] \right\}, \quad (8)$$

where $h_{22}^{(0)}$ and $l_{22}^{(0)}$ of the semidiurnal tides are chosen as the nominal values h_2 and l_2 . These values depend on whether anelasticity is included in the computation or not, but no imaginary parts are included at this stage. In equation (8),

GM_j = gravitational parameter for the Moon ($j = 2$) or the Sun ($j = 3$),

GM_{\oplus} = gravitational parameter for the Earth,

\hat{R}_j, R_j = unit vector from the geocenter to Moon or Sun and the magnitude of that vector,

R_e = Earth's equatorial radius,

\hat{r}, r = unit vector from the geocenter to the station and the magnitude of that vector,

h_2 = nominal degree 2 Love number,

l_2 = nominal degree 2 Shida number.

Note that the part proportional to h_2 gives the radial (not vertical) component of the tide-induced station displacement, and the terms in l_2 represent the vector displacement transverse to the radial direction (and not in the horizontal plane).

The computation just described may be generalized to include the latitude dependence arising through $h^{(2)}$ by simply adding $h^{(2)}[(3/2)\sin^2 \phi - (1/2)]$ to the constant nominal value given above, with $h^{(2)} = -0.0006$. The addition of a similar term (with $l^{(2)} = 0.0002$) to the nominal value of l_2 takes care of the corresponding contribution to the transverse displacement. The resulting incremental displacements are small, not exceeding 0.4 *mm* radially and 0.2 *mm* in the transverse direction.

Displacements due to degree 3 tides

The Love numbers of the degree 3 tides may be taken as real and constant in computations to the degree of accuracy aimed at here. The vector displacement due to these tides is then given by

$$\Delta \vec{r} = \sum_{j=2}^3 \frac{GM_j R_e^5}{GM_{\oplus} R_j^4} \left\{ h_3 \hat{r} \left(\frac{5}{2} (\hat{R}_j \cdot \hat{r})^3 - \frac{3}{2} (\hat{R}_j \cdot \hat{r}) \right) + l_3 \left(\frac{15}{2} (\hat{R}_j \cdot \hat{r})^2 - \frac{3}{2} \right) [\hat{R}_j - (\hat{R}_j \cdot \hat{r}) \hat{r}] \right\}. \quad (9)$$

Only the Moon's contribution ($j = 2$) need be computed, the term due to the Sun being quite ignorable. The transverse part of the displacement (9) does not exceed 0.2 *mm*, but the radial displacement can reach 1.7 *mm*.

Contributions to the transverse displacement due to the $l^{(1)}$ term

The imaginary part of $l^{(1)}$ (anelastic case) is completely ignorable, and so is the difference between the real part and the elastic Earth value, as well as the intra-band frequency dependence; and $l^{(1)}$ is effectively zero in the zonal band.

In the expressions given below, and elsewhere in this Chapter,

Φ_j = body fixed geocentric latitude of Moon or Sun, and

λ_j = body fixed east longitude (from Greenwich) of Moon or Sun.

The following formulae may be employed when the use of Cartesian coordinates X_j, Y_j, Z_j of the body relative to the terrestrial reference frame is preferred:

$$P_2^0(\sin \Phi_j) = \frac{1}{R_j^2} \left(\frac{3}{2} Z_j^2 - \frac{1}{2} R_j^2 \right), \quad (10a)$$

$$P_2^1(\sin \Phi_j) \cos \lambda_j = \frac{3X_j Z_j}{R_j^2}, \quad P_2^1(\sin \Phi_j) \sin \lambda_j = \frac{3Y_j Z_j}{R_j^2}, \quad (10b)$$

$$P_2^2(\sin \Phi_j) \cos 2\lambda_j = \frac{3}{R_j^2} (X_j^2 - Y_j^2), \quad P_2^2(\sin \Phi_j) \sin 2\lambda_j = \frac{6}{R_j^2} X_j Y_j. \quad (10c)$$

Contribution from the diurnal band (with $l^{(1)} = 0.0012$):

$$\delta \vec{t} = -l^{(1)} \sin \phi \sum_{j=2}^3 \frac{GM_j R_e^4}{GM_{\oplus} R_j^3} P_2^1(\sin \Phi_j) [\sin \phi \cos(\lambda - \lambda_j) \hat{n} - \cos 2\phi \sin(\lambda - \lambda_j) \hat{e}]. \quad (11)$$

Contribution from the semidiurnal band (with $l^{(1)} = 0.0024$):

$$\delta \vec{t} = -\frac{1}{2} l^{(1)} \sin \phi \cos \phi \sum_{j=2}^3 \frac{GM_j R_e^4}{GM_{\oplus} R_j^3} P_2^2(\sin \Phi_j) [\cos 2(\lambda - \lambda_j) \hat{n} + \sin \phi \sin 2(\lambda - \lambda_j) \hat{e}]. \quad (12)$$

The contributions of the $l^{(1)}$ term to the transverse displacements caused by the diurnal and semidiurnal tides could be up to 0.8 mm and 1.0 mm respectively.

Out of phase contributions from the imaginary parts of $h_{2m}^{(0)}$ and $l_{2m}^{(0)}$

In the following, h^I and l^I stand for the imaginary parts of $h_{2m}^{(0)}$ and $l_{2m}^{(0)}$, which do not exist in the elastic case.

Contributions δr to radial and $\delta \vec{t}$ to transverse displacements from diurnal tides (with $h^I = -0.0025$, $l^I = -0.0007$):

$$\delta r = -\frac{3}{4}h^I \sum_{j=2}^3 \frac{GM_j R_e^4}{GM_\oplus R_j^3} \sin 2\Phi_j \sin 2\phi \sin(\lambda - \lambda_j), \quad (13a)$$

$$\delta \vec{t} = -\frac{3}{2}l^I \sum_{j=2}^3 \frac{GM_j R_e^4}{GM_\oplus R_j^3} \sin 2\Phi_j [\cos 2\phi \sin(\lambda - \lambda_j) \hat{n} + \sin \phi \cos(\lambda - \lambda_j) \hat{e}]. \quad (13b)$$

Contributions from semidiurnal tides (with $h^I = -0.0022$, $l^I = -0.0007$):

$$\delta r = -\frac{3}{4}h^I \sum_{j=2}^3 \frac{GM_j R_e^4}{GM_\oplus R_j^3} \cos^2 \Phi_j \cos^2 \phi \sin 2(\lambda - \lambda_j), \quad (14a)$$

$$\delta \vec{t} = \frac{3}{4}l^I \sum_{j=2}^3 \frac{GM_j R_e^4}{GM_\oplus R_j^3} \cos^2 \Phi_j [\sin 2\phi \sin 2(\lambda - \lambda_j) \hat{n} - 2 \cos \phi \cos 2(\lambda - \lambda_j) \hat{e}]. \quad (14b)$$

The out of phase contributions from the zonal tides has no closed expression in the time domain.

Computations of **Step 2** are to take account of the intraband variation of $h_{2m}^{(0)}$ and $l_{2m}^{(0)}$. Variations of the imaginary parts (anelastic case) are ignorable except as stated below. For the zonal tides, however, the contributions from the imaginary part have to be computed in Step 2.

A FORTRAN program for computing the various corrections is available at ftpserver.oma.be, subdirectory /pub/astro/dehant/IERS (anonymous-ftp system).

Correction for frequency dependence of the Love and Shida numbers

(a) Contributions from the diurnal band

Corrections to the radial and transverse station displacements δr and $\delta \vec{t}$ due to a diurnal tidal term of frequency f are obtainable from equation (5b):

$$\delta r = \delta R_f \sin 2\phi \sin(\theta_f + \lambda), \quad (15a)$$

$$\delta \vec{t} = \delta T_f [\sin \phi \cos(\theta_f + \lambda) \hat{e} + \cos 2\phi \sin(\theta_f + \lambda) \hat{n}], \quad (15b)$$

where

$$\delta R_f = -\frac{3}{2} \sqrt{\frac{5}{24\pi}} \delta h_f H_f \quad \text{and} \quad \delta T_f = -3 \sqrt{\frac{5}{24\pi}} \delta l_f H_f, \quad (15c)$$

and

δh_f = difference of $h^{(0)}$ at frequency f from the nominal value of h_2 ,

δl_f = difference of $l^{(0)}$ at frequency f from the nominal value of l_2 .

Values of ΔR_f and ΔT_f listed in Tables 7.3a and 7.3b are for the constituents that must be taken into account to ensure an accuracy of 1 *mm*. ΔR_f^{el} and ΔT_f^{el} are for the elastic case, and ΔR_f^{anel} and ΔT_f^{anel} are for use when anelasticity effects are included. It should be noted that different nominal values are used for the two cases in order to minimize the number of terms for which corrections are needed.

Corrections to the out-of-phase parts, arising from variation of the imaginary parts of $h_{21}^{(0)}$ and $l_{21}^{(0)}$, are very small. The only one with an amplitude exceeding the cutoff of 0.05 *mm* used for the table is 0.06 *mm* in the vertical component due to the K_1 tide. Its contribution to the displacement is $0.06 \sin 2\phi \cos(\theta_g + \pi + \lambda)$ *mm*.

Table 7.3a. Corrections due to frequency variation of Love and Shida numbers for diurnal tides. Units: *mm*. All terms with radial correction ≥ 0.05 *mm* are shown. Nominal values are $h = 0.6026$ and $l = 0.0831$ for the elastic case, and $h^R = 0.6078$ and $l^R = 0.0847$ for the real parts in the anelastic case. Frequencies shown are in degrees per hour.

Name	Frequency	Doodson	τ	s	h	p	N'	p_s	ℓ	ℓ'	F	D	Ω	ΔR_f^{el}	ΔT_f^{el}	ΔR_f^{anel}	ΔT_f^{anel}
Q ₁	13.39866	135,655	1	-2	0	1	0	0	1	0	2	0	2	-0.11	-0.01	-0.09	0.00
	13.94083	145,545	1	-1	0	0	-1	0	0	0	2	0	1	-0.12	-0.01	-0.10	0.00
O ₁	13.94303	145,555	1	-1	0	0	0	0	0	0	2	0	2	-0.63	-0.04	-0.53	0.02
NO ₁	14.49669	155,655	1	0	0	1	0	0	1	0	0	0	0	0.07	0.00	0.06	-0.00
π_1	14.91787	162,556	1	1	-3	0	0	1	0	1	2	-2	2	-0.06	0.00	-0.05	0.00
P ₁	14.95893	163,555	1	1	-2	0	0	0	0	0	2	-2	2	-1.29	0.05	-1.23	0.07
	15.03886	165,545	1	1	0	0	-1	0	0	0	0	0	-1	-0.23	0.01	-0.22	0.01
K ₁	15.04107	165,555	1	1	0	0	0	0	0	0	0	0	0	12.25	-0.65	12.04	-0.72
	15.04328	165,565	1	1	0	0	1	0	0	0	0	0	1	1.77	-0.09	1.74	-0.10
ψ_1	15.08214	166,554	1	1	1	0	0	-1	0	-1	0	0	0	-0.51	0.03	-0.50	0.03
ϕ_1	15.12321	167,555	1	1	2	0	0	0	0	0	-2	2	-2	-0.11	0.01	-0.11	0.01

(b) Contributions from the long period band

Corrections δr and $\delta \vec{t}$ due to a zonal tidal term of frequency f include both in phase (*ip*) and out of phase (*op*) parts. From equations (5a) and (7) one finds that

$$\delta r = \left(\frac{3}{2} \sin^2 \phi - \frac{1}{2} \right) (\delta R_f^{(ip)} \cos \theta_f + \delta R_f^{(op)} \sin \theta_f), \quad (16a)$$

and

$$\delta \vec{t} = \sin 2\phi (\delta T_f^{(ip)} \cos \theta_f + \delta T_f^{(op)} \sin \theta_f) \hat{n}, \quad (16b)$$

where

$$\delta R(ip)_f = \sqrt{\frac{5}{4\pi}} \delta h_f^R H_f \quad \text{and} \quad \delta R(op)_f = -\sqrt{\frac{5}{4\pi}} \delta h_f^I H_f, \quad (16c)$$

$$\delta T(ip)_f = \frac{3}{2} \sqrt{\frac{5}{4\pi}} \delta l_f^R H_f \quad \text{and} \quad \delta T(op)_f = -\frac{3}{2} \sqrt{\frac{5}{4\pi}} \delta l_f^I H_f. \quad (16d)$$

Table 7.3b. Corrections due to frequency variation of Love and Shida numbers for zonal tides. Units: *mm*. All terms with radial correction ≥ 0.05 *mm* are shown. Nominal values are $h = 0.6026$ and $l = 0.0831$ for the elastic case, and $h^R = 0.6078$ and $l^R = 0.0847$ for the real parts in the anelastic case. For each frequency, the in phase amplitudes $\Delta R_f^{(ip)}$ and $\Delta T_f^{(ip)}$ are shown on the first line, and the out of phase amplitudes $\Delta R_f^{(op)}$ and $\Delta T_f^{(op)}$ on the second line. Frequencies shown are in degrees per hour.

Name	Frequency	Doodson	τ	s	h	p	N'	p_s	ℓ	ℓ'	F	D	Ω	ΔR_f^{elas}	ΔT_f^{elas}	ΔR_f^{anel}	ΔT_f^{anel}
	0.00221	55,565	0	0	0	0	1	0	0	0	0	0	1	-0.05	0.00	0.47	0.23
																0.16	0.07
S_{sa}	0.08214	57,555	0	0	2	0	0	0	0	0	-2	2	-2	0.05	0.00	-0.20	-0.12
																-0.11	-0.05
M_m	0.54438	65,455	0	1	0	-1	0	0	-1	0	0	0	0	0.06	0.00	-0.11	-0.08
																-0.09	-0.04
M_f	1.09804	75,555	0	2	0	0	0	0	0	0	-2	0	-2	0.12	0.00	-0.13	-0.11
																-0.15	-0.07
	1.10024	75,565	0	2	0	0	1	0	0	0	-2	0	-1	0.05	0.00	-0.05	-0.05
																-0.06	-0.03

Permanent deformation

The zonal part of the degree 2 potential contains a time-independent constituent of amplitude (-0.31460) *m*. A permanent deformation due to this constituent forms a part of the site displacement computed from Equation (8) using the nominal values $h_2 = 0.6026$ and $l_2 = 0.0831$ when ignoring anelasticity. The permanent part of radial displacement thus computed is

$$\sqrt{\frac{5}{4\pi}}(0.6026)(-0.31460)\left(\frac{3}{2}\sin^2\phi - \frac{1}{2}\right) = -0.1196\left(\frac{3}{2}\sin^2\phi - \frac{1}{2}\right) \text{ meters,} \quad (17a)$$

and the transverse component, which is in the northward direction, is

$$\sqrt{\frac{5}{4\pi}}(0.0831)(-0.31460)3\cos\phi\sin\phi = -0.0247\sin 2\phi \text{ meters.} \quad (17b)$$

This permanent deformation must be removed from the displacement vector computed by the procedure described above in order to obtain the temporally varying part of the tide-induced site displacement. If the nominal values for the anelastic case ($h_2 = 0.6078, l_2 = 0.0847$) were used in the first step computation, one should have -0.1206 and -0.0252 respectively in the expressions for the radial and northward components (instead of -0.1196 and -0.0247).

If the $h^{(2)}$ -latitude dependence of the Love numbers were accounted for in the first step, *i.e.* if the change $h_2 \rightarrow h(\phi) = h^{(0)} + h^{(2)}[(3\sin^2\phi - 1)/2]$ and $l_2 \rightarrow l(\phi) = l^{(0)} + l^{(2)}[(3\sin^2\phi - 1)/2]$ were made, the values will change accordingly.

The restitution of the indirect effect of the permanent tide is done to be consistent with the XVIII IAG General Assembly Resolution 16; but to get the permanent tide at the station, one should

use the same formula (equations (17a) and (17b)) replacing the Love numbers by the fluid limit Love numbers which are $l = 0$ and $h = 1 + k$ with $k = 0.94$.

Rotational Deformation Due to Polar Motion

The variation of station coordinates caused by the pole tide is recommended to be taken into account. Let us choose \hat{x}, \hat{y} and \hat{z} as a terrestrial system of reference. The \hat{z} axis is oriented along the Earth's mean rotation axis, the \hat{x} axis is in the direction of the adopted origin of longitude and the \hat{y} axis is orthogonal to the \hat{x} and \hat{z} axes and in the plane of the 90° E meridian.

The centrifugal potential caused by the Earth's rotation is

$$V = \frac{1}{2}[r^2|\vec{\Omega}|^2 - (\vec{r} \cdot \vec{\Omega})^2], \quad (18)$$

where $\vec{\Omega} = \Omega(m_1\hat{x} + m_2\hat{y} + (1 + m_3)\hat{z})$. Ω is the mean angular velocity of rotation of the Earth, m_i are small dimensionless parameters, m_1, m_2 describing polar motion and m_3 describing variation in the rotation rate, r is the radial distance to the station.

Neglecting the variations in m_3 which induce displacements that are below the mm level, the m_1 and m_2 terms give a first order perturbation in the potential V (Wahr, 1985)

$$\Delta V(r, \theta, \lambda) = -\frac{\Omega^2 r^2}{2} \sin 2\phi (m_1 \cos \lambda + m_2 \sin \lambda). \quad (19)$$

The radial displacement S_r and the horizontal displacements S_θ and S_λ (positive upwards, south and east respectively in a horizon system at the station) due to ΔV are obtained using the formulation of tidal Love numbers (Munk and MacDonald, 1960):

$$\begin{aligned} S_r &= h_2 \frac{\Delta V}{g}, \\ S_\theta &= \frac{\ell_2}{g} \partial_\theta \Delta V, \\ S_\lambda &= \frac{\ell_2}{g} \frac{1}{\sin \theta} \partial_\lambda \Delta V. \end{aligned} \quad (20)$$

In general, these computed displacements have a non-zero average over any given time span because m_1 and m_2 , used to find ΔV , have a non-zero average. Consequently, the use of these results will lead to a change in the estimated mean station coordinates. When mean coordinates produced by different users are compared at the centimeter level, it is important to ensure that this effect has been handled consistently. It is recommended that m_1 and m_2 used in Equation 9 be replaced by parameters defined to be zero for the Terrestrial Reference Frame discussed in Chapter 4.

Thus, define

$$\begin{aligned} x_p &= m_1 - \bar{m}_1, \\ y_p &= -(m_2 - \bar{m}_2), \end{aligned} \quad (21)$$

where \bar{m}_1 and \bar{m}_2 are the values of m_1 and m_2 for the Terrestrial Reference Frame. Then, using Love number values appropriate to the pole tide ($h = 0.6027$, $l = 0.0836$) and $r = a = 6.378 \times 10^6$ m, one finds

$$\begin{aligned} S_r &= -32 \sin 2\theta(x_p \cos \lambda - y_p \sin \lambda) \text{ mm}, \\ S_\theta &= -9 \cos 2\theta(x_p \cos \lambda - y_p \sin \lambda) \text{ mm}, \\ S_\lambda &= 9 \cos \theta(x_p \sin \lambda + y_p \cos \lambda) \text{ mm}. \end{aligned} \tag{22}$$

for x_p and y_p in seconds of arc.

Taking into account that x_p and y_p vary, at most, 0.8 arcsec, the maximum radial displacement is approximately 25 mm, and the maximum horizontal displacement is about 7 mm.

If X , Y , and Z are Cartesian coordinates of a station in a right-handed equatorial coordinate system, we have the displacements of coordinates

$$[dX, dY, dZ]^T = R^T[S_\theta, S_\lambda, S_r]^T, \tag{23}$$

where

$$R = \begin{pmatrix} \cos \theta \cos \lambda & \cos \theta \sin \lambda & -\sin \theta \\ -\sin \lambda & \cos \lambda & 0 \\ \sin \theta \cos \lambda & \sin \theta \sin \lambda & \cos \theta \end{pmatrix}.$$

The deformation caused by the pole tide also leads to time dependent perturbations in the C_{21} and S_{21} geopotential coefficients (see Chapter 6).

Antenna Deformation

Changes in antenna height and axis offset due to temperature changes can be modeled simply.

Let V be the antenna height and A the axis offset. changes due to temperature, T , are then given by

$$\begin{aligned} dV &= kV(T - T_0), \text{ and} \\ dA &= k'A(T - T_0), \end{aligned}$$

where k and k' are estimated constants and T_0 is the reference temperature. Typically k and k' are of the order of 10^{-6} .

Atmospheric Loading

Temporal variations in the geographic distribution of atmospheric mass load the Earth and deform its surface. Displacement variations are dominated by effects of synoptic pressure systems; length scales of 1000-2000 km and periods of two weeks. Pressure loading effects are larger at high latitudes due to the larger storms found there. Effects are smaller at low latitude sites (35S to 35N) and at sites within 300 km of the sea or ocean. Theoretical studies by Rabbel and Zschau (1985), Rabbel and Schuh (1986), vanDam and Wahr (1987), and Manabe *et al.* (1991) demonstrate that vertical displacements of up to 25 mm are possible with horizontal effects of one-third this amount.

All pressure loading analyses make the assumption that the response of the ocean to changes in air pressure is inverse barometric. It is likely that the ocean responds to pressure as an inverted

barometer at periods of a few days to a few years. (See Chelton and Enfield (1986) or Ponte *et al.* (1991) for a summary of observational evidence for the inverted barometer response.) A local inverted barometer response is probably appropriate for periods as short as 3 or 4 days. On the other hand, the decidedly nonequilibrium diurnal ocean tides imply that the global response is certainly not an inverted barometer at periods close to a day.

There are many methods for computing atmospheric loading corrections. In contrast to ocean tidal effects, analysis of the situation in the atmospheric case does not benefit from the presence of a well-understood periodic driving force. Otherwise, estimation of atmospheric loading via Green's function techniques is analogous to methods used to calculate ocean loading effects. Rabbel and Schuh (1986) recommend a simplified form of the dependence of the vertical crustal displacement on pressure distribution. It involves only the instantaneous pressure at the site in question, and an average pressure over a circular region C with a 2000 km radius surrounding the site. The expression for the vertical displacement (mm) is

$$\Delta r = -0.35p - 0.55\bar{p} \quad (15)$$

where p is the local pressure anomaly with respect to the standard pressure of 101.3 kPA (equivalent to 1013 mbar), and \bar{p} the pressure anomaly within the 2000 km circular region mentioned above. Both quantities are in 10^{-1} kPA (equivalent to mbar). Note that the reference point for this displacement is the site location at standard pressure. Equation 15 permits one to estimate the seasonal displacement due to the large-scale atmospheric loading with an error less than ± 1 mm (Rabbel and Schuh, 1986).

An additional mechanism for characterizing \bar{p} may be applied. The two-dimensional surface pressure distribution surrounding a site is described by

$$p(x, y) = A_0 + A_1x + A_2y + A_3x^2 + A_4xy + A_5y^2,$$

where x and y are the local East and North distances of the point in question from the VLBI site. The pressure anomaly \bar{p} may be evaluated by the simple integration

$$\bar{p} = \frac{\int \int_C dx dy p(x, y)}{\int \int_C dx dy}$$

giving

$$\bar{p} = A_0 + (A_3 + A_5)R^2/4,$$

where $R^2 = (x^2 + y^2)$.

It remains the task of the data analyst to perform a quadratic fit to the available weather data to determine the coefficients A_{0-5} .

vanDam and Wahr (1987) computed the displacements due to atmospheric loading by performing a convolution sum between barometric pressure data and the mass loading Green's Function. They found that the corrections based on Equation 15 are inadequate for stations close to the coast. For these coastal stations, Equation 15 can be improved by extending the regression equation.

A few investigators (Manabe *et al.*, 1991; MacMillan and Gipson, 1994; vanDam and Herring, 1994; vanDam *et al.*, 1994) have attempted to calculate site dependent pressure responses by regressing local pressure changes with theoretical, VLBI or GPS height variations. For example vanDam and Herring (1994) find significant site displacements in some VLBI stations which can be modeled by a simple linear regression. Table 7.4 shows the relationship between variations in local atmospheric pressure and theoretical radial surface displacements for these sites as found in their analysis. This rate is available by anonymous ftp to `gracie.grdl.noaa.gov`.

Table 7.4. Regression Coefficients

Station	Slope (mm/mbar)
GILC	$-0.45 \pm .001$
ONSA	$-0.32 \pm .001$
WETT	$-0.46 \pm .002$
WEST	$-0.43 \pm .002$
HATC	$-0.40 \pm .002$
NRAO	$-0.41 \pm .002$
KASH	$-0.04 \pm .020$
MOJA	$-0.42 \pm .004$
GRAS	$-0.55 \pm .002$
RICH	$-0.35 \pm .002$
KAUA	$-0.26 \pm .005$

Postglacial Rebound

The current state-of-the-art model of the global process of postglacial rebound is that described in Peltier (1994). The model consists of a history of the variations in ice thickness from the time of the last glacial maximum (LGM) until the present coupled with a radial profile of viscosity in the planetary mantle. The ice model, called ICE-4G, is a significant improvement over the previous model of Tushingham and Peltier (1991) called ICE-3G in that it has been constrained to fit the detailed history of relative sea level rise at Barbados that is derivative of dated coral sequences that extend from the LGM to the present.

The planet's response to the model deglaciation event is computed by first solving an integral equation to determine the site dependent variation of ocean bathymetry since the LGM in order to ensure that the ocean surface remains a gravitational equipotential. Time dependent, three dimensional displacement fields are then determined by spectral convolution of the visco-elastic impulse response Green function for the planet with the complete history of surface mass loading (with its distinct ice and ocean components). A succinct review of the complete theory for the three dimensional displacement calculation and a recent application to the computation of VLBI baseline variations will be found in Peltier (1995).

A file containing a listing of the radial and horizontal displacements for a number of sites is available by anonymous ftp. ftp to maia.usno.navy.mil. Change directories to standards (cd standards). The file is called pgr.model. Any comments or corrections to this file should be directed to Prof. Richard Peltier (peltier@rainbow.physics.utoronto.ca).

References

- Cartwright, D. E. and Tayler, R. J., 1971, "New Computations of the Tide-Generating Potential," *Geophys. J. Roy. Astron. Soc.*, **23**, pp. 45–74.
- Cartwright, D. E. and Edden, A. C., 1973, "Corrected Tables of Tidal Harmonics," *Geophys. J. Roy. Astron. Soc.*, **33**, pp. 253–264.
- Chelton, D. B. and Enfield, D. B., 1986, "Ocean Signals in Tide Gauge Records," *J. Geophys.*, **91**, pp. 9081–9098.

- Dehant, V., 1987, "Tidal parameters for an inelastic Earth," *Phys. Earth Plan. Int.*, **49**, pp. 97–116.
- Doodson, A. T., 1928, "The Analysis of Tidal Observations," *Phil. Trans. Roy. Soc. Lond.*, **227**, pp. 223–279.
- Farrell, W. E., 1972, "Deformation of the Earth by Surface Loads," *Rev. Geophys. Space Phys.*, **10**, pp. 761–797.
- Flather, R. A., 1981, *Proc. Norwegian Coastal Current Symp. Geilo, 1980*, Saetre and Mork (eds), pp. 427–457.
- Le Provost, C., Genco, M. L., Lyard, F., Incent, P., and Canceil, P., 1994, "Spectroscopy of the world ocean tides from a finite element hydrological model," *J. Geophys. Res.*, **99**, pp. 24777–24798.
- MacMillan, D.S. and J.M. Gipson, 1994, "Atmospheric Pressure Loading Parameters from Very Long Baseline Interferometry Observations," *J. Geophys. Res.*, **99**, pp. 18081–18088.
- Manabe, S.T., T. Sato, S. Sakai, and K. Yokoyama, 1991, "Atmospheric Loading Effects on VLBI Observations," in Proceedings of the AGU Chapman Conference on Geodetic VLBI: Monitoring Global Change, *NOAA Tech. Rep. NOS 137 NGS 49*, pp. 111–122.
- Mathews, P. M., Buffett, B. A., and Shapiro, I. I., 1995, "Love numbers for a rotating spheroidal Earth: New definitions and numerical values," *Geophys. Res. Lett.*, **22**, pp. 579–582.
- Munk, W. H. and MacDonald, G. J. F., 1960, *The Rotation of the Earth*, Cambridge Univ. Press, New York, pp. 24–25.
- Peltier, W. R., 1994, "Ice Age Paleotopography," *Science*, **265**, pp. 195–201.
- Peltier, W.R., 1995, "VLBI baseline variations from the ICE-4G model of postglacial rebound," *Geophys. Res. Lett.*, **22**, pp. 465–468.
- Ponte, R. M., Salstein, D. A., and Rosen, R. D., 1991, "Sea Level Response to Pressure Forcing in a Barotropic Numerical Model," *J. Phys. Oceanogr.*, **21**, pp. 1043–1057.
- Rabbell, W. and Schuh, H., 1986, "The Influence of Atmospheric Loading on VLBI Experiments," *J. Geophys.*, **59**, pp. 164–170.
- Rabbell, W. and Zschau, J., 1985, "Static Deformations and Gravity Changes at the Earth's Surface due to Atmospheric Loading," *J. Geophys.*, **56**, pp. 81–99.
- Row, L. W., Hastings, D. A., and Dunbar, P. K., 1995, "TerrainBase Worldwide Digital Terrain Data," NOAA, National Geophysical Data Center, Boulder CO.
- Scherneck, H. G., 1983, *Crustal Loading Affecting VLBI Sites*, University of Uppsala, Institute of Geophysics, Dept. of Geodesy, Report No. 20, Uppsala, Sweden.

- Scherneck, H. G., 1990, "Loading Green's functions for a continental shield with a Q-structure for the mantle and density constraints from the geoid," *Bull. d'Inform. Marées Terr.*, **108**, pp. 7757–7792.
- Scherneck, H. G., 1991, "A Parameterized Solid Earth Tide Model and Ocean Tide Loading Effects for Global Geodetic Baseline Measurements," *Geophys. J. Int.*, **106**, pp. 677–694.
- Scherneck, H. G., 1993, "Ocean Tide Loading: Propagation of Errors from the Ocean Tide into Loading Coefficients," *Man. Geod.*, **18**, pp. 59–71.
- Schwiderski, E. W., 1983, "Atlas of Ocean Tidal Charts and Maps, Part I: The Semidiurnal Principal Lunar Tide M_2 ," *Marine Geodesy*, **6**, pp. 219–256.
- Schwiderski, E. W. and Szeto, L. T., 1981, NSWC-TR 81-254, Naval Surface Weapons Center, Dahlgren Va., 19 pp.
- Tamura, Y., 1987, "A harmonic development of the tide-generating potential," *Bull. d'Inform. Marées Terr.*, **99**, pp. 6813–6855.
- Tushingham, A. M. and Peltier, W. R., 1991, "Ice-3G: A New Global Model of Late Pleistocene Deglaciation Based Upon Geophysical Predictions of Post-Glacial Relative Sea Level Change," *J. Geophys. Res.*, **96**, pp. 4497–4523.
- Tushingham, A. M. and Peltier, W. R., 1991, "Validation of the ICE-3G Model of Wurm-Wisconsin Deglaciation Using a Global Data Base of Relative Sea Level Histories," *J. Geophys. Res.*, **97**, pp. 3285–3304.
- vanDam, T. M. and Wahr, J. M., 1987, "Displacements of the Earth's Surface due to Atmospheric Loading: Effects on Gravity and Baseline Measurements," *J. Geophys. Res.*, **92**, pp. 1281–1286.
- vanDam, T. M. and Herring, T. A., 1994, "Detection of Atmospheric Pressure Loading Using Very Long Baseline Interferometry Measurements," *J. Geophys. Res.*, **99**, pp. 4505–4517.
- vanDam, T. M., Blewitt, G., and Heflin, M. B., 1994, "Atmospheric Pressure Loading Effects on Global Positioning System Coordinate Determinations," *J. Geophys. Res.*, **99**, pp. 23,937–23,950.
- Verheijen and Schrama, 1995, personal communication.
- Wahr, J. M., 1981, "The Forced Nutations of an Elliptical, Rotating, Elastic, and Oceanless Earth," *Geophys. J. Roy. Astron. Soc.*, **64**, pp. 705–727.
- Wahr, J. M., 1985, "Deformation Induced by Polar Motion," *J. Geophys. Res.*, **90**, pp. 9363–9368.
- Wang, R., 1994, "Effect of rotation and ellipticity on earth tides," *Geophys. J. Int.*, **117**, pp. 562–565.
- Zschau, J., 1983, "Rheology of the Earth's mantle at tidal and Chandler Wobble periods," *Proc. Ninth Int. Symp. Earth Tides*, New York, 1981, J. T. Kuo (ed), Schweitzerbart'sche Verlagsbuchhandlung, Stuttgart, pp. 605–630.

CHAPTER 8 TIDAL VARIATIONS IN THE EARTH'S ROTATION

Periodic variations in UT1 due to tidal deformation of the polar moment of inertia were derived by Yoder *et al.* (1981) including the tidal deformation of the Earth with a decoupled core. This model uses effective Love numbers that differ from the bulk value of 0.301 because of the oceans and the fluid core giving rise to different theoretical values of the ratio k/C for the fortnightly and monthly terms. However, Yoder *et al.* recommend the value of 0.94 for k/C for both cases. Oceanic tides also cause variations in UT1 represented by models given by Brosche *et al.* (1991, 1989), Dickman (1993, 1991, 1990, 1989), Gross (1993), Herring and Dong (1994), and Ray *et al.* (1994). The contribution of the oceanic tides is split into a part which is in phase with the solid Earth tides and an out-of-phase part.

Table 8.1 provides corrections for the tidal variations in UT1–UTC with periods between five and 35 days. This is identical to tables in IERS Technical Notes 3 and 13 which defined UT1R–UTC, $\Delta - \Delta R$, and $\omega - \omega R$. Table 8.1 continues to define UT1R–UTC, $\Delta - \Delta R$, and $\omega - \omega R$.

$$\begin{aligned} \text{UT1} - \text{UT1R} &= \sum_{i=1}^{41} A_i \sin \xi_i \\ \Delta - \Delta R &= \sum_{i=1}^{41} A'_i \cos \xi_i \\ \omega - \omega R &= \sum_{i=1}^{41} A''_i \cos \xi_i \\ \xi_i &= \sum_{j=1}^5 a_{ij} \alpha_j \end{aligned}$$

a_{ij} = integer multipliers of the α_j (l, l', F, D or Ω) for the i^{th} tide given in the first five columns of Table 8.1. A_i, A'_i, A''_i are given in columns 7-9 respectively in Table 8.1.

Table 8.2 is identical to Table 8.2 in IERS Technical Note 13 which defined UT1S–UTC, $\Delta - \Delta S$, and $\omega - \omega S$ except that the table below corrects one misprint in the out-of-phase term for the 18.6-year tide. Table 8.2 provides corrections for the tidal variations with periods from five days to 18.6 years and incorporates the most significant effects of oceanic tides using the model of Dickman (1993).

$$\begin{aligned} \text{UT1} - \text{UT1S} &= \sum_{i=1}^{62} B_i \sin \xi_i + C_i \cos \xi_i \\ \Delta - \Delta S &= \sum_{i=1}^{62} B'_i \cos \xi_i + C'_i \sin \xi_i \\ \omega - \omega S &= \sum_{i=1}^{62} B''_i \cos \xi_i + C''_i \sin \xi_i \end{aligned}$$

ξ_i are defined the same way as for UT1R above except the a_{ij} are given in the first five columns of Table 8.2. $B_i, C_i, B'_i, C'_i, B''_i$, and C''_i are given in columns 7-12 respectively in Table 8.2.

Table 8.3 provides corrections for daily and sub-daily tidal variations in the Earth's rotation from Ray (1995). Values corrected using Table 8.3 are referred to as UT1D, $\Delta - \Delta D$, and $\omega - \omega D$. Those corrected using Table 8.1 and 8.3 will then be called UT1DR, $\Delta - \Delta DR$, and $\omega - \omega DR$, and those corrected using Table 8.2 and 8.3 will be called UT1DS, $\Delta - \Delta DS$, and $\omega - \omega DS$.

$$\begin{aligned} \text{UT1} - \text{UT1D} &= \sum_{i=1}^8 D_i \sin \xi_i + E_i \cos \xi_i \\ \Delta - \Delta D &= \sum_{i=1}^8 D'_i \cos \xi_i + E'_i \sin \xi_i \\ \omega - \omega D &= \sum_{i=1}^8 D''_i \cos \xi_i + E''_i \sin \xi_i \\ \xi_i &= \sum_{j=1}^6 c_{ij} \gamma_j + \phi_i \end{aligned}$$

c_{ij} = integer multipliers of the γ_j (l, l', F, D, Ω , or θ) for the i^{th} tide given in columns 2-7 of Table 8.3. ϕ_i = the phase given in column 8 of Table 8.3.

Table 8.4 provides corrections for daily and subdaily tidal variations in polar motion from Ray (1995). Values corrected by using this table are referred to as xD and yD and are obtained by

$$\begin{aligned} xD - x &= \sum_{i=1}^8 F_i \sin \xi_i + G_i \cos \xi_i, \\ yD - y &= \sum_{i=1}^8 H_i \sin \xi_i + K_i \cos \xi_i, \end{aligned}$$

where F_i, G_i, H_i , and K_i are given in the table and

$$\xi_i = \sum_{j=1}^6 c_{ij} \gamma_j + \phi_i.$$

c_{ij} = integer multipliers of the γ_j (l, l', F, D, Ω , or θ) for the i^{th} tide given in columns 2-7 of Table 8.4. ϕ_i = the phase given in column 8 of Table 8.4.

Table 8.1. Zonal Tide Terms With Periods Up to 35 Days. UT1R, Δ R, and ω R represent the regularized forms of UT1, the duration of the day Δ , and the angular velocity of the Earth, ω . The units are 10^{-4} s for UT, 10^{-5} s for Δ , and 10^{-14} rad/s for ω .

ARGUMENT*				PERIOD	UT1-UT1R	$\Delta - \Delta$ R	$\omega - \omega$ R	
l	l'	F	D					Coefficient of
			Ω	Days	Sin (Argument)	Cos (Argument)		
1	0	2	2	2	5.64	-0.02	0.3	-0.2
2	0	2	0	1	6.85	-0.04	0.4	-0.3
2	0	2	0	2	6.86	-0.10	0.9	-0.8
0	0	2	2	1	7.09	-0.05	0.4	-0.4
0	0	2	2	2	7.10	-0.12	1.1	-0.9
1	0	2	0	0	9.11	-0.04	0.3	-0.2
1	0	2	0	1	9.12	-0.41	2.8	-2.4
1	0	2	0	2	9.13	-0.99	6.8	-5.8
3	0	0	0	0	9.18	-0.02	0.1	-0.1
-1	0	2	2	1	9.54	-0.08	0.5	-0.5
-1	0	2	2	2	9.56	-0.20	1.3	-1.1
1	0	0	2	0	9.61	-0.08	0.5	-0.4
2	0	2	-2	2	12.81	0.02	-0.1	0.1
0	1	2	0	2	13.17	0.03	-0.1	0.1
0	0	2	0	0	13.61	-0.30	1.4	-1.2
0	0	2	0	1	13.63	-3.21	14.8	-12.5
0	0	2	0	2	13.66	-7.76	35.7	-30.1
2	0	0	0	-1	13.75	0.02	-0.1	0.1
2	0	0	0	0	13.78	-0.34	1.5	-1.3
2	0	0	0	1	13.81	0.02	-0.1	0.1
0	-1	2	0	2	14.19	-0.02	0.1	-0.1
0	0	0	2	-1	14.73	0.05	-0.2	0.2
0	0	0	2	0	14.77	-0.73	3.1	-2.6
0	0	0	2	1	14.80	-0.05	0.2	-0.2
0	-1	0	2	0	15.39	-0.05	0.2	-0.2
1	0	2	-2	1	23.86	0.05	-0.1	0.1
1	0	2	-2	2	23.94	0.10	-0.3	0.2
1	1	0	0	0	25.62	0.04	-0.1	0.1
-1	0	2	0	0	26.88	0.05	-0.1	0.1
-1	0	2	0	1	26.98	0.18	-0.4	0.3
-1	0	2	0	2	27.09	0.44	-1.0	0.9
1	0	0	0	-1	27.44	0.53	-1.2	1.0
1	0	0	0	0	27.56	-8.26	18.8	-15.9
1	0	0	0	1	27.67	0.54	-1.2	1.0
0	0	0	1	0	29.53	0.05	-0.1	0.1
1	-1	0	0	0	29.80	-0.06	0.1	-0.1
-1	0	0	2	-1	31.66	0.12	-0.2	0.2
-1	0	0	2	0	31.81	-1.82	3.6	-3.0
-1	0	0	2	1	31.96	0.13	-0.3	0.2
1	0	-2	2	-1	32.61	0.02	0.0	0.0
-1	-1	0	2	0	34.85	-0.09	0.2	-0.1

Table 8.2. Zonal Tide Terms. UT1S1, Δ S1, and ω S1 represent the regularized forms of UT1, the duration of the day Δ , and the angular velocity of the Earth, ω . The units are 10^{-4} s for UT, 10^{-5} s for Δ , and 10^{-14} rad/s for ω .

ARGUMENT*					PERIOD	UT1-UT1S		$\Delta - \Delta$ S		$\omega - \omega$ S	
l	l'	F	D	Ω	Days	Sin	Cos	Coefficient of		Cos	Sin
1	0	2	2	2	5.64	-0.02		Cos	Sin	-0.2	
2	0	2	0	1	6.85	-0.04		Cos		-0.3	
2	0	2	0	2	6.86	-0.10		Cos		-0.8	
0	0	2	2	1	7.09	-0.05		Cos		-0.4	
0	0	2	2	2	7.10	-0.12		Cos		-0.9	
1	0	2	0	0	9.11	-0.04		Cos		-0.2	
1	0	2	0	1	9.12	-0.40	0.01	Cos	0.1	-2.3	-0.1
1	0	2	0	2	9.13	-0.98	0.03	Cos	0.2	-5.7	-0.2
3	0	0	0	0	9.18	-0.02		Cos		-0.1	
-1	0	2	2	1	9.54	-0.08		Cos		-0.5	
-1	0	2	2	2	9.56	-0.20		Cos		-1.1	
1	0	0	2	0	9.61	-0.08		Cos		-0.4	
2	0	2	-2	2	12.81	0.02		Cos		0.1	
0	1	2	0	2	13.17	0.03		Cos		0.1	
0	0	2	0	0	13.61	-0.30		Cos		-1.2	
0	0	2	0	1	13.63	-3.20	0.09	Cos	0.4	-12.4	-0.4
0	0	2	0	2	13.66	-7.73	0.21	Cos	1.0	-30.0	-0.8
2	0	0	0	-1	13.75	0.02		Cos		0.1	
2	0	0	0	0	13.78	-0.34		Cos		-1.3	
2	0	0	0	1	13.81	0.02		Cos		0.1	
0	-1	2	0	2	14.19	-0.02		Cos		-0.1	
0	0	0	2	-1	14.73	0.05		Cos		0.2	
0	0	0	2	0	14.77	-0.72	0.02	Cos	0.1	-2.6	-0.1
0	0	0	2	1	14.80	-0.05		Cos		-0.2	
0	-1	0	2	0	15.39	-0.05		Cos		-0.2	
1	0	2	-2	1	23.86	0.05		Cos		0.1	
1	0	2	-2	2	23.94	0.10		Cos		0.2	
1	1	0	0	0	25.62	0.04		Cos		0.1	
-1	0	2	0	0	26.88	0.05		Cos		0.1	
-1	0	2	0	1	26.98	0.18		Cos		0.3	
-1	0	2	0	2	27.09	0.44		Cos		0.9	
1	0	0	0	-1	27.44	0.53		Cos		1.0	
1	0	0	0	0	27.56	-8.33	0.12	Cos	0.3	-16.0	-0.2
1	0	0	0	1	27.67	0.54		Cos		1.0	
0	0	0	1	0	29.53	0.05		Cos		0.1	
1	-1	0	0	0	29.80	-0.06		Cos		-0.1	
-1	0	0	2	-1	31.66	0.12		Cos		0.2	
-1	0	0	2	0	31.81	-1.84	0.02	Cos	0.0	-3.0	0.0
-1	0	0	2	1	31.96	0.13		Cos		0.2	
1	0	-2	2	-1	32.61	0.02		Cos		0.0	
-1	-1	0	2	0	34.85	-0.09		Cos		-0.1	
0	2	2	-2	2	91.31	-0.06		Cos		0.0	

0	1	2	-2	1	119.61	0.03			0.0		0.0		
0	1	2	-2	2	121.75	-1.88			1.0		-0.8		
0	0	2	-2	0	173.31	0.25			-0.1		0.1		
0	0	2	-2	1	177.84	1.17			-0.4		0.3		
0	0	2	-2	2	182.62	-48.84	0.11		16.8	0.0	-14.2	0.0	
0	2	0	0	0	182.63	-0.19			0.1		-0.1		
2	0	0	-2	-1	199.84	0.05			0.0		0.0		
2	0	0	-2	0	205.89	-0.55			0.2		-0.1		
2	0	0	-2	1	212.32	0.04			0.0		0.0		
0	-1	2	-2	1	346.60	-0.05			0.0		0.0		
0	1	0	0	-1	346.64	0.09			0.0		0.0		
0	-1	2	-2	2	365.22	0.83			-0.1		0.1		
0	1	0	0	0	365.26	-15.55	0.02		2.6	0.0	-2.2	0.0	
0	1	0	0	1	386.00	-0.14			0.0		0.0		
1	0	0	-1	0	411.78	0.03			0.0		0.0		
2	0	-2	0	0	1095.17	-0.14			0.0		0.0		
-2	0	2	0	1	1305.47	0.42			0.0		0.0		
-1	1	0	1	0	3232.85	0.04			0.0		0.0		
0	0	0	0	2	3399.18	7.90			0.1		-0.1		
0	0	0	0	1	6790.36	-1637.68	-0.10		-10.4	0.0	8.8	0.0	

Table 8.3. Diurnal and subdiurnal zonal tide terms. The units are 10^{-4} s for UT, 10^{-5} s for Δ , and 10^{-14} rad/s for ω .

Tide	l	l'	F	D	Ω	θ	phase	Period	UT1-UT1D		$\Delta - \Delta D$		$\omega - \omega D$	
									Sin	Cos	Cos	Sin	Cos	Sin
Q_1	-1	0	-2	0	-2	1	-90	26.868	0.02	0.05	-1.4	2.8	1.2	-2.4
O_1	0	0	-2	0	-2	1	-90	25.819	0.12	0.16	-7.1	9.4	6.0	-7.9
P_1	0	0	-2	2	-2	1	-90	24.066	0.03	0.05	-1.8	3.2	1.5	-2.7
K_1	0	0	0	0	0	1	90	23.935	0.09	0.18	-5.4	11.2	4.6	-9.4
N_2	-1	0	-2	0	-2	2	0	12.658	-0.04	-0.02	4.5	-1.8	-3.8	1.6
M_2	0	0	-2	0	-2	2	0	12.421	-0.16	-0.07	19.6	-8.7	-16.6	7.4
S_2	0	0	-2	2	-2	2	0	12.000	-0.08	0.00	9.5	-0.5	-8.1	0.4
K_2	0	0	0	0	0	2	0	11.967	-0.02	0.00	2.5	-0.5	-2.1	0.4

$\theta = 180^\circ + 360^\circ 993326(\text{MJD}-51544.5)$ Earth's rotation angle
 See Chapter 5 for definitions of l, l', F, D, Ω .

Table 8.4. Diurnal and subdiurnal tide terms for polar motion. The units are msec. of arc for Δx and Δy .

Tide	l	l'	F	D	Ω	θ	phase (deg.)	Period (hours)	Δx Δy			
									Coefficients of			
								Sin	Cos	Sin	Cos	
Q ₁	-1	0	-2	0	-2	1	-90	26.868	-0.026	0.006	-0.006	0.026
O ₁	0	0	-2	0	-2	1	-90	25.819	-0.133	0.049	-0.049	0.133
P ₁	0	0	-2	2	-2	1	-90	24.066	-0.050	0.025	-0.025	0.050
K ₁	0	0	0	0	0	1	90	23.935	-0.152	0.078	-0.078	0.152
N ₂	-1	0	-2	0	-2	2	0	12.658	-0.057	-0.013	0.011	-0.033
M ₂	0	0	-2	0	-2	2	0	12.421	-0.330	-0.028	0.037	-0.196
S ₂	0	0	-2	2	-2	2	0	12.000	-0.145	0.064	0.059	-0.087
K ₂	0	0	0	0	0	2	0	11.967	-0.036	0.017	0.018	-0.022

References

- Brosche, P., Seiler, U., Sündermann, J., and Wunsch, J., 1989, "Periodic Changes in Earth's Rotation due to Oceanic Tides," *Astron. Astrophys.*, **220**, pp. 318–320.
- Brosche, P., Wunsch, J., Campbell, J., and Schuh, H., 1991, "Ocean Tide Effects in Universal Time detected by VLBI," *Astron. Astrophys.*, **245**, pp. 676–682.
- Dickman, S. R., 1989, "A Complete Spherical Harmonic Approach to Luni-Solar Tides," *Geophys. J.*, **99**, pp. 457–468.
- Dickman, S. R., 1990, "Experiments in Tidal Mass Conservation" (research note), *Geophys. J.*, **102**, pp. 257–262.
- Dickman, S. R., 1991, "Ocean Tides for Satellite Geodesy," *Mar. Geod.*, **14**, pp. 21–56.
- Dickman, S. R., 1993, "Dynamic ocean-tide effects on Earth's rotation," *Geophys. J. Int.*, **112**, pp. 448–470.
- Gross, R. S., 1993, "The Effect of Ocean Tides on the Earth's Rotation as Predicted by the Results of an Ocean Tide Model," *Geophys. Res. Lett.*, **20**, pp. 293–296.
- Herring, T. A. and Dong, D., 1994, "Measurement of Diurnal and Semidiurnal Rotational Variations and Tidal Parameters of Earth," *J. Geophys. Res.*, **99**, pp. 18051–18071.
- Ray, R. D., Steinberg, D. J., Chao, B. F., and Cartwright, D. E., 1994, "Diurnal and Semidiurnal Variations in the Earth's Rotation Rate Induced by Oceanic Tides," *Science*, **264**, pp. 830–832.
- Ray, R. D., 1995, Personal Communication.
- Yoder, C. F., Williams, J. G., Parke, M. E., 1981, "Tidal Variations of Earth Rotation," *J. Geophys. Res.*, **86**, pp. 881–891.

CHAPTER 9 TROPOSPHERIC MODEL

Optical Techniques

The formulation of Marini and Murray (1973) is commonly used in laser ranging. The formula has been tested by comparison with ray-tracing radiosonde profiles.

The correction to a one-way range is

$$\Delta R = \frac{f(\lambda)}{f(\phi, H)} \cdot \frac{A + B}{\sin E + \frac{B/(A+B)}{\sin E + 0.01}}, \quad (1)$$

where

$$A = 0.002357P_0 + 0.000141e_0, \quad (2)$$

$$B = (1.084 \times 10^{-8})P_0T_0K + (4.734 \times 10^{-8})\frac{P_0^2}{T_0} \frac{2}{(3 - 1/K)}, \quad (3)$$

$$K = 1.163 - 0.00968 \cos 2\phi - 0.00104T_0 + 0.00001435P_0, \quad (4)$$

where

ΔR = range correction (meters),

E = true elevation of satellite,

P_0 = atmospheric pressure at the laser site (in 10^{-1} kPa, equivalent to millibars),

T_0 = atmospheric temperature at the laser site (degrees Kelvin),

e_0 = water vapor pressure at the laser site (10^{-1} kPa, equivalent to millibars),

$f(\lambda)$ = laser frequency parameter (λ = wavelength in micrometers), and

$f(\phi, H)$ = laser site function.

Additional definitions of these parameters are available. The water vapor pressure, e_0 , can be calculated from a relative humidity measurement, R_h (%) by

$$e_0 = \frac{R_h}{100} \times 6.11 \times 10^{\frac{7.5(T_0 - 273.15)}{237.3 + (T_0 - 273.15)}}.$$

The laser frequency parameter, $f(\lambda)$, is

$$f(\lambda) \equiv 0.9650 + \frac{0.0164}{\lambda^2} + \frac{0.000228}{\lambda^4}.$$

$f(\lambda) = 1$ for a ruby laser, [*i.e.* $f(0.6943) = 1$], while $f(\lambda_G) = 1.02579$ and $f(\lambda_{IR}) = 0.97966$ for green and infrared YAG lasers.

The laser site function is

$$f(\phi, H) = 1 - 0.0026 \cos 2\phi - 0.00031H,$$

where ϕ is the latitude and H is the geodetic height (km).

Radio Techniques

The differences between mathematical tropospheric models are often less than the errors which would be introduced by the character and distribution of the wet component and by the departures of

the refractivity from azimuthal symmetry. For this reason it is customary in the analysis of geodetic data to estimate the zenith atmospheric delay and to model only the mapping function, which is the ratio of delay at a given elevation angle to the zenith delay. The mapping function may be for the hydrostatic, wet, or total troposphere delay. Accordingly, the IERS conventional model applies primarily to the mapping functions. For the most accurate *a priori* hydrostatic delay, desirable when the accuracy of the estimate of the zenith wet delay is important, the formula of Saastamoinen (1972) as given by Davis *et al.* 1985) should be used.

Comparisons of many mapping functions with the ray tracing of a global distribution of radiosonde data have been made by Janes *et al.* (1991) and by Mendes and Langley (1994). For observations below 10° elevation, which may be included in geodetic programs in order to increase the precision of the vertical component of site position, the mapping functions of Lanyi (1984), Ifadis (1986), Herring (1992, designated MTT) and Niell (1996, designated NMF) are the most accurate. Only the last three were developed for observations below an elevation of 6°, with MTT and NMF being valid to 3° and Ifadis to 2°.

Each of these mapping functions consists of a component for the water vapor and a component for either the total atmosphere (Lanyi) or the hydrostatic contribution to the total delay (Ifadis, MTT, and NMF). In all cases the wet mapping should be used as the function partial derivative for estimating the residual atmosphere zenith delay.

The parameters of the atmosphere that are readily accessible at the time of the observation are the surface temperature, pressure, and relative humidity. The mapping functions of Lanyi, Ifadis, and Herring were developed to make use of this information. Lanyi additionally allows for parameterization in terms of the height of a surface isothermal layer, the lapse rate from the top of this layer to the tropopause, and the height of the tropopause. Including the surface meteorology without these data results in larger discrepancies from radiosonde data than the Ifadis and Herring models.

The hydrostatic mapping function of Niell differs from the other three by being independent of surface meteorology. It relies instead on the greater contribution by the conditions in the atmosphere above approximately 1 km, which are strongly seasonal dependent. The RMS variation is comparable to those using Ifadis and MTT, and all three are less than that from the Lanyi model when only surface data are available. Thus NMF offers comparable precision and accuracy to Ifadis and MTT, when they are provided with accurate surface meteorology data, but with no dependence on external measurements.

Thus, if information is available on the vertical temperature distribution in the atmosphere, Lanyi is preferred. Otherwise one of the other three mapping functions should be used.

References

- Davis, J. L., Herring, T. A., Shapiro, I. I., Rogers, A. E. E., and Elgered, G., 1985, "Geodesy by Radio Interferometry: Effects of Atmospheric Modelling Errors on Estimates of Baseline Length," *Radio Science*, **20**, No. 6, pp. 1593–1607.
- Herring, T. A., 1992, "Modeling Atmospheric Delays in the Analysis of Space Geodetic Data," *Proceedings of Refraction of Transatmospheric Signals in Geodesy*, Netherlands Geodetic Commission Series, **36**, The Hague, Netherlands, pp. 157–164.

- Ifadis, I. I., 1986, "The Atmospheric Delay of Radio Waves: Modeling the Elevation Dependence on a Global Scale," *Technical Report No. 38L*, Chalmers U. of Technology, Göteborg, Sweden.
- Janes, H. W., Langley, R. B., and Newby, S. P., 1991, "Analytical Tropospheric Delay Prediction Models: Comparison with Ray-tracing and Implications for GPS Relative Positioning," *Bull. Géod.*, **65**, pp 151–161.
- Lanyi, G., 1984, "Tropospheric Delay Affecting Radio Interferometry," *TDA Progress Report*, pp. 152–159; see also *Observation Model and Parameter Partial for the JPL VLBI Parameter Estimation Software 'MASTERFIT'-1987*, 1987, JPL Publication 83-39, Rev. 3.
- Marini, J. W. and Murray, C. W., 1973, "Correction of Laser Range Tracking Data for Atmospheric Refraction at Elevations Above 10 Degrees," NASA GSFC X-591-73-351.
- Mendes, V. B. and Langley, R. B., 1994, "A Comprehensive Analysis of Mapping Functions Used in Modeling Tropospheric Propagation Delay in Space Geodetic Data," International Symposium on Kinematic Systems in Geodesy, Geomatics and Navigation, Banff Canada.
- Niell, A. E., 1996, "Global Mapping Functions for the Atmospheric Delay of Radio Wavelengths," *J. Geophys. Res.*, **101**, pp. 3227–3246.
- Saastamoinen, J., 1972, "Atmospheric Correction for the Troposphere and Stratosphere in Radio Ranging of Satellites," *Geophysical Monograph 15*, Henriksen (ed), pp. 247–251.

CHAPTER 10 RADIATION PRESSURE REFLECTANCE MODEL

For a near-Earth satellite the solar radiation pressure acceleration, is given by:

$$\ddot{\vec{r}} = \kappa \left[\frac{A}{R} \right]^2 C_R \frac{a}{m} \frac{\vec{R}}{R},$$

where

- $\kappa = 4.560 \times 10^{-6}$ newtons/m² (1367 watts/m²),
- A = astronomical unit in meters,
- R = heliocentric radius vector to the satellite,
- a = cross-sectional area (m²) of the satellite perpendicular to \vec{R} ,
- m = satellite mass,
- C_R = reflectivity coefficient, usually an adjusted parameter.

The radiation pressure due to backscatter from the Earth is ignored. The model for the Earth's and Moon's shadows should include the umbra and the penumbra (Haley, 1973).

Earth Radius	6402 km
Moon Radius	1738 km
Solar Radius	696000 km

Global Positioning System

For GPS satellites, the solar radiation pressure models T10 (for Block I and IIA) and T20 (for Block II) of Fliegel *et al.* (1992), (Gallini and Fliegel, 1995) are recommended. These models include thermal reradiation. A preliminary model for the forthcoming Block IIR satellites, which may begin to replace Block II/IIA as early as January 1997, is given here as T30.

Those models provide the X and Z components of the total nominal solar pressure force as functions of the angle B between the Sun and the $+Z$ axis of the satellite. For Block I, II, and IIA, $0 < B < 180$ degrees, but Block IIR, $0 < B < 360$ degrees (no "noon turn").

The model formulae for T10 are (angles in radians):

$$X = -4.55 \sin B + 0.08 \sin(2B + 0.9) - 0.06 \cos(4B + 0.08) + 0.08,$$

$$Z = -4.54 \cos B + 0.20 \sin(2B - 0.3) - 0.03 \sin 4B.$$

The model formulae for T20 are:

$$X = -8.96 \sin B + 0.16 \sin 3B + 0.10 \sin 5B - 0.07 \sin 7B,$$

$$Z = -8.43 \cos B.$$

The model formulae for T30 (Fliegel, 1995) are:

$$X = -11.0 \sin B - 0.2 \sin 3B + 0.2 \sin 5B,$$

$$Z = -11.3 \cos B + 0.1 \cos 3B + 0.2 \cos 5B.$$

In both cases the units are 10^{-5} N.

References

- Fliegel, H. F., Gallini, T. E., and Swift, E., 1992, "Global Positioning System Radiation Force Models for Geodetic Applications," *J. Geophys. Res.*, **97**, No. B1, pp. 559–568.
- Fliegel, H. F. and Gallini, T. E., 1996, "Solar Force Modelling of Block IIR GPS Satellites," *J. of Space Craft and Rockets*, in press.
- Gallini, T. E. and Fliegel, H. F., 1995, *The Generalized Solar Force Model*, Aerospace Report No. TOR-95(5473)-2, The Aerospace Corporation, El Segundo, CA.
- Haley, D., 1973, *Solar Radiation Pressure Calculations in the Geodyn Program*, EG&G Report 008-73, Prepared for NASA Goddard Space Flight Center.

CHAPTER 11 GENERAL RELATIVISTIC MODELS FOR TIME, COORDINATES AND EQUATIONS OF MOTION

The relativistic treatment of the near-Earth satellite orbit determination problem includes corrections to the equations of motion, the time transformations, and the measurement model. The two coordinate systems generally used when including relativity in near-Earth orbit determination solutions are the solar system barycentric frame of reference and the geocentric or Earth-centered frame of reference.

Ashby and Bertotti (1986) constructed a locally inertial E-frame in the neighborhood of the gravitating Earth and demonstrated that the gravitational effects of the Sun, Moon, and other planets are basically reduced to their tidal forces, with very small relativistic corrections. Thus the main relativistic effects on a near-Earth satellite are those described by the Schwarzschild field of the Earth itself. This result makes the geocentric frame more suitable for describing the motion of a near-Earth satellite (Ries *et al.*, 1988).

The time coordinate in the inertial E-frame is Terrestrial Time (designated TT) (Guinot, 1991) which can be considered to be equivalent to the previously defined Terrestrial Dynamical Time (TDT). This time coordinate (TT) is realized in practice by International Atomic Time (TAI), whose rate is defined by the atomic second in the International System of Units (SI). Terrestrial Time adopted by the International Astronomical Union in 1991 differs from Geocentric Coordinate Time (TCG) by a scaling factor:

$$\text{TCG} - \text{TT} = L_G \times (\text{MJD} - 43144.0) \times 86400 \text{ seconds},$$

where MJD refers to the modified Julian date. Figure 11.1 shows graphically the relationships between the time scales. See *IERS Technical Note 13*, pages 137–142 for copies of the IAU Recommendations relating to these time scales.

Equations of Motion for an Artificial Earth Satellite

The correction to the acceleration of an artificial Earth satellite $\Delta\vec{a}$ is

$$\Delta\vec{a} = -\frac{GM_\oplus}{c^2 r^3} \left\{ [2(\beta + \gamma)\frac{GM_\oplus}{r} - \gamma v^2]\vec{r} + 2(1 + \gamma)(\vec{r} \cdot \vec{v})\vec{v} \right\}, \quad (1)$$

where

- c = speed of light,
- β, γ = PPN parameters equal to 1 in General Relativity,
- $\vec{r}, \vec{v}, \vec{a}$ = geocentric satellite position, velocity, and acceleration, respectively,
- GM_\oplus = geocentric constant of gravitation.

The effects of Lense-Thirring precession (frame-dragging), geodesic (de Sitter) precession, and the relativistic effects of the Earth's oblateness have been neglected.

Equations of Motion in the Barycentric Frame

The n-body equations of motion for the solar system frame of reference (the isotropic Parameterized Post-Newtonian system with Barycentric Coordinate Time (TCB) as the time coordinate) are required to describe the dynamics of the solar system and artificial probes moving about the solar

system (for example, see Moyer, 1971). These are the equations applied to the Moon’s motion for Lunar Laser Ranging (Newhall *et al.*, 1987). In addition, relativistic corrections to the laser range measurement, the data timing, and the station coordinates are required (see Chapter 12).

Scale Effect and Choice of Time Coordinate

A previous IAU definition of the time coordinate in the barycentric frame required that only periodic differences exist between Barycentric Dynamical Time (TDB) and Terrestrial Dynamical Time (TDT) (Kaplan, 1981). As a consequence, the spatial coordinates in the barycentric frame had to be rescaled to keep the speed of light unchanged between the barycentric and the geocentric frames (Misner, 1982; Hellings, 1986). Thus, when barycentric (or TDB) units of length were compared to geocentric (or TDT) units of length, a scale difference, L , appeared. This is no longer required with the use of the TCG time scale.

The difference between TCB and TDB is given in seconds by

$$\text{TCB} - \text{TDB} = L_B \times (\text{MJD} - 43144.0) \times 86400.$$

The difference between Barycentric Coordinate Time (TCB) and Geocentric Coordinate Time (TCG) involves a four-dimensional transformation,

$$\text{TCB} - \text{TCG} = c^{-2} \left\{ \int_{t_0}^t \left[\frac{v_e^2}{2} + U_{ext}(\vec{x}_e) \right] dt + \vec{v}_e \cdot (\vec{x} - \vec{x}_e) \right\},$$

where \vec{x}_e and \vec{v}_e denote the barycentric position and velocity of the Earth’s center of mass and \vec{x} is the barycentric position of the observer. U_{ext} is the Newtonian potential of all of the solar system bodies apart from the Earth evaluated at the geocenter. t_0 is chosen to be consistent with 1977 January 1, 0^h0^m0^s TAI and t is TCB. An approximation is given in seconds by

$$(\text{TCB} - \text{TCG}) = L_C \times (\text{MJD} - 43144.0) \times 86400 + c^{-2} \vec{v}_e \cdot (\vec{x} - \vec{x}_e) + P.$$

with MJD measured in TAI. Table 4.1 lists the values of the rates L_B , L_C , and L_G . Periodic differences denoted by P have a maximum amplitude of around 1.6 ms. These can be evaluated by the “FBL” model of Fairhead, Bretagnon and Lestrade (1995). A comparison with the numerical time ephemeris TE245 (Fukushima, 1995) revealed that this series provides the smallest deviation from TE245 for the years 1980–1999 after removing a linear trend. Users may expect the FBL model to provide the periodic part in TCB-TT within a few ns for a few decades around the present time. This is sufficient for all precision measurement including timing observations of millisecond pulsars.

Software to implement the FBL model is available by anonymous ftp to [maia.usno.navy.mil](ftp://maia.usno.navy.mil) and is located in the directory `/conventions/chapter11`. The files of interest are called `fbl.f` and `fbl.results`. This model is based on earlier works (Fairhead *et al.*, 1988; Fairhead and Bretagnon, 1990).

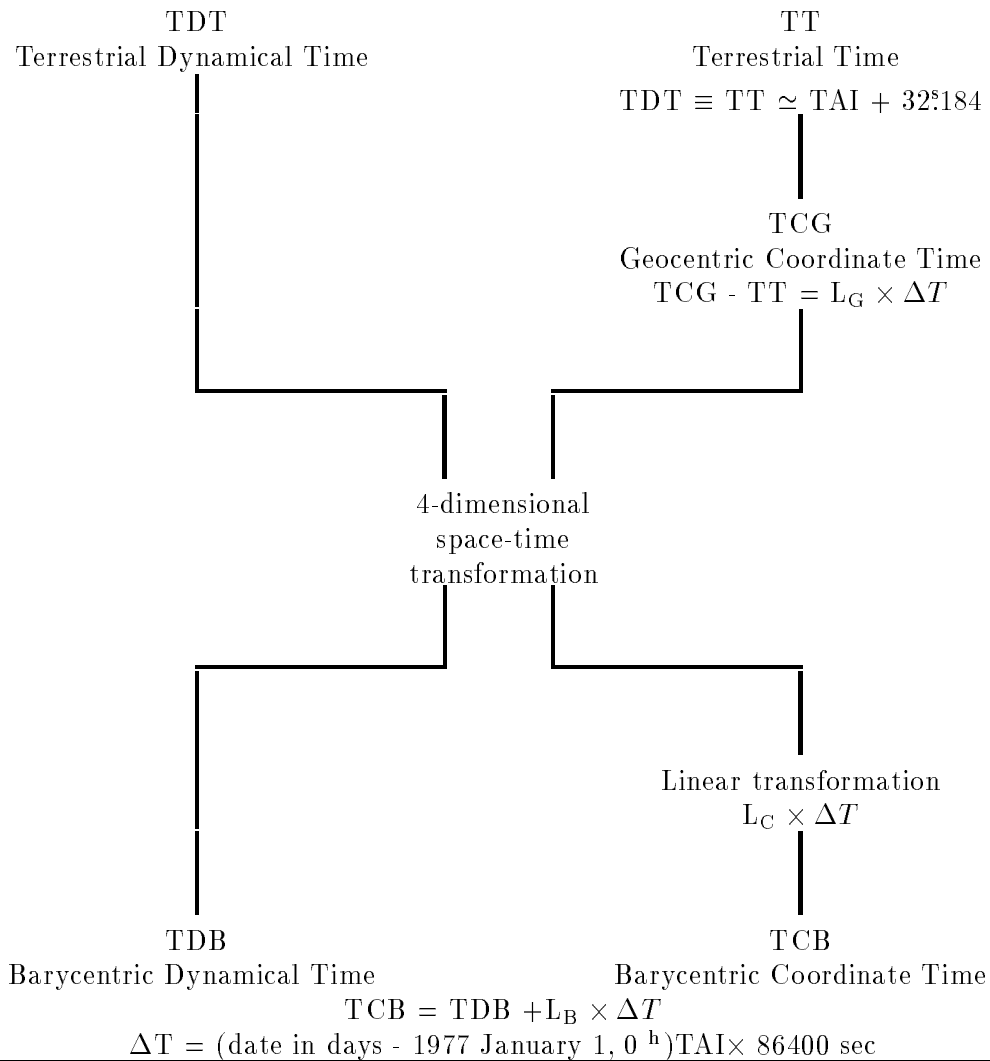


Fig 11.1 Relations between time scales.

References

- Ashby, N. and Bertotti, B., 1986, "Relativistic Effects in Local Inertial Frames," *Phys. Rev. D*, **34** (8), p. 2246.
- Fairhead, L. and Bretagnon, P., 1990, "An Analytic Formula for the Time Transformation TB-TT," *Astron. Astrophys.*, **229**, pp. 240–247.
- Fairhead, L., Bretagnon, P., and Lestrade, J.-F., 1988, "The Time Transformation TDB-TDT: An Analytical Formula and Related Problem of Convention," in *The Earth's Rotation and Reference Frames for Geodesy and Geophysics*, A. K. Babcock and G. A. Wilkins (eds.), Kluwer Academic Publishers, Dordrecht, pp. 419–426.
- Fairhead, L., Bretagnon, P., and Lestrade, J.-F., 1995, Private Communication.
- Fukushima, T., 1995, "Time Ephemeris," *Astron. Astrophys.*, **294**, pp. 895–906.

- Guinot, B., 1991, "Report of the Sub-group on Time," in Reference Systems, J. A. Hughes, C. A. Smith, and G. H. Kaplan (eds), U. S. Naval Observatory, Washington, D. C., pp. 3–16.
- Hellings, R. W., 1986, "Relativistic Effects in Astronomical Timing Measurement," *Astron. J.*, **91** (3), pp. 650–659. Erratum, *ibid.*, p. 1446.
- Kaplan, G. H., 1981, *The IAU Resolutions on Astronomical Constants, Time Scale and the Fundamental Reference Frame*, U. S. Naval Observatory Circular No. 163.
- Misner, C. W., 1982, *Scale Factors for Relativistic Ephemeris Coordinates*, NASA Contract NAS5-25885, Report, EG&G, Washington Analytical Services Center, Inc.
- Moyer, T. D., 1971, *Mathematical Formulation of the Double-precision Orbit Determination Program*, JPL Technical Report 32-1527.
- Newhall, X X, Williams, J. G., and Dickey, J. O., 1987, "Relativity Modeling in Lunar Laser Ranging Data Analysis," in *Proceedings of the International Association of Geodesy (IAG) Symposia*, Vancouver, pp. 78–82.
- Ries, J. C., Huang, C., and Watkins, M. M., 1988, "Effect of General Relativity on a Near-Earth Satellite in the Geocentric and Barycentric Reference Frames," *Phys. Rev. Let.*, **61**, pp. 903–906.

CHAPTER 12 GENERAL RELATIVISTIC MODELS FOR PROPAGATION

VLBI Time Delay

There have been many papers dealing with relativistic effects which must be accounted for in VLBI processing; see (Robertson, 1975), (Finkelstein *et al.*, 1983), (Hellings, 1986), (Pavlov, 1985), (Cannon *et al.*, 1986), (Soffel *et al.*, 1986), (Zeller *et al.*, 1986), (Sovers and Fanselow, 1987), (Zhu and Groten, 1988), (Shahid-Saless *et al.*, 1991), (Soffel *et al.*, 1991). As pointed out by Boucher (1986), the relativistic correction models proposed in various articles are not quite compatible. To resolve differences between the procedures and to arrive at a standard model, a workshop was held at the U. S. Naval Observatory on 12 October 1990. The proceedings of this workshop have been published (Eubanks, 1991) and the model given here is based on the consensus model resulting from that workshop. Much of this chapter dealing with VLBI time delay is taken directly from that work and the reader is urged to consult that publication for further details. One change from that model has been made in order to adopt the IAU/IUGG conventions for the scale of the terrestrial reference system, in accord with 1991 resolutions (see Appendix in McCarthy, 1992). Geodetic lengths should be expressed in “SI units,” *i.e.*, be consistent with the second as realized by a clock running at the TAI rate at sea level. The only change needed to the 1992 formulation to satisfy the IAU/IUGG Resolutions is to include the Earth’s potential, U_{\oplus} , in the total potential U in the delay equation (Equation 9). The only observable effect of this change will be an increase of the VLBI terrestrial scale by 1.39385806 parts in 10^9 .

As pointed out by Eubanks, the use of clocks running at the geoid and delays calculated “at the geocenter” ignoring the scale change induced by the Earth’s gravitational potential means that terrestrial distances calculated from the consensus model will not be the same as those calculated using the expressions in this chapter which are equivalent to using meter sticks on the surface of the Earth. The accuracy limit chosen for the consensus VLBI relativistic delay model is 10^{-12} seconds (one picosecond) of differential VLBI delay for baselines less than two Earth radii in length. In the model all terms of order 10^{-13} seconds or larger were included to ensure that the final result was accurate at the picosecond level. Source coordinates derived from the consensus model will be solar system barycentric and should have no apparent motions due to solar system relativistic effects at the picosecond level.

The consensus model was derived from a combination of five different relativistic models for the geodetic delay. These are the Masterfit/Modest model, due to Fanselow and Thomas (see Treuhaft and Thomas, in (Eubanks, 1991), and (Sovers and Fanselow, 1987)), the I. I. Shapiro model (see Ryan, in (Eubanks, 1991)), the Hellings-Shahid-Saless model (Shahid-Saless *et al.*, 1991) and in (Eubanks, 1991), the Soffel, Muller, Wu and Xu model (Soffel *et al.*, 1991) and in (Eubanks, 1991), and the Zhu-Groten model (Zhu and Groten, 1988) and in (Eubanks, 1991). Baseline results are expressed in “local” or “SI” coordinates appropriate for clocks running at the TAI rate on the surface of the Earth, to be consistent with the more general IERS conventions on the terrestrial reference system scale. This means that the gravitational potential of the Earth is now included in U ; the scale effects of the geocentric station velocities can still be ignored as they will at most cause scale changes of order 1 part in 10^{12} (see Zhu and Groten, Soffel *et al.*, and Fukushima, all in Eubanks (1991) and Shahid-Saless *et al.* (1991) for further details on the implications of these choices). As the time argument is now based on TAI, which is a quasi-local time on the geoid, distance estimates from these conventions will now be consistent in principle with “physical” distances.

The model is designed for use in the reduction of VLBI observations of extra-galactic objects acquired from the surface of the Earth. The delay error caused by ignoring the annual parallax is > 1 psec for objects closer than several hundred thousand light years, which includes all of the Milky Way galaxy. The model is not intended for use with observations of sources in the solar system, nor is it intended for use with observations made from space-based VLBI, from either low or high Earth orbit, or from the surface of the Moon (although it would be suitable with obvious changes for observations made entirely from the Moon).

It is assumed that the inertial reference frame is defined kinematically and that very distant objects, showing no apparent motion, are used to estimate precession and the nutation series. This frame is not truly inertial in a dynamical sense, as included in the precession constant and nutation series are the effects of the geodesic precession (~ 19 milli arc seconds / year). Soffel *et al.* (in Eubanks (1991)) and Shahid-Saless *et al.* (1991) give details of a dynamically inertial VLBI delay equation. At the picosecond level, there is no practical difference for VLBI geodesy and astrometry except for the adjustment in the precession constant.

Although the delay to be calculated is the time of arrival at station 2 minus the time of arrival at station 1, it is the time of arrival at station 1 that serves as the time reference for the measurement. Unless explicitly stated otherwise, all vector and scalar quantities are assumed to be calculated at t_1 , the time of arrival at station 1 including the effects of the troposphere.

The notation follows that of Hellings (1986) and Hellings and Shahid-Saless in Eubanks (1991) as closely as possible. It is assumed that the standard IAU models for precession, nutation, Earth rotation and polar motion have been followed and that all geocentric vector quantities have thus been rotated into a nearly non-rotating celestial frame. The errors in the standard IAU models are negligible for the purposes of the relativistic transformations. The notation itself is given in Table 12.1. The consensus model separates the total delay into a classical delay and a general relativistic delay, which are then modified by relativistic transformations between geocentric and solar system barycentric frames.

Table 12.1. Notation used in the model

t_i	the time of arrival of a radiointerferometric signal at the i^{th} VLBI receiver in terrestrial time (TAI)
T_i	the time of arrival of a radiointerferometric signal at the i^{th} VLBI receiver in barycentric time (TCB or TDB)
t_{g_i}	the “geometric” time of arrival of a radiointerferometric signal at the i^{th} VLBI receiver including the gravitational “bending” delay and the change in the geometric delay caused by the existence of the atmospheric propagation delay but neglecting the atmospheric propagation delay itself
t_{v_i}	the “vacuum” time of arrival of a radiointerferometric signal at the i^{th} VLBI receiver including the gravitational delay but neglecting the atmospheric propagation delay and the change in the geometric delay caused by the existence of the atmospheric propagation delay
t_{i_j}	the approximation to the time that the ray path to station i passed closest to gravitating body J
δt_{atm_i}	the atmospheric propagation delay for the i^{th} receiver = $t_i - t_{g_i}$
Δt_{grav}	the differential gravitational time delay, commonly known as the gravitational “bending delay”
$\vec{x}_i(t_i)$	the geocentric radius vector of the i^{th} receiver at the geocentric time t_i
\vec{b}	$\vec{x}_2(t_1) - \vec{x}_1(t_1)$ and is thus the geocentric baseline vector at the time of arrival t_1
\vec{b}_0	the <i>a priori</i> geocentric baseline vector at the time of arrival t_1
$\delta \vec{b}$	$\vec{b}(t_1) - \vec{b}_0(t_1)$

- \vec{w}_i the geocentric velocity of the i^{th} receiver
 - \hat{K} the unit vector from the barycenter to the source in the absence of gravitational or aberrational bending
 - \hat{k}_i the unit vector from the i^{th} station to the source after aberration
 - \vec{X}_i the barycentric radius vector of the i^{th} receiver
 - \vec{X}_\oplus the barycentric radius vector of the geocenter
 - \vec{X}_J the barycentric radius vector of the J^{th} gravitating body
 - \vec{R}_{i_J} the vector from the J^{th} gravitating body to the i^{th} receiver
 - \vec{R}_{\oplus_J} the vector from the J^{th} gravitating body to the geocenter
 - $\vec{R}_{\oplus\odot}$ the vector from the Sun to the geocenter
 - \hat{N}_{i_J} the unit vector from the J^{th} gravitating body to the i^{th} receiver
 - \vec{V}_\oplus the barycentric velocity of the geocenter
 - U the gravitational potential at the geocenter plus the terrestrial potential at the surface of the Earth. At the picosecond level, only the solar and terrestrial potentials need be included in U so that $U = GM_\odot/|\vec{R}_{\oplus\odot}|c^2 + GM_\oplus/a_\oplus c^2$
 - M_i the mass of the i^{th} gravitating body
 - M_\oplus the mass of the Earth
 - γ a PPN Parameter = 1 in general relativity
 - c the speed of light in meters / second
 - G the Gravitational Constant in Newtons meters² kilograms⁻²
 - a_\oplus the equatorial radius of the Earth
-

Vector magnitudes are expressed by the absolute value sign [$|x| = (\sum x_i^2)^{\frac{1}{2}}$]. Vectors and scalars expressed in geocentric coordinates are denoted by lower case (*e.g.* \vec{x} and t), while quantities in barycentric coordinates are in upper case (*e.g.* \vec{X} and T). MKS units are used throughout. For quantities such as V_\oplus , \vec{w}_i , and U it is assumed that a table (or numerical formula) is available as a function of TAI and that they are evaluated at the atomic time of reception at station 1, t_1 , unless explicitly stated otherwise. A lower case subscript (*e.g.* \vec{x}_i) denotes a particular VLBI receiver, while an upper case subscript (*e.g.* \vec{x}_J) denotes a particular gravitating body.

Gravitational Delay

The general relativistic delay, Δt_{grav} , is given for the J^{th} gravitating body by

$$\Delta t_{grav_J} = (1 + \gamma) \frac{GM_J}{c^3} \ln \frac{|\vec{R}_{1_J}| + \vec{K} \cdot \vec{R}_{1_J}}{|\vec{R}_{2_J}| + \vec{K} \cdot \vec{R}_{2_J}}. \quad (1)$$

At the picosecond level it is possible to simplify the delay due to the Earth, Δt_{grav_\oplus} , which becomes

$$\Delta t_{grav_\oplus} = (1 + \gamma) \frac{GM_\oplus}{c^3} \ln \frac{|\vec{x}_1| + \vec{K} \cdot \vec{x}_1}{|\vec{x}_2| + \vec{K} \cdot \vec{x}_2}. \quad (2)$$

The Sun, the Earth and Jupiter must be included, as well as the other planets in the solar system along with the Earth's Moon, for which the maximum delay change is several picoseconds. The major satellites of Jupiter, Saturn and Neptune should also be included if the ray path passes close to them. This is very unlikely in normal geodetic observing but may occur during planetary occultations.

The effect on the bending delay of the motion of the gravitating body during the time of propagation along the ray path is small for the Sun but can be several hundred picoseconds for Jupiter (see Sovers and Fanselow (1987) page 9). Since this simple correction, suggested by Sovers and Fanselow (1987) and Hellings (1986) among others, is sufficient at the picosecond level, it was adapted for the consensus model. It is also necessary to account for the motion of station 2 during the propagation time between station 1 and station 2. In this model \vec{R}_{iJ} , the vector from the J^{th} gravitating body to the i^{th} receiver, is iterated once, giving

$$t_{1J} = \min[t_1, t_1 - \hat{K} \cdot (\vec{X}_J(t_1) - \vec{X}_1(t_1))], \quad (3)$$

so that

$$\vec{R}_{1J}(t_1) = \vec{X}_1(t_1) - \vec{X}_J(t_{1J}), \quad (4)$$

and

$$\vec{R}_{2J} = \vec{X}_2(t_1) - \frac{\vec{V}_\oplus}{c}(\hat{K} \cdot \vec{b}_0) - \vec{X}_J(t_{1J}). \quad (5)$$

Only this one iteration is needed to obtain picosecond level accuracy for solar system objects. If more accuracy is required, it is probably better to use the rigorous approach of Shahid-Saless *et al.* (1991). $\vec{X}_1(t_1)$ is not tabulated, but can be inferred from $\vec{X}_\oplus(t_1)$ using

$$\vec{X}_i(t_1) = \vec{X}_\oplus(t_1) + \vec{x}_i(t_1), \quad (6)$$

which is of sufficient accuracy for use in equations 3, 4, and 5, when substituted into equation 1 but not for use in computing the geometric delay. The total gravitational delay is the sum over all gravitating bodies including the Earth,

$$\Delta t_{grav} = \sum_J \Delta t_{gravJ}. \quad (7)$$

Geometric Delay

In the barycentric frame the vacuum delay equation is, to a sufficient level of approximation:

$$T_2 - T_1 = -\frac{1}{c} \hat{K} \cdot (\vec{X}_2(T_2) - \vec{X}_1(T_1)) + \Delta t_{grav}. \quad (8)$$

This equation is converted into a geocentric delay equation using known quantities by performing the relativistic transformations relating the barycentric vectors \vec{X}_i to the corresponding geocentric vectors \vec{x}_i , thus converting equation 8 into an equation in terms of \vec{x}_i . The related transformation between barycentric and geocentric time can be used to derive another equation relating $T_2 - T_1$ and $t_2 - t_1$, and these two equations can then be solved for the geocentric delay in terms of the geocentric baseline vector \vec{b} . The papers by Soffel *et al.* in Eubanks (1991), Hellings and Shahid-Saless in Eubanks (1991), Zhu and Groten (1988) and Shahid-Saless *et al.* (1991) give details of the derivation of the vacuum delay equation. To conserve accuracy and simplify the equations the delay was expressed as much as is possible in terms of a rational polynomial. In the rational polynomial form the total geocentric vacuum delay is given by

$$t_{v_2} - t_{v_1} = \frac{\Delta t_{grav} - \frac{\hat{K} \cdot \vec{b}_0}{c} [1 - (1 + \gamma)U - \frac{|\vec{V}_\oplus|^2}{2c^2} - \frac{\vec{V}_\oplus \cdot \vec{w}_2}{c^2}] - \frac{\vec{V}_\oplus \cdot \vec{b}_0}{c^2} (1 + \hat{K} \cdot \vec{V}_\oplus / 2c)}{1 + \frac{\hat{K} \cdot (\vec{V}_\oplus + \vec{w}_2)}{c}}. \quad (9)$$

Given this expression for the vacuum delay, the total delay is found to be

$$t_2 - t_1 = t_{v_2} - t_{v_1} + (\delta t_{atm_2} - \delta t_{atm_1}) + \delta t_{atm_1} \frac{\hat{K} \cdot (\vec{w}_2 - \vec{w}_1)}{c}. \quad (10)$$

For convenience the total delay can be divided into separate geometric and propagation delays. The geometric delay is given by

$$t_{g_2} - t_{g_1} = t_{v_2} - t_{v_1} + \delta t_{atm_1} \frac{\hat{K} \cdot (\vec{w}_2 - \vec{w}_1)}{c}, \quad (11)$$

and the total delay can be found at some later time by adding the propagation delay:

$$t_2 - t_1 = t_{g_2} - t_{g_1} + (\delta t_{atm_2} - \delta t_{atm_1}). \quad (12)$$

The tropospheric propagation delay in equations 11 and 12 need not be from the same model. The estimate in equation 12 should be as accurate as possible, while the δt_{atm} model in equation 11 need only be accurate to about an air mass (~ 10 nanoseconds). If equation 10 is used instead, the model should be as accurate as is possible.

If the difference, $\delta \vec{b}$, between the *a priori* baseline vector \vec{b}_0 used in equation 9 and the true baseline vector is less than roughly three meters, then it suffices to add $-(\hat{K} \cdot \delta \vec{b})/c$ to $t_2 - t_1$. If this is not the case, however, the delay must be modified by adding

$$\Delta(t_{g_2} - t_{g_1}) = -\frac{\frac{\hat{K} \cdot \delta \vec{b}_0}{c}}{1 + \frac{\hat{K} \cdot (\vec{V}_\oplus + \vec{w}_2)}{c}} - \frac{\vec{V}_\oplus \cdot \delta \vec{B}}{c^2} \quad (13)$$

to the total time delay $t_2 - t_1$ from equation 10 or 12.

Observations Close to the Sun

For observations made very close to the Sun, higher order relativistic time delay effects become increasingly important. The largest correction is due to the change in delay caused by the bending of the ray path by the gravitating body described in Richter and Matzner (1983) and Hellings (1986). The change to Δt_{grav} is

$$\delta t_{grav_i} = \frac{(1 + \gamma)^2 G^2 M_i^2}{c^5} \frac{\vec{b} \cdot (\hat{N}_{1_i} + \hat{K})}{(|\vec{R}|_{1_i} + \vec{R}_{1_i} \cdot \hat{K})^2}, \quad (14)$$

which should be added to the Δt_{grav} in equation 1.

Summary

Assuming that time t_1 is the Atomic (TAI) time of reception of the VLBI signal at receiver 1, the following steps are recommended to correct the VLBI time delay for relativistic effects.

1. Use equation 6 to estimate the barycentric station vector for receiver 1.
2. Use equations 3, 4, and 5 to estimate the vectors from the Sun, the Moon, and each planet except the Earth to receiver 1.

3. Use equation 1 to estimate the differential gravitational delay for each of those bodies.
4. Use equation 2 to find the differential gravitational delay due to the Earth.
5. Sum to find the total differential gravitational delay.
6. Add Δt_{grav} to the rest of the *a priori* vacuum delay from equation 9.
7. Calculate the aberrated source vector for use in the calculation of the tropospheric propagation delay:

$$\vec{k}_i = \hat{K} + \frac{\vec{V}_\oplus + \vec{w}_i}{c} - \hat{K} \frac{\hat{K} \cdot (\vec{V}_\oplus + \vec{w}_i)}{c}. \quad (15)$$

8. Add the geometric part of the tropospheric propagation delay to the vacuum delay, equation 11.
9. The total delay can be found by adding the best estimate of the tropospheric propagation delay

$$t_2 - t_1 = t_{g_2} - t_{g_1} + [\delta t_{atm_2}(t_1 - \frac{\hat{K} \cdot \vec{b}_0}{c}, \vec{k}_2) - \delta t_{atm_1}(\vec{k}_1)]. \quad (16)$$

10. If necessary, apply equation 13 to correct for “post-model” changes in the baseline by adding equation 13 to the total time delay from equation step 9.

Propagation Correction for Laser Ranging

The space-time curvature near a massive body requires a correction to the Euclidean computation of range, ρ . This correction in seconds, Δt , is given by (Holdridge, 1967)

$$\Delta t = \frac{(1 + \gamma)GM}{c^3} \ln \left(\frac{R_1 + R_2 + \rho}{R_1 + R_2 - \rho} \right), \quad (17)$$

where

- c = speed of light,
- γ = PPN parameter equal to 1 in General Relativity,
- R_1 = distance from the body’s center to the beginning of the light path,
- R_2 = distance from the body’s center to the end of the light path,
- GM = gravitational parameter of the deflecting body.

For near-Earth satellites, working in the geocentric frame of reference, the only body to be considered is the Earth (Ries *et al.*, 1989). For lunar laser ranging, which is formulated in the solar system barycentric reference frame, the Sun and the Earth must be considered (Newhall *et al.*, 1987).

In the computation of the instantaneous space-fixed positions of a station and a lunar reflector in the analysis of LLR data, the body-centered coordinates of the two sites are affected by a scale reduction and a Lorentz contraction effect (Martin *et al.*, 1985). The scale effect is about 15 cm in the height of a tracking station, while the maximum value of the Lorentz effect is about 3 cm.

The equation for the transformation of \vec{r} , the geocentric position vector of a station expressed in the geocentric frame, is

$$\vec{r}_b = \vec{r} \left(1 - \frac{\gamma \Phi}{c^2} \right) + \frac{1}{2} \left(\frac{\vec{V} \cdot \vec{r}}{c^2} \right) \vec{V}, \quad (18)$$

where

- \vec{r}_b = station position expressed in the barycentric frame,
- Φ = gravitational potential at the geocenter (excluding the Earth's mass),
- \vec{V} = barycentric velocity of the Earth,

A similar equation applies to the selenocentric reflector coordinates; the maximum value of the Lorentz effect is about 1 cm (Newhall *et al.*, 1987).

References

- Boucher, C., 1986, "Relativistic effects in Geodynamics" in *Relativity in Celestial Mechanics and Astrometry*, J. Kovalevsky and V. A. Brumberg (eds), pp. 241–253.
- Cannon, W. H., Lisewski, D., Finkelstein, A. M., Kareinovich, and V. Ya, 1986, "Relativistic Effects in Earth Based and Cosmic Long Baseline Interferometry," *ibid.*, pp. 255–268.
- Eubanks, T. M., ed, 1991, *Proceedings of the U. S. Naval Observatory Workshop on Relativistic Models for Use in Space Geodesy*, U. S. Naval Observatory, Washington, D. C.
- Finkelstein, A. M., Kreinovitch, V. J., and Pandey, S. N., 1983, "Relativistic Reductions for Radiointerferometric Observables," *Astrophys. Space Sci.*, **94**, pp. 233–247.
- Hellings, R. W., 1986, "Relativistic effects in Astronomical Timing Measurements," *Astron. J.*, **91**, pp. 650–659. Erratum, *ibid.*, p. 1446.
- Holdridge, D. B., 1967, *An Alternate Expression for Light Time Using General Relativity*, JPL Space Program Summary 37-48, III, pp. 2–4.
- Martin, C. F., Torrence, M. H., and Misner, C. W., 1985, "Relativistic Effects on an Earth Orbiting Satellite in the Barycentric Coordinate System," *J. Geophys. Res.*, **90**, p. 9403.
- McCarthy, D. D., 1992, IERS Standards, IERS Technical Note 13, Observatoire de Paris, Paris.
- Newhall, X X, Williams, J. G., and Dickey, J. O., 1987, "Relativity Modelling in Lunar Laser Ranging Data Analysis," in *Proceedings of the International Association of Geodesy (IAG) Symposia*, Vancouver, pp. 78–82.
- Pavlov, B. N., 1985, "On the Relativistic Theory of Astrometric Observations. III. Radio Interferometry of Remote Sources," *Soviet Astronomy*, **29**, pp. 98–102.
- Richter, G. W. and Matzner, R. A., 1983, "Second-order Contributions to Relativistic Time Delay in the Parameterized Post-Newtonian Formalism," *Phys. Rev. D*, **28**, pp. 3007–3012.

- Ries, J. C., Huang, C., and Watkins, M. M., 1988, "The Effect of General Relativity on Near-Earth Satellites in the Solar System Barycentric and Geocentric Reference Frames," *Phys. Rev. Let.*, **61**, pp. 903–906.
- Robertson, D. S., 1975, "Geodetic and Astrometric Measurements with Very-Long-Baseline Interferometry," Ph. D. Thesis, Massachusetts Institute of Technology.
- Shahid-Saless, B., Hellings, R. W., and Ashby, N., 1991, "A Picosecond Accuracy Relativistic VLBI Model via Fermi Normal Coordinates," *Geophys. Res. Let.*, **18**, pp. 1139–1142.
- Soffel, M., Ruder H., Schneider, M., Campbell, J., and Schuh, H., 1986, "Relativistic Effects in Geodetic VLBI Measurements," in *Relativity in Celestial Mechanics and Astrometry*, J. Kovalevsky and V. A. Brumberg (eds), pp. 277–282.
- Soffel M. H., Muller, J., Wu, X., and Xu, C., 1991, "Consistent Relativistic VLBI Theory with Picosecond Accuracy," *Astron. J.*, **101**, pp. 2306–2310.
- Sovers, O. J. and Fanselow, J. L., 1987, *Observation Model and Parameter Partial for the JPL VLBI Parameter Estimation Software 'Masterfit'-1987*, JPL Pub. 83-89, Rev. 3.
- Zeller, G., Soffel, M., Ruder, H., and Schneider, M., 1986, *Astr. Geod. Arbeiten*, Heft 48, Bay. Akad. d. Wiss., pp. 218–236.
- Zhu, S. Y. and Groten, E., 1988, "Relativistic Effects in the VLBI Time Delay Measurement," *Man. Geod.*, **13**, pp. 33–39.

GLOSSARY

AAM	Atmospheric Angular Momentum
BIH	Bureau International de l'Heure
BIPM	Bureau International des Poids et Mesures
CEP	Celestial Ephemeris Pole
CERGA	Centre d'Etudes et de Recherches Geodynamiques et Astronomiques
CCIR	International Radio Consultative Committee
CIO	Conventional International Origin
CODE	Center for Orbit Determination in Europe
CSR	Center for Space Research, University of Texas
DORIS	Doppler Orbit determination and Radiopositioning Integrate on Satellite
DUT	Delft University of Technology
ECMWF	European Centre for Medium-range Weather Forecasting
EMR	See NRCan
EOP	Earth Orientation Parameters
ESOC	European Space Operations Center
GFZ	GeoForschungsZentrum
GMST	Greenwich Mean Sidereal Time
GPS	Global Positioning System
IAG	International Association of Geodesy
IAU	International Astronomical Union
IERS	International Earth Rotation Service
ICRF	IERS Celestial Reference Frame
IGS	International GPS Service for geodynamics
ITRF	IERS Terrestrial Reference Frame
IRP	IERS Reference Pole
IRM	IERS Reference Meridian
JPL	Jet Propulsion Laboratory
LLR	Lunar Laser Ranging
MCC	Russian Mission Control
NEOS	National Earth Orientation Service
NOAA	National Oceanic and Atmospheric Administration
NRCan	Natural Resources Canada , formerly EMR
SLR	Satellite Laser Ranging
SI	Systeme International
SIO	Scripps Institution of Oceanography
TAI	Temps Atomique International
TT	Terrestrial Time
UKMO	U.K. Meteorological Office
USNO	United States Naval Observatory
UTC	Coordinated Universal Time
UTXMO	Dept. of Astronomy. The University of Texas at Austin.
VLBI	Very Long Baseline Interferometry